Investigation of Dielectric Properties of Recycled Polyolefins

by

Iman SHIRZAEI SANI

MANUSCRIPT-BASED THESIS PRESENTED TO ÉCOLE DE TECHNOLOGIE SUPÉRIEURE IN PARTIAL FULFILLEMENT FOR THE DEGREE OF DOCTOR OF PHILOSOPHY
PH.D

MONTREAL, OCTOBER 23, 2025

ÉCOLE DE TECHNOLOGIE SUPÉRIEURE
UNIVERSITÉ DU QUÉBEC

BOARD OF EXAMINERS

THIS THESIS HAS BEEN EVALUATED

BY THE FOLLOWING BOARD OF EXAMINERS

Mr. Éric David, Thesis Supervisor
Department of Mechanical Engineering, École de technologie supérieure

Mrs. Nicole R. Demarquette, Thesis Co-supervisor
Department of Mechanical Engineering, École de technologie supérieure

Mrs. Claudiane Ouellet-Plamondon, President of the Board of Examiners
Department of Construction Engineering, École de technologie supérieure

Mr. Ilyass Tabiai, Member of the jury
Department of Mechanical Engineering, École de technologie supérieure

Mr. Issouf Fofana, External Evaluator
Department of applied sciences, Chicoutimi (Québec)

THIS THESIS WAS PRENSENTED AND DEFENDED

IN THE PRESENCE OF A BOARD OF EXAMINERS AND PUBLIC

OCTOBER 8, 2025

AT ECOLE DE TECHNOLOGIE SUPERIEURE

ACKNOWLEDGMENT

I would like to express my deepest gratitude to my PhD thesis supervisor, Professor Éric David, for his unwavering support, insightful guidance, and steady patience throughout my PhD. I extend my sincere thanks to my thesis co-supervisor, Professor Nicole R. Demarquette, for her valuable feedback, thoughtful advice, and consistent support, which have been invaluable to my research.

I would like to express my appreciation to the members of my thesis committee, Prof. Claudiane Ouellet-Plamondon, and Prof. Ilyass Tabiai from École de technologie supérieure and Prof. Issouf Fofana, from Chicoutimi university for their time to evaluate this work.

I wish to express my gratitude to the Natural Sciences and Engineering Research Council of Canada (NSERC) for their financial support and to ETS for providing the essential facilities and resources that made this research possible.

This dissertation is dedicated to the loving memory of my late father, whom I lost during my PhD journey. Thank you for your support and guidance throughout my life. To my mother and my siblings, your love and emotional support carried me through the most challenging times. This accomplishment belongs to my entire family.

Finally, I wish to express my heartfelt thanks to my friends whose friendship and encouragement made this journey more meaningful and memorable.

ÉTUDE DES PROPRIÉTÉS DIÉLECTRIQUES DES POLYOLÉFINES RECYCLÉES

Iman SHIRZAEI SANI

RÉSUMÉ

Cette thèse étudie le comportement diélectrique des polyoléfines recyclées post-consommation, en particulier le polyéthylène haute densité recyclé et les mélanges recyclés de polyéthylène–polypropylène, en vue d'une utilisation potentielle dans des applications d'isolation électrique. L'étude comprend une évaluation détaillée de leurs propriétés diélectriques, thermiques et chimiques dans diverses conditions, notamment à l'état sec, humide et non traité. Le mélange avec du HDPE vierge a été utilisé comme stratégie pour évaluer s'il pouvait améliorer les performances diélectriques des matériaux recyclés.

La caractérisation chimique a révélé la présence d'impuretés organiques et inorganiques dans le PE recyclé et les mélanges PE–PP, ce qui a fortement affecté leur comportement diélectrique. Ces impuretés ont entraîné des pertes diélectriques jusqu'à 24 à 28 fois supérieures à celles du HDPE vierge à 60 Hz et ont influencé la rigidité diélectrique. Le HDPE recyclé a montré une rigidité diélectrique de 115 kV/mm, contre 128 kV/mm pour le HDPE vierge, ce qui indique que les impuretés de grande taille ont un impact négatif sur les performances diélectriques.

L'absorption d'humidité affecte de manière significative le comportement diélectrique des polyoléfines recyclées. Les résultats montrent que le pic de relaxation se déplace vers des fréquences plus élevées dans les échantillons humides, avec une augmentation notable des pertes diélectriques aux hautes fréquences et une diminution à basses fréquences. À 60 Hz, la perte diélectrique du PE–PP recyclé humide était 71 fois plus élevée que celle du HDPE vierge non traité, tandis que le HDPE humide ne montrait qu'une augmentation de 2 fois, ce qui souligne la plus grande sensibilité à l'humidité du matériau recyclé.

Le mélange de polyoléfines recyclées avec du HDPE vierge améliore significativement leurs performances diélectriques. Même une faible addition de HDPE vierge, comme 15 %, a permis de réduire les pertes diélectriques jusqu'à 40 %, tandis qu'un ajout de 50 % a réduit les pertes jusqu'à près de 70 % et a amélioré la rigidité diélectrique. Cette stratégie permet d'atténuer efficacement les effets négatifs des impuretés et rend les matériaux recyclés plus adaptés aux applications d'isolation.

Mots-clés : polyoléfines recyclées, relaxation diélectrique, résistance à la rupture, impuretés, absorption d'eau, matériaux durables, fonction havriliak-negami

INVESTIGATION OF DIELECTRIC PROPERTIES OF RECYCLED POLYOLEFINS

Iman SHIRZAEI SANI

ABSTRACT

This thesis investigates the dielectric behavior of post-consumer recycled polyolefins, specifically recycled high-density polyethylene and recycled polyethylene–polypropylene blends, for potential use in electrical insulation applications. The study includes detailed evaluation of their dielectric, thermal, and chemical properties under various conditions, including dry, wet, and untreated states. Blending with virgin HDPE was used as a strategy to assess whether it could improve the dielectric performance of the recycled materials.

Chemical characterization revealed the presence of organic and inorganic impurities in recycled PE and PE–PP blends, which significantly affected their dielectric behavior. These impurities led to dielectric losses up to 24–28 times higher than virgin HDPE at 60 Hz and influenced breakdown strength. Recycled HDPE showed a breakdown strength of 115 kV/mm compared to 128 kV/mm for virgin HDPE, indicating that large-sized impurities negatively impact dielectric performance.

Moisture absorption significantly affects the dielectric behavior of recycled polyolefins. The results show that the relaxation peak shifts to higher frequencies in wet samples, with a significant increase in dielectric loss at high frequencies and a decrease at low frequencies. At 60 Hz, the dielectric loss of wet recycled PE-PP was 71 times higher than that of untreated virgin HDPE, while wet HDPE showed only a 2-times increase, highlighting the greater moisture sensitivity of the recycled material.

Blending recycled polyolefins with virgin HDPE significantly improves their dielectric performance. Even a small addition of virgin HDPE, such as 15%, reduced the dielectric loss by up to 40%, while 50% of virgin HDPE reduce the losses up to almost 70 % and improved breakdown strength. This strategy effectively moderates the negative effects of impurities and makes recycled materials more suitable for insulation applications.

Kewwords: recycled polyolefins, dielectric relaxation, breakdown strength, impurities, water absorption, sustainable materials, havriliak–negami function

TABLE OF CONTENTS

Page

LIST OF TABLES

Page

LIST OF FIGURES

Page

LIST OF ABREVIATIONS

AC	Alternating current
BDS	Broadband Dielectric Spectroscopy
DC	Direct current
DSC	Differential Scanning Calorimetry
EDX	Energy Dispersive X-ray
FTIR	Fourier Transform Infrared spectroscopy
HDPE	High-density- Polyethylene
HN function	Havriliak-Negami function
LDPE	Low-density- Polyethylene
LLDPE	Linear-low-density- Polyethylene
MFI	Melt-flow-index
MWS	Maxwell–Wagner–Sillars
PC	polycarbonate
PCRF	Post-consumer recycled-flake
PCRP	Post-consumer recycled-pellet
PE	Polyethylene
PP	Polypropylene
rHDPE	recycled High-density- Polyethylene
rPE	recycled Polyethylene
r(PE-PP)	recycled Polyethylene/ polypropylene
rPP	recycled polypropylene
SEM	Scanning Electron Microscopy

TGA	Thermogravimetric Analysis
V	Voltage
Vrms	root-mean-square voltage

LIST OF SYMBOLS

E_b	Dielectric strength (v/m)
E_{Br}	Electrical breakdown
f_{max}	Maximum frequency at relaxation peak
P	Cumulative probability
T_g	Glass transition temperature
T_m	Melting temperature
tan δ	Loss tangent
X_c	Degree of crystallinity
α_k	Width parameter
β_k	Asymmetry parameter
$\hat{\varepsilon}$	Complex dielectric permittivity
ε_0	Vacuum permittivity
ε_∞	Real permittivity at much higher frequencies
ε''	Imaginary permittivity
ε'	Real permittivity
σ	Electrical direct conductivity
τ_k	Relaxation time
ΔH_m	Melting enthalpy
$\Delta\varepsilon$	Dielectric relaxation strength

INTRODUCTION

0.1 Context of the Research

The rapid growth in plastic consumption has led to a significant increase in plastic waste accumulation, most of which ends up in landfills or the natural environment. Despite the ease of processing thermoplastics and their potential for reuse, less than 10% of plastic waste is currently recycled (Geyer et al., 2017; Jambeck et al., 2015). This results in substantial environmental and economic losses. Because of their recyclable nature, plastics are increasingly being considered in circular economy strategies, which aim to reintroduce waste materials into new applications. However, to make recycling truly effective, it is crucial to enhance the properties of recycled materials, especially post-consumer plastics that often contain impurities and signs of degradation.

Around 50% of global plastic waste consists of polyolefins (Singh et al., 2023), mainly polyethylene (PE) and polypropylene (PP). These materials, widely used in electrical cables due to their good dielectric properties and low cost, are non-biodegradable and contribute significantly to long-term pollution. It has been reported that approximately 14% of globally produced polyethylene (PE) is currently used in the wire and cable industry ("Polyethylene Insulation Materials Market Size and Forecast 2030," 2022; "Polyethylene Market Size to Hit US$ 151.85 Billion by 2030," 2021). Although polyolefins can be easily separated from other plastics using float-sink methods, further separation into PE and PP is economically challenging (Ragaert et al., 2017). Therefore, recycling strategies often rely on using mixed polyolefin waste as-is, despite the drop in material performance caused by polymer aging and contamination.

While numerous studies have investigated various characteristics of waste materials—particularly their mechanical, thermal, and chemical properties (Borovanska et al., 2014; Calero et al., 2018; Gala et al., 2020; Gall et al., 2021; Mylläri et al., 2016)—only limited attention has been given to their dielectric behavior. Although the effects of factors such as water absorption (Couderc Hugues et al., 2014; Hosier et al., 2017; Hui et al., 2013; Kochetov

et al., 2016) and aging (Densley, 2001; Li et al., 2024; Liang et al., 2023; Tantipattarakul et al., 2020; Zheng et al., 2023) on polyolefins and their composites have been extensively explored, their influence on the dielectric properties of recycled materials remains underexplored.

To improve the performance of polyolefins, researchers have proposed various strategies. One common approach is the incorporation of particles, especially nanoparticles, to enhance dielectric properties. For example, Tiemblo et al. (Tiemblo et al., 2008) demonstrated that particle shape and orientation can significantly influence the breakdown strength of polymer-based systems. However, unlike the controlled addition of engineered nanoparticles, recycled materials inherently contain uncontrolled impurities, which often lead to a decline in dielectric performance.

Blending recycled polyolefins with virgin polymers is another widely adopted method to enhance overall material performance. Numerous studies have shown that such blends can improve the mechanical and thermal properties of recycled polyolefins (Cecon et al., 2021; X. Huang et al., 2019; Zhang et al., 2023), and in some cases, also contribute to better dielectric behavior (X. Huang et al., 2019). Despite these findings, the majority of existing literature has focused primarily on mechanical and thermal enhancements, with dielectric performance receiving comparatively little attention. This represents a critical knowledge gap, especially considering the significance of dielectric properties in applications such as electrical insulation. Given these insights, blending stands out as a promising strategy not only for improving the mechanical and thermal properties of recycled polyolefins but also for potentially enhancing their dielectric behavior. This study seeks to address the current research gap by investigating the dielectric performance of recycled polyolefin blends, with a focus on their potential use in electrical insulation applications.

0.2 Objectives

The main purpose of this research is to advance the application of recycled polyolefins in electrical insulation by investigating the impact of impurities and environmental conditions on their dielectric properties. Additionally, the study explores practical strategies, including the

incorporation of virgin polymers, to address performance drawbacks of recycled polyolefins. Through this approach, the work aims to contribute to more sustainable and efficient use of recycled polymers in industrial electrical applications. The specific objectives are as follows:

1. To understand how impurities influence the dielectric behavior and performance of recycled polyolefins used in insulation applications.
2. To investigate the dielectric properties of recycled polyolefins under varying thermal and environmental conditions (dry, wet, and ambient) in order to determine their impact on dielectric performance.
3. To explore performance-enhancing techniques, such as blending with virgin polymer, to restore the dielectric performance of recycled polyolefins in insulation applications.

0.3 Methodology

Prior to conducting any analytical techniques, it is crucial to determine the composition of the recycled materials. This involves identifying the type of polymer present and measuring any potential contaminants in the sample. This analysis facilitates a more precise interpretation of the results from the subsequent analyses.

Thermal characterization: Differential Scanning Calorimetry (DSC) and Thermogravimetric Analysis (TGA) were utilized to assess the thermal properties of recycled materials. DSC provides valuable results such as glass transition temperature (T_g), percentage of crystallinity (X_c), and melting temperature (T_m), which help in understanding the polymer waste composition and distinguishing different types of polymers based on their melting temperatures. While optical equipment is used to separate various polymers before storage, DSC ensures that no guest polymers remain in the mixture. If a significant amount of guest components is present, related peaks will appear at different temperatures. TGA, on the other hand, was used to evaluate the thermal stability and decomposition behavior of the materials. It helps identify inorganic impurities in the polymeric matrix, which may significantly impact electrical insulation properties and overall material performance.

Chemical characterization: While DSC is an effective method for distinguishing different polymer types, the melting temperature of a polymer may overlap with that of other polymers

(e.g., HDPE and LDPE). In such cases, FT-IR can help distinguish between different polymers by comparing the blended pure polymer with the waste material. Additionally, FT-IR can detect polymer degradation during reprocessing, as specific peaks corresponding to degradation products will become observable.

EDX, which is an additional feature of the SEM device, provides more detailed information about the type of impurities present in the polymeric matrix. While TGA can quantify the amount of impurities, it does not identify the specific types. Different impurities can influence dielectric properties in various ways due to their differing conductivities. Therefore, EDX is a valuable tool for identifying the chemical elements present in the material, offering insights into the composition and potential impact on the polymer's performance.

Dielectric characterization: The dielectric properties of the recycled materials were examined using a Novocontrol broadband spectrometer and a Bauer DTA100, which were employed to analyze the complex permittivity and breakdown strength of the nanocomposites, respectively. Impurities present in the waste polymer matrix, whether present in the source material or introduced during reprocessing, can influence the loss factor observed in both the real and imaginary permittivity. These impurities, along with elements released during degradation, can also influence the electrical breakdown strength. The analysis helps assess dielectric insulation properties, particularly in recycled materials, where impurities, both organic and inorganic, can significantly affect the dielectric response and increase conductivity compared to virgin materials. Varying conditions, including temperature-dependent and time-dependent analyses, as well as different environments dry, wet, and ambient were studied.

Short-term AC breakdown testing is a common method for analyzing dielectric behavior by assessing the dielectric strength of recycled materials. Samples were tested following a standardized protocol, and statistical analysis was performed to evaluate variability in breakdown performance. This test provides valuable data on the materials' electrical insulation characteristics, indicating the maximum electric field they can withstand before failure.

Finally, the experimental data obtained from BDS were fitted to standard dielectric models using commercial software. This fitting process enabled the identification of key parameters influencing the dielectric behavior and provided insights into the polarization and relaxation mechanisms involved.

This methodology ensures a comprehensive understanding of the chemical, thermal, and electrical properties of the recycled materials. By studying the factors influencing dielectric behavior, we can identify strategies to enhance their performance for industrial applications.

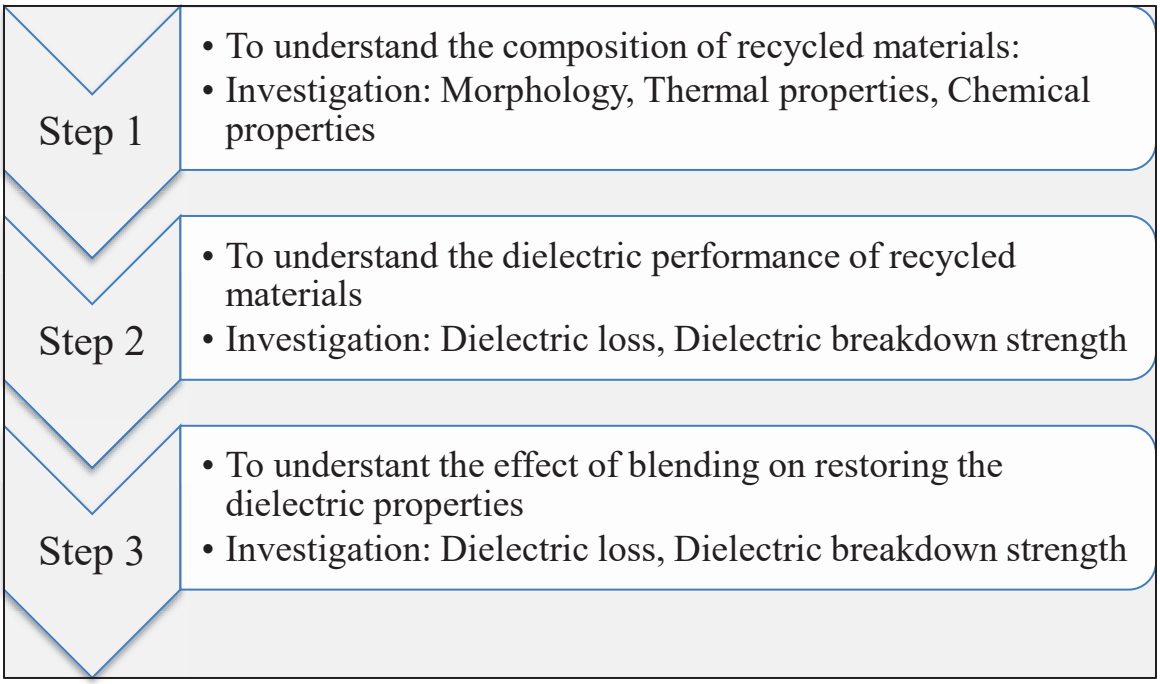

Figure 0.1 The outline of Ph.D project

CHAPTER 1

BASIC CONCEPT OF DIELECTRIC POLYMERS

1.1 Introduction to Dielectric Materials

Dielectric materials, commonly referred to as electrical insulators, are materials that do not conduct electric current under normal conditions. When placed in an external electric field, they do not allow current to flow due to the absence of free electrons, unlike conductors. However, they do experience a phenomenon called polarization, where the electric charges within the material shift slightly, aligning in response to the applied field. This internal rearrangement of bound charges leads to the development of electric dipoles, a fundamental feature of dielectric behavior.

1.2 Polarization

In dielectric materials, polarization occurs through various mechanisms depending on the structure and composition of the material. The four primary types of polarization are:

1.2.1 Electronic Polarization

Electronic polarization arises when an external electric field distorts the electron cloud of an atom relative to its nucleus, creating a temporary dipole moment. This is typically the fastest form of polarization and occurs in all dielectric materials. It is more pronounced in materials with weakly bound outer electrons. In materials with strong covalent bonds, such as some polymers, electronic polarization is limited due to the restricted mobility of electrons.

1.2.2 Ionic Polarization

This type of polarization occurs in ionic solids when the positively and negatively charged ions are displaced in opposite directions under an external electric field. The relative motion of cations and anions creates dipole moments. Ionic polarization is commonly observed in crystalline ionic compounds and, to a lesser extent, in certain polymeric materials.

1.2.3 Dipolar (Orientation) Polarization

Dipolar polarization occurs in materials containing permanent dipoles, such as polar molecules. In the absence of an electric field, these dipoles are randomly oriented. When a field is applied, they tend to align with it, resulting in net polarization. In polymers, the presence and arrangement of polar side groups strongly influence this effect.

1.2.4 Interfacial (Maxwell-Wagner) Polarization

Interfacial polarization occurs in heterogeneous systems, such as composites, where different phases have unequal electrical conductivities. Charge carriers accumulate at the interfaces under an applied field, creating large dipole moments. This effect is more dominant at low frequencies and is influenced by factors like impurities, crystal-amorphous boundaries, and phase discontinuities in polymer blends or composites.

As frequency changes, the dominant polarization mechanism shifts, whereas electronic polarization is most effective at high frequencies, while interfacial polarization is most effective at low frequencies.

1.3 Complex permittivity

The polarization behavior of a dielectric material is described using the complex permittivity (ε^*), which is expressed as equation 1.1.

$$\varepsilon^* = \varepsilon' - j\varepsilon'' \quad (1.1)$$

In this equation, ε′ is the real part of permittivity, associated with the material's ability to store electrical energy (also known as the dielectric constant). Also, ε″ is the imaginary part, which corresponds to dielectric loss or the energy dissipated as heat due to lagging polarization.

The real component, ε′, is influenced by the number of polarizable charges (electrons, ions, or dipoles) and their mobility within the material. As such, both temperature and frequency play crucial roles. Higher temperatures generally increase charge mobility, while higher frequencies can reduce the ability of dipoles or charges to reorient in time with the Alternating electric field.

When an alternating electric field is applied, dipolar and ionic entities attempt to align with the changing field direction. If the frequency is too high, dipoles and ions cannot respond quickly enough, and this delay leads to energy dissipation, resulting in a higher dielectric loss (ε″). Conversely, at low frequencies, these entities can fully reorient, reducing energy loss. This dynamic behavior explains the frequency and temperature dependence of both ε′ and ε″(Jonscher, 1983; Kremer and Schönhals, 2003).

The dielectric constant (ε′) reflects a material's capacity to concentrate electrostatic field lines and store energy under an electric field. A higher ε′ indicates greater energy storage potential, which is critical for applications in capacitors, insulators, and high-frequency devices.

It should be noted that the imaginary part of the complex permittivity (ε″), as measured in dielectric spectroscopy, includes two main contributions. The first is due to polarization relaxation losses, which result from the time delay in the response of dipoles or polarizable groups to an alternating electric field. The second component arises from conductive losses, which are associated with the electrical conductivity (σ) of the material. Unlike relaxation losses, conductive losses are caused by the movement of free charges, such as ions or electrons, through the material under an electric field. These losses are different from polarization effects and do not involve the reorientation or displacement of dipoles.

These two contributions to dielectric loss are mathematically related and can be expressed as:

$$\varepsilon_r'' = \varepsilon_{relaxation}'' + \frac{\sigma}{\varepsilon_0 \omega} \quad (1.2)$$

In this expression, ε_0 is the vacuum permittivity, ω is the angular frequency ($\omega = 2\pi f$), and σ is the electrical direct conductivity of the material (conductivity at low frequency).
The first term represents energy loss due to relaxation processes, while the second term reflects conduction losses. Conduction losses are typically more significant at low frequencies, where charges have more time to move over longer distances through the material. In contrast, relaxation involves localized charge displacements that occur much more quickly (higher frequencies).

1.4 Dissipation factor

The dissipation factor, also known as the loss tangent (tan δ) indicates how efficiently a material performs in an electric field. It is defined by the following equation (Equation 1.3):

$$\tan\delta = \frac{\varepsilon''}{\varepsilon'} \tag{1.3}$$

The dissipation factor reflects the ratio of energy lost- including both conduction and relaxation losses- to the energy stored during each cycle of the applied electric field. A lower tan δ indicates that the material stores energy efficiently with minimal energy dissipation.
In capacitors, a low dissipation factor is essential for effective energy storage with reduced heat loss. Similarly, in insulating materials, a low tan δ is crucial as it reflects the material's reliability and stability under electrical stress. Therefore, minimizing the dissipation factor is a key objective in designing materials for both energy storage and electrical insulation applications.

1.5 Dielectric breakdown

The breakdown of polymeric insulation is a critical failure mode that occurs when the applied electric field exceeds the material’s ability to maintain its insulating properties. Despite low-level degradation processes such as physical, chemical, and electrical aging contribute to long-term degradation processes, they typically operate at electric fields far below the breakdown strength and typically do not cause sudden breakdown

In contrast, breakdown mechanisms, including electrical, thermal, electromechanical, and partial discharge processes can lead to fast failure depending on the intensity and duration of the applied stress.

1.5.1 Electrical Breakdown:

Electrical breakdown occurs when the electric field surpasses the dielectric strength of the material, often at localized defects or imperfections. The intrinsic dielectric strength depends on the material type and temperature (Kuffel, 2000). It can be calculated by the following equation (Blythe and Bloor, 2005):

$$E_b = \frac{V}{t_{insulator}} \tag{1.4}$$

Where:

E_b: Dielectric strength (v/m)

V: Breakdown voltage (v)

$t_{insulator}$: Thickness of insulator (m)

1.5.2 Thermal Breakdown:

Thermal breakdown occurs when the heat generated by electrical stress exceeds the material's capacity to dissipate it. This overheating enhances ionic mobility and electrical conductivity, potentially leading to thermal runaway a process that can result in the polymer melting or burning.

1.5.3 Partial Discharge:

Partial discharge is triggered by the ionization of gas within voids present in the insulating material. These voids often unavoidable during the manufacturing process, intensify the local electric field due to the difference in dielectric properties between the gas and the adjacent

polymer. The ionized gas can gradually erode the insulation or lead to sudden failure, especially in thicker samples (Fothergill et al., 2003).

Overall, breakdown can occur suddenly or gradually, depending on whether the dominant mechanism is field-driven failure or long-term aging. While aging weakens the insulation over time, direct breakdown mechanisms are responsible for the final failure under high stress conditions.

CHAPTER 2

INVESTIGATION AND CHARACTERIZATION OF DIELECTRIC, THERMAL, AND CHEMICAL PROPERTIES OF RECYCLED HDPE BLENDED WITH VIRGIN HDPE

Iman Shirzaei Sani [a], Nicole R. Demarquette [b], Eric David [c]

[a,b,c] Department of Mechanical Engineering, École de Technologie Supérieure, 1100 Notre-Dame West, Montreal, Quebec, Canada H3C 1K3

Paper published in *Polymer Engineering and Science journal*, August 2023
DOI: 10.1002/pen.26441

Chapter outline: Chapter 2 investigate the dielectric performance of post-consumer recycled material mainly HDPE blended with virgin HDPE. It focuses on chemical characterization and dielectric properties of recycled material. It begins with an abstract highlighting key finding, followed by an introduction that outlines the importance of recycling and the challenges posed by unknown impurities in recycled polymers. The materials and methods section describe the techniques (TGA, DSC, and EDX) used for compositional characterization. The results and discussion section presents the impurity profiles, dielectric behavior, and breakdown strength of the materials, along with the improvements observed through virgin HDPE blending. The chapter concludes with a summary of the findings, underscoring the critical role of material characterization in assessing the electrical suitability of recycled HDPE.

Abstract: Dielectric performance of post-consumer recycled HDPE blended with virgin HDPE was investigated in order to evaluate the possibility of using these materials for the insulation of electrical wires and cables. The presence of organic and inorganic impurities was investigated using thermal and chemical methods (TGA, DSC, and EDX). The characterization of impurities revealed different amount of inorganic impurities in recycled material that was depending on the execution of melt filtration by the recycler to prepare the recycled material.

Higher values of both dielectric losses and dielectric constant were observed for post-consumer recycled PE, with the dielectric loss of recycled material almost 17 times higher than the one of virgin PE at power frequency (60 Hz). The short-term breakdown strength of post-consumer recycled HDPE was observed to be slightly lower than that of virgin PE.
The experimental result showed that blending the recycled stream with virgin materials was effective in order to enhance dielectric properties of recycled material. In this regards, dielectric losses decreased by almost 50% when 50% of virgin HDPE was added to the recycled material. Also, breakdown strength was improved when virgin HDPE was added.

Keywords: waste material; recycled polyethylene; dielectric loss; impurity; permittivity; breakdown strength

2.1 Introduction

Polyolefins are widely used as a dielectric material in all types of electrical cables, from low or medium voltage cables to high and ultra-high voltage cables, which, for most of their industrial applications, do not need high thermal or mechanical properties. Polyethylene can usually provide all the needed requirements such as very good dielectric properties, sufficient thermal and mechanical properties in addition to excellent processability and low cost. Furthermore the use of non-renewable and non-biodegradable plastics, such as these polyolefins, rises more and more concern since it has led to accumulation of millions of tons of plastic waste that ends up in landfills, or somewhere else in the environment (Jambeck et al., 2015). Only a small amount (~9 %) of plastic wastes are recycled (Geyer et al., 2017), although they could be easily reused due to their ability to be processed and re-processed. Moreover, plastics can be a sustainable substitute to most materials such as ceramics and metals. Hence, there is a growing interest in utilizing waste materials for new applications as part of circular economy strategies that are in consideration worldwide.

Around 14% of global produced PE are currently used in wires & cables industry (“Polyethylene Insulation Materials Market Size and Forecast 2030,” 2022; “Polyethylene

Market Size to Hit US$ 151.85 Billion by 2030," 2021). Consequently, promoting the use of recycled material in this industry would certainly increase material circularity. In order to do, it is necessary to determine the extent to which the properties, particularly the dielectric properties, are influenced by the presence of contaminants - that are commonly encountered in recycled polymers supplied by sorting centers. Extensive investigations have been carried out on recycled polymers, contributing to our understanding of their performance characteristics. For instance, detrimental effect of recycled polypropylene (rPP) as the polymeric contamination has been investigated by Erdal et al. (Karaagac et al., 2021). They highlighted that the presence of inevitable recycled PP resulted in a reduction in the mechanical properties of recycled HDPE. Moreover, chemical, thermal, rheological, and mechanical properties of recycled materials have been studied by other researchers(Boz Noyan et al., 2022; Gall et al., 2021; Garofalo et al., 2021; Roosen et al., 2020).

Even though several studies have been done on above mentioned properties, there is a limited amount of research available on the dielectric properties of recycled materials. Cruz et al.(Cruz and Zanin, 2004; S. A. Cruz and M. Zanin, 2004) evaluated the incorporation of recycled HDPE in virgin polymer blends and its impact on dielectric strength. Their results showed a decrease in dielectric strength when using 100% recycled material compared to virgin HDPE. However, they reported formulations with up to 50% recycled material exhibited potential for electric insulating systems. In addition to the limited research available on the dielectric properties of recycled polymers, it is worth noting that several studies and review articles have examined the dielectric properties of virgin materials(Angalane and Kasinathan, 2022; Gao et al., 2023b, 2023a; Pandey and Singh, 2021). These studies provide valuable insights into understanding the behavior of dielectric properties of recycled materials.

In this study, we evaluated to what extend recycled materials can be used in the electrical cable industry. In particular, the effects of impurities on the dielectric properties of the recycled materials are evaluated. In the second phase of our study, we evaluated how the polymers' properties could be reclaimed by blending them with virgin materials. Blending was investigated as a potential strategy to overcome the drawbacks of using waste material.

2.2 Materials and Methods

2.2.1 Materials

High-density polyethylene (HDPE) pellets with a melt flow index (MFI) of 6.8 g/10 min (measured at 190 °C under a 2.16 kg load) and a density of 0.952 g/cm^3 was supplied from Dow. The post-consumer recycled polyethylene was supplied in two forms, flakes and pellets. The flake form of post-consumer recycled materials (PCRF) that were only collected, sorted and grinded by the recycler and the pellets form of post-consumer recycled material (PCRP) is the same material but with an additional cleaning step and was melt processed by the recycler. The MFI of these two materials were measured at 190 °C with a load of 2.16 kg. MFI were 0.59 ± 0.02 and 0.64 ± 0.03 for the flake and pellet forms of recycled polyethylene respectively.

2.2.2 Sample Preparation

The flake form of post-consumer recycled material (PCRF) consisted of colorful pieces of diverse origin. To ensure the preparation of uniform samples (as shown in Figure 2.1), they were subjected to two extrusion processes before any characterization. In this regard, a twin-screw extruder (L/D=40) was used for sample preparation (model: Haake Rheomix OSPTW16, Thermo Fisher Scientific Inc., USA). The temperature was set at 180 °C from hopper to die and the screw rate was adjusted at 100 rpm.

To analyze the dielectric properties, the recycled materials were hot-pressed into the disc shape using a hydraulic press. The same method and conditions were used to press the samples that were composed of recycled PCRF or PCRP blended with virgin HDPE, at different ratios of 15, 30, 50, 70 and 85 wt% of recycled material. The mold thickness that was used for the dielectric measurements was approximately 300 μm. After being preheated for approximately 5 minutes, the material underwent hot-pressing for another 5 minutes at a temperature of 170 °C and a pressure of 5 MPa. Finally, the prepared samples were then cooled down to ambient

temperature while maintaining the applied pressure using circulating water. The cooling process was carried out at a rate of 10 °C /min.

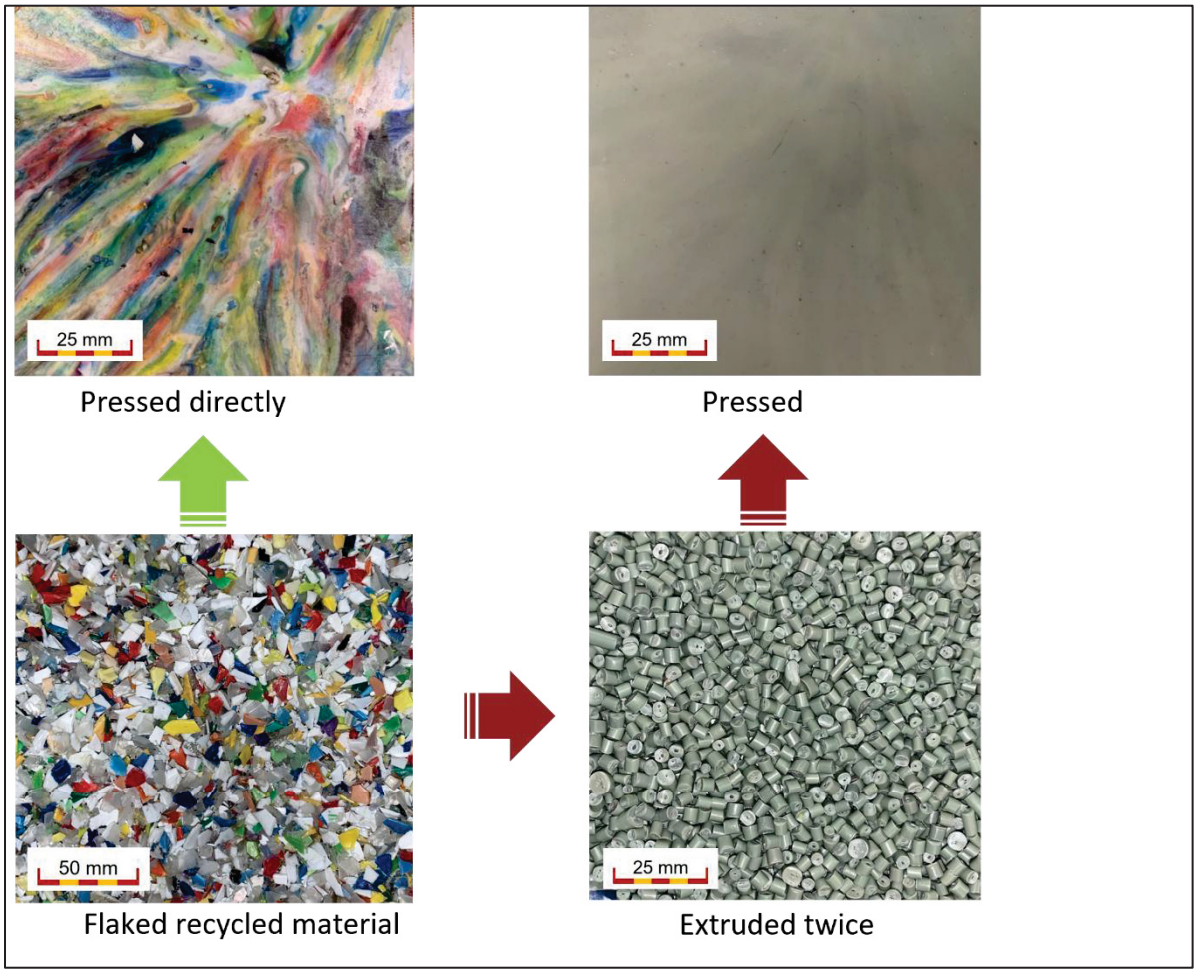

Figure 2.1 Prepared samples of flaked recycled PE, using hot-press directly or after twice extruding

2.3 Characterization

2.3.1 Chemical Properties

To analyze the organic composition of recycled materials, a Fourier transform infrared spectrometer (FT-IR, Nicolet 6700) was employed in transmission mode, over a wavenumber range of 400 to 4000 cm^{-1}. The presence of inorganic impurities was assessed by element

analysis of the surface of waste materials using SEM–energy dispersive X-ray spectroscopy (EDX) with a SEM Hitachi SU3500.

2.3.2 Thermal Characterization

Differential scanning calorimetry (DSC) model Perkin Elmer, Pyris1, USA, were used to characterize melting temperature, crystallization temperature, and degree of crystallinity. To ensure accuracy and eliminate the thermal history, the samples were heated from 70 to 170°C at a rate of 10°C/min under a nitrogen flow rate of 20 ml/min. Then cooled from 170 to 70°C at a cooling rate of 10°C/min, and finally heated again from 70 to 170°C at the same rate. The values obtained during the second heating cycle were utilized to determine the crystallization temperature, melting temperature, and degree of crystallinity. Prior to the experiments, empty pans were used to establish the baseline. The degree of crystallinity (x_c) was then determined using Equation (2.1) in accordance with ASTM D-3418 (*ASTM D-3418, Standard Test Method for Transition Annual book of ASTM,* 2015),

$$x_c = 100 \times \frac{\Delta H_m}{\Delta H_m^{\circ}} \tag{2.1}$$

where x_c is the weight fraction of the crystalline phase, ΔH_m and ΔH_m° are the fusion enthalpy of examined sample and 100% crystalline PE (293.6 J/g) respectively. The first was extracted from DSC thermograms.

A Pyris Diamond thermogravimetric analyzer (TG/DTA, PerkinElmer technology, Shelton, CT, USA) was employed to illustrate the thermal degradation of the materials and quantify the weight percentage of inorganic impurities. The analysis was performed by heating the samples from 50°C to 600°C at a heating rate of 10°C/min under a nitrogen flow of 100 ml/min. To verify the accuracy of the TGA findings, larger samples were subjected to pyrolysis at 450°C in an oven.

2.3.3 Dielectric Spectroscopy

Measurements of the dielectric response in the frequency domain were conducted using a broadband dielectric spectrometer (Novocontrol Technologies GmbH & Co. KG, Montabaur, Germany) at temperatures from 25 to 85 ºC. The measurements were isothermal and covered a frequency range of 10^{-1} to 1×10^{6} Hz. The samples were disk-shaped with a thickness of 300 μm, and a diameter of 40 mm and were positioned between two parallel plate electrodes. The thickness of electrodes was 2 mm, and the excitation voltage was set at 3 Vrms. To measure the real permittivity, a gold coating with a thickness of around 10 nm was applied to each side of the sample using a metallizer.

2.3.4 Dielectric Breakdown Strength

The Baur DTA100 device was used to perform AC short-term breakdown tests, in which samples were placed between two semispherical electrodes immersed in mineral oil. The electrodes had a diameter of 12.7mm, and the tests were conducted using the ASTM D-149 standard-method A, short-time test (*ASTM D-149, Standard Test Method for Dielectric Breakdown Voltage and Dielectric Strength of Solid Electrical Insulating Materials at Commercial Power Frequencies*, 2020) at a rate of rise of 5 kV/s and 60 Hz. Prior to the test, the mineral oil was degassed for at least two hours in a vacuum oven in order to increase its dielectric strength and reduce the likelihood of a flashover. To ensure accuracy, the surrounding medium and electrodes were periodically cleaned, and for each series of tests, a new clean and degassed oil was used. Since the thickness of the samples varied from one sample to another, measurements were adjusted to a normalized thickness of 400 μm using a power-law relationship expressed in Equation (2.2).

$$E_2 = E_1\left(\frac{d_2}{d_1}\right)^{-0.4} \tag{2.2}$$

where breakdown strength is estimated (E_2) at a reference thickness of 400 μm (d_2). E_1 is the measured breakdown strength at the actual thickness of dielectric material(d_1) (*IEEE-930, IEEE Guide for the Statistical Analysis of Electrical Insulation Breakdown Data*, 2005). In

order to take into account, the intrinsic statistical nature of dielectric breakdown, multiple samples of the same material were tested, and the resulting breakdown data were analyzed using the two-parameter Weibull distribution, as described by Equation (2.3).

$$P = 1 - \exp\left[-\frac{E}{E_0}\right]^{\beta} \quad (2.3)$$

If the electrical field is equal to or less than E, the probability of failure up to that point can be represented by the cumulative probability, denoted as P. The scale parameter, E_0, is the electrical field value at which 63.2% of the sample breakdown occurred. The shape parameter, β, indicates the scattering of data. Large values of β means that the standard deviation of the breakdown strength measurements is low. The scale and shape parameters of the distribution were calculated using the maximum likelihood method and the 95 % confidence bounds of the distribution were numerically calculated. For each material, the breakdown strength value was determined using the scale parameter, as described in literature (David et al., 2013; Helal et al., 2017). Further information on the statistical analysis of breakdown measurements can be found in IEEE-930 (*IEEE-930, IEEE Guide for the Statistical Analysis of Electrical Insulation Breakdown Data*, 2005).

2.4 Results and Discussion

2.4.1 Characterization of Contaminant of Recycled PE

In Figure 2.2, FT-IR spectra of virgin and recycled HDPE are presented, showing three main vibration modes can be identified for both recycled and virgin materials. The peaks at 2915 and 2850 cm^{-1} were corresponded to asymmetric and symmetric stretching vibrations of C-H bonds in methylene groups, respectively. Also, bending and the rocking vibration mode of C-H bonds can be identified at 1460 cm^{-1} and 720 cm^{-1} respectively (Gala et al., 2020; Heydariaraghi et al., 2016). Comparing FT-IR spectra of waste materials with virgin polyethylene revealed that both PCRF and PCRP samples were mainly composed of polyethylene, as their IR spectra were very similar. The only noticeable difference was related to the presence of a weak absorbance band at 1377 cm^{-1} in the IR spectrum of PCRF and PCRP

samples. The peak can be attributed to the symmetrical bending vibrations of C-H bonds in methyl groups and could be related to contamination with polypropylene (Gala et al., 2020; Heydariaraghi et al., 2016). Furthermore, the band at 1377 cm^{-1} can be utilized as an indicator to differentiate between different types of branched polyethylene (PE) such as LDPE, LLDPE, and HDPE. HDPE, for instance, typically displays a highest peak between 1400 and 1300 cm^{-1}, without the presence of an additional band at 1377 cm^{-1} (Gall et al., 2021).

Further analysis reveals the presence of split peaks at 720 and 1460 cm^{-1}. Figure 2.2b, illustrates two distinct in-phase and out-of-phase rocking vibrations, resulting in separate peaks at 720 and 730 cm^{-1}. This splitting phenomenon is characteristic of solid, long chain alkanes like HDPE. In contrast, a polymer like LDPE lacks this splitting due to the presence of side chains that hinder the crystallization of methylene chains by keeping them apart. Likewise, a similar split peak is observed at 1460 and 1470 cm^{-1} (Figure 2.2c), which corresponds to the crystalline structure of HDPE(Smith, 2021a).

Figure 2.3 displays the result of differential scanning calorimetry (DSC) for both virgin and recycled materials. The virgin high-density polyethylene (HDPE) and low-density polyethylene (LDPE) exhibit a solitary melting transition (T_m) at 137 and 113 °C, respectively, which is in line with what is expected for the pure resins. Melting temperature corresponding to both recycled PCRF and PCRP materials appears around 133 °C which is consistent with the fact it was identified by the recycler as mainly HDPE. No trace of a lower or higher melting peak that would indicate contamination with LDPE and PP respectively was observed. Therefore, it can be concluded that both of post-consumer recycled materials, PCRP and PCRF, are almost composed of HDPE without any significant amount of other organic impurities. This method is commonly employed to ascertain the component of polymer blends using the melt enthalpy since for blends of immiscible polyolefins each component can be distinguished based on their specific melting temperature (T_m) (Juan et al., 2021; Wong and Lam, 2002). Indeed, some researchers (Juan et al., 2021; Larsen et al., 2021; Wong and Lam, 2002) have studied the organic impurities quantitatively using enthalpy directly or the relation between the polymer mass and enthalpy.

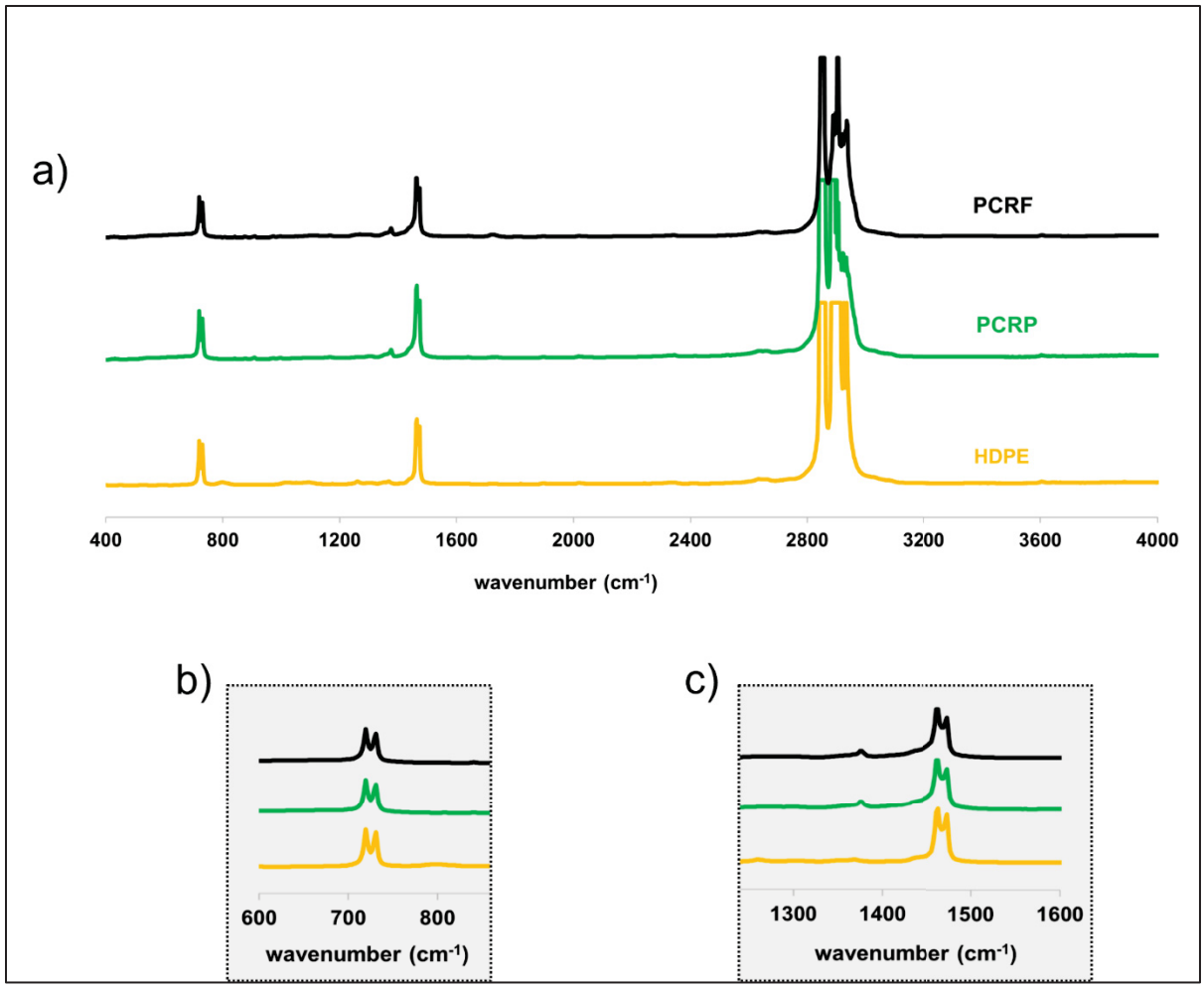

Figure 2.2 FT-IR spectra of recycled waste materials, and virgin HDPE at the spectrum range from a) 4000 to 400 cm^{-1}, b) 600 to 800cm^{-1}, and c)1300 to 1600 cm^{-1}

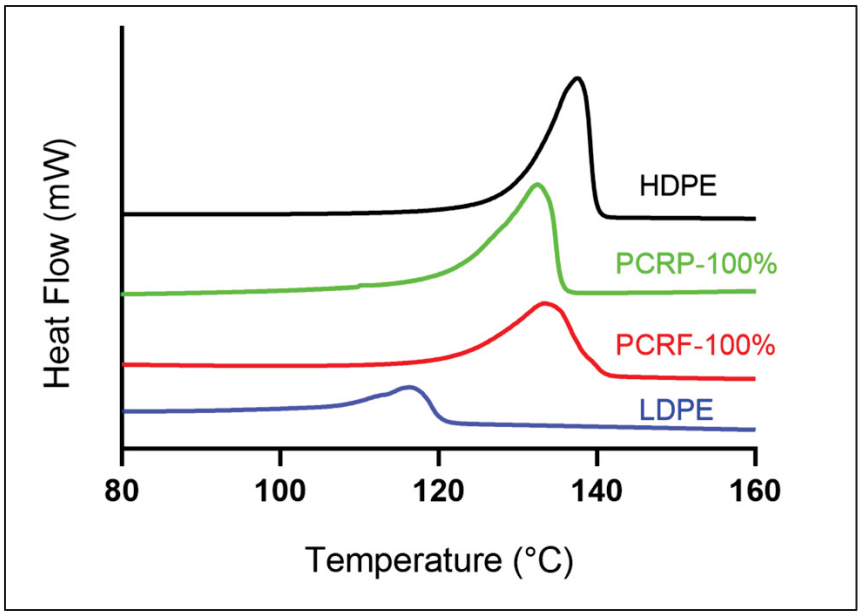

Figure 2.3 DSC curve of LDPE, PCRF-100%, PCRP-100%, and HDPE at temperatures from 80 to 160°C

SEM-EDX has been used to determine what type of inorganic impurities were present within the recycled material. The different elements which were detected with EDX are shown in Table 1. The detected elements might come from various sources. According to Table 1, Ti, Ca, Si, and Al, were the most founded elements in the waste materials. The possible source of inorganic impurities in recycled PE has been reported by other researchers (Turku et al., 2017). Soil impurities are the most possible sources for silicon (Si). Titanium could also come from components of pigments. It was reported that the components of fire retardants or catalysts used during polymerization might be another source of impurity (Turku et al., 2017). In the case of the neat HDPE, no amount of catalyst components or other types of inorganic impurities was detected from EDX. SEM-EDX map of PCRF sample can be seen in Figure 2.4. Some elements such as Ca and Si or Al and Si were detected simultaneously at the same locations, suggesting inorganic contamination with calcium silicate or aluminosilicate-type components. The confocal microscopy and SEM pictures of the PCRF sample can be seen in Figure 2.5. The presence of micro-size inorganic particles was confirmed by Figure 2.5.

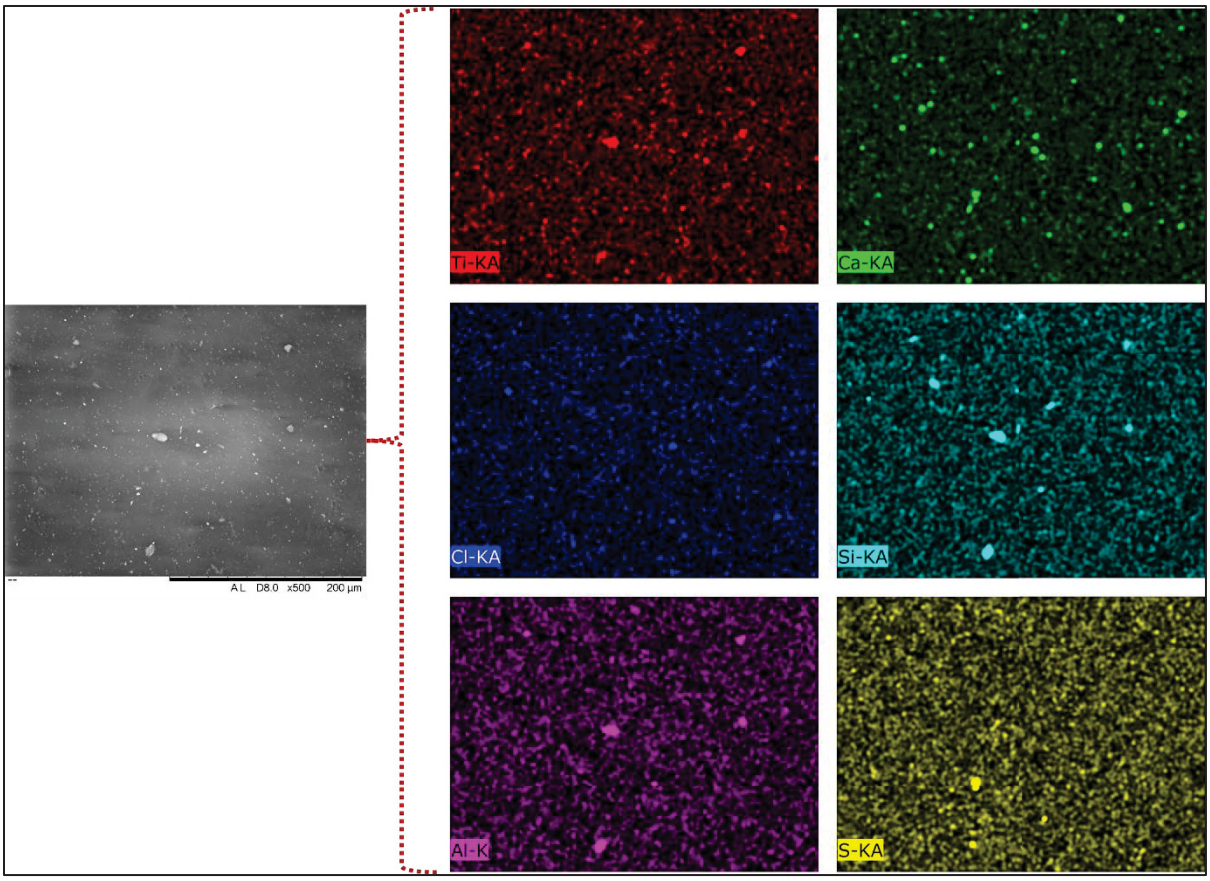

Figure 2.4 SEM-EDX map of post-consumer recycled polyethylene in flake form (PCRF)

Table 2.1 Proportions of elements (%) on the surface of virgin and recycled materials

Sample/ Element	C	O	Ti	Ca	Si	Al	S	Cl	Mg	Na	K
HDPE	98.67	1.33	-	-	-	-	-	-	-	-	-
PCRF	95.23	1.53	1.36	0.82	0.27	0.20	0.17	0.15	0.09	0.09	0.08
PCRP	94.72	1.97	0.87	0.3	2.06	0.05	-	0.02	-	-	-

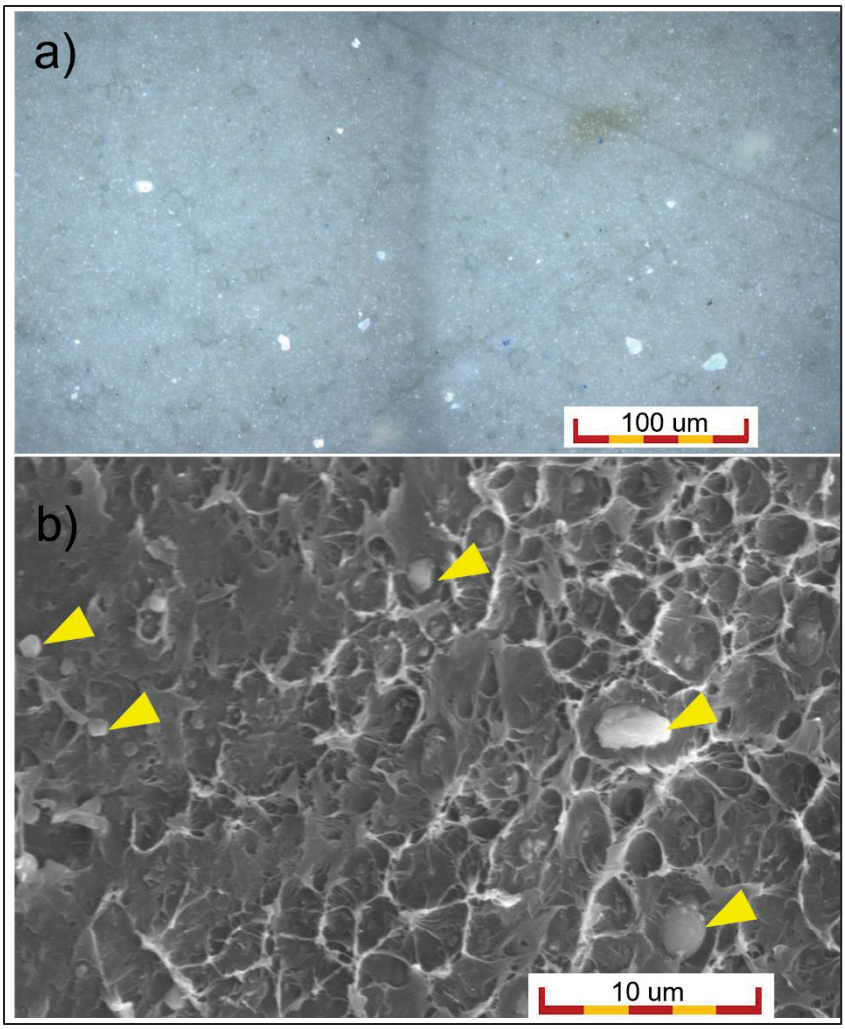

Figure 2.5 a) Confocal microscopy of the surface of recycled polyethylene in flake form (PCRF), b) Cross section of the recycled polyethylene in flake form (PCRF)

2.4.2 Thermal analysis (TGA, pyrolysis) of recycled PE

TGA curves of recycled materials, both pellet (PCRP) and flake (PCRF) form, are shown in Figure 2.6. Decomposition of recycled materials was observed to start at around 350°C. The main weight loss took place in the 400 to 500°C temperature window, which is in good agreement with what can be found elsewhere in the literature for the pyrolysis of PE (Gala et al., 2020). The remaining mass at 600 °C was found to be around 1.4 and 0.8 wt % for PCRF and PCRP samples respectively. In order to assess these values that are subjected to sample-

to-samples variation due to inaccurate estimation of impurity with TGA which arise from inhomogeneous dispersion of impurities and the inherent limitation of the technique (±0.1%), conventional pyrolysis was conducted in a pyrolysis oven on larger samples. The results showed impurity contents of 1.45 ± 0.01 wt% and 1.11 ± 0.01 wt% for PCRF and PCRP respectively. This was in relatively good agreement with both SEM-EDX and TGA measurements. Post-consumer recycled material in pellet form (PCRP) had lower levels of impurity because of the cleaning process that was performed during pelletizing process using a screen changer.

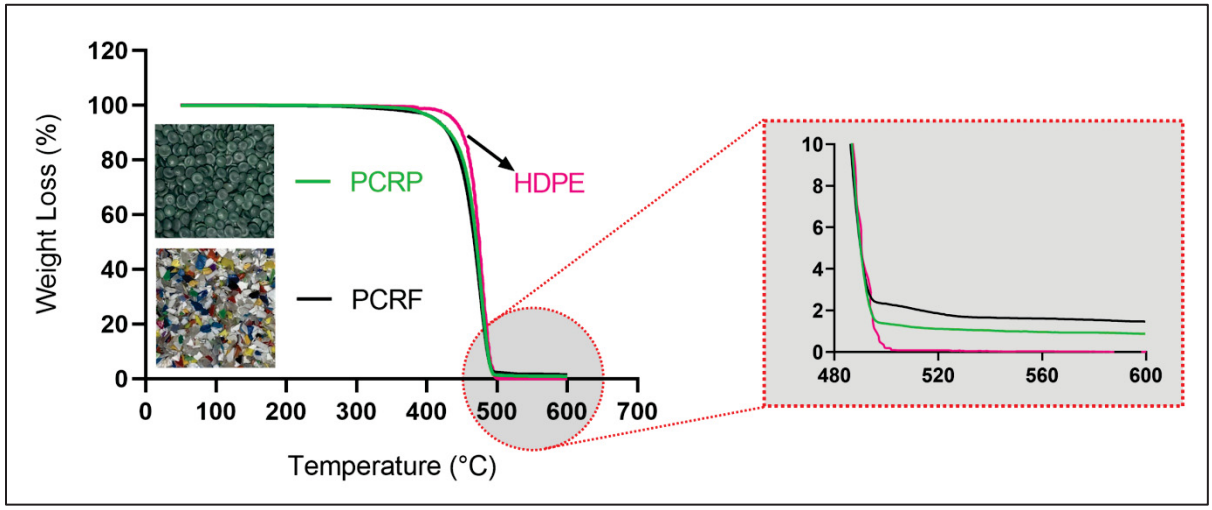

Figure 2.6 TGA curve of post-consumer recycled polyethylene in pellet (PCRP) and flake (PCRF) forms

2.4.3 Dielectric response of recycled PE

In Figure 2.7, the frequency-dependent imaginary part of permittivity of both virgin HDPE and recycled materials is presented for temperatures ranging from 25 to 85 °C. The imaginary permittivity of virgin HDPE, which is known as low-loss dielectric, was observed to be indeed very low (~10^{-4}) and remained relatively constant across the frequency range. This is indicative of a dielectric response known as flat dielectric losses (Jonscher, 1983). Actually, it can be observed that some data points were lower than the sensitivity of the measuring device, resulting in negative values (Figure 2.7c). This dielectric behavior is generally associated with

the nonpolar structure of the polymer. Furthermore, due to the inherently low dielectric losses of PE, these properties are extremely sensitive to inorganic contamination or molecular contamination to a lesser extent.

The dielectric losses of post-consumer recycled material in flake form (PCRF) are shown in Figure 2.7a. A relaxation peak was observed at low frequencies at around 1 to 10^2 Hz. It was most likely related to an interfacial polarization mechanism also known as Maxwell Wagner polarization (T. W. Dakin, 2006). It comes from either accumulation of ionic carriers at the polymer/electrode interfaces, a mechanism called electrode polarization, or at the contaminant particles/polymer interfaces that are distributed in the bulk of the sample. The bulk interfacial polarization observed in composites is primarily attributed to differences in the electrical conductivity of its constituents. As shown in Figure 2.7a, the relaxation peak shifts to higher frequencies with increasing temperature, which is likely due to an increase in the conductivity of either the ionic impurities or the second phase of micro scale impurities. The later explanation is more likely and is in agreement with the previous research on the frequency-domain dielectric response of low concentration of metallic oxide-filled polyethylene (F. Ciuprina et al., 2010). The dielectric response may either exhibit a relaxation peak that moves to higher frequencies with increasing temperature (as in Figure 2.7a), or simply an increase of the dielectric losses towards low frequencies, known as low frequency dispersion phenomena, without a designable relaxation peak (Jonscher, 1991) (as in Figure 2.7b), or a combination of both phenomena. The type of response exhibited is dependent on the chemical nature, the size and the concentration of the filler. In the case of hydrophilic impurities, moisture absorption was also found to play a significant role in the frequency position of the relaxation peak (Couderc Hugues et al., 2014). No similar relaxation peak was observed in dielectric loss spectrum of PCRP, because of lower content of impurity that did not lead to an obvious phase separation (Figure 2.7b). Furthermore, the cleaning process has removed the larger particles that are the most likely to cause Maxwell-Wagner polarization. Indeed, there is some agreement in the literature that the decrease of size of inorganic particles inside polyethylene can lead to the suppression of the interfacial relaxation process, particularly in the case of nano-composites (M. Roy et al., 2005). Figure 2.7b shows an increase in dielectric loss at low frequencies with rising temperatures. This can be explained by the influence of pure dc-

conductivity or charge fluctuations resulting from low-frequency dispersion. Typically, it is a combination of both factors (I. Shirzaei Sani et al., 2021). This behavior was also observed for nanofillers (F. Ciuprina et al., 2010). At the two highest temperatures, there was a small loss peak indicating some accumulation of charge carriers at the microstructure boundaries or at the electrode interfaces.

Dielectric loss of virgin HDPE, PCRF, and PCRP were compared to each other at room temperature over a frequency range of 10^{-1} to 1×10^{6} Hz (Figure 2.7d). It was observed that the recycled materials, in both flake and pellet form, exhibited greater dielectric losses compared to virgin PE, especially at low frequencies. At 10^{-1} Hz, the dielectric loss of virgin HDPE, PCRP, and PCRF were found to be 0.86×10^{-3}, 5.8×10^{-3} and 9.8×10^{-3}, respectively. Similarly, at power frequency (60 Hz), the dielectric loss of virgin HDPE, PCRP, and PCRF were 0.12×10^{-3}, 0.7×10^{-3}, and 2.1×10^{-3}, respectively. The higher dielectric losses observed in the recycled materials were most likely attributed to the presence of inorganic impurities.

In addition to inorganic impurities, molecular impurities such as additives, polymer-degrading substances like alkanes and alkenes, and residual product residues, can significantly impact the dielectric properties of materials, particularly in the case of recycled materials that hold higher value compared to virgin materials. The extent of molecular impurities present in recycled materials varies depending on the quality of sorting and recycling procedures employed. For instance, Mallari et al.(Mylläri et al., 2016) conducted simulations involving the use of detergent in the washing process of recycling and observed higher levels of volatile content in the recycled material compared to the virgin material without washing process. Although molecular impurities have a greater impact on the properties of recycled materials compared to virgin materials, their effects are less significant than that of inorganic impurities due to the incomparable size and content. From the other side, although organic impurities make up a few content of the total composition of studied recycled material, rendering them undetectable through techniques like DSC, they still have the potential to influence the properties of recycled materials, as demonstrated in other studies focusing on mechanical properties (Gall et al., 2021; Karaagac et al., 2021; Thoden van Velzen et al., 2021). Similar considerations can be envisioned for dielectric properties (Mylläri et al., 2016).

The real part of the complex permittivity is affected by polarization mechanisms at low frequencies, as expected due to the mathematical interconnection (known as the Kramers-Kronig relations) linking dielectric loss and dielectric constant. Isothermal curves of the real permittivity versus frequency for temperatures ranging from 25°C to 85°C were plotted in Figure 8 for both virgin and recycled HDPE, showing a dielectric constant between 2.4 and 2.6 that decreased with increasing temperature. This is due to the changes in density predicted by the Clausius–Mossotti equation (G and Hauver, 2014). The dielectric constant was also relatively frequency-independent because of the non-polar nature of polyethylene which is consistent with previous reports for PE (Eesaee et al., 2020). Figure 2.8b shows the isothermal curve of PCRF as a function of frequency for temperatures ranging from 25 to 85 ^{o}C. At high frequencies, the curves were similar to the virgin HDPE, but at low frequencies, significant discrepancy was found due to the contribution of charge carrier fluctuation to the overall polarization. Indeed, The real and imaginary parts of the permittivity were affected by phenomena such as Maxwell-Wagner polarization, electrode polarization, and low-frequency dispersion, unlike pure dc conductivity, which only affects the imaginary part, as reported in previous literature (Kremer and Schönhals, 2003).

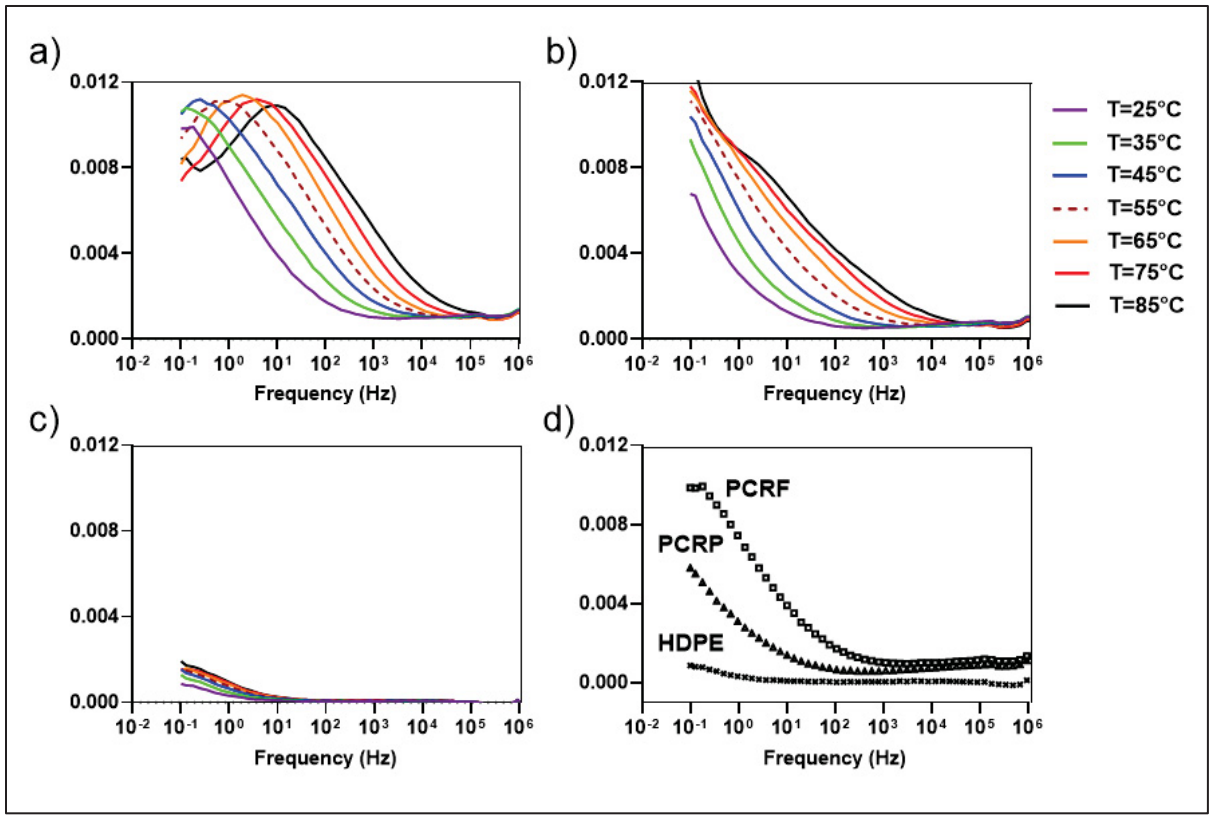

Figure 2.7 Dielectric loss of a) Recycled polymer in flake form (PCRF), b) Recycled polymer in pellet form (PCRP), c) Virgin HDPE, at temperatures from 25 to 85 °C; and d) Comparison of dielectric loss of recycled polymer with pure polymer at 25 °C

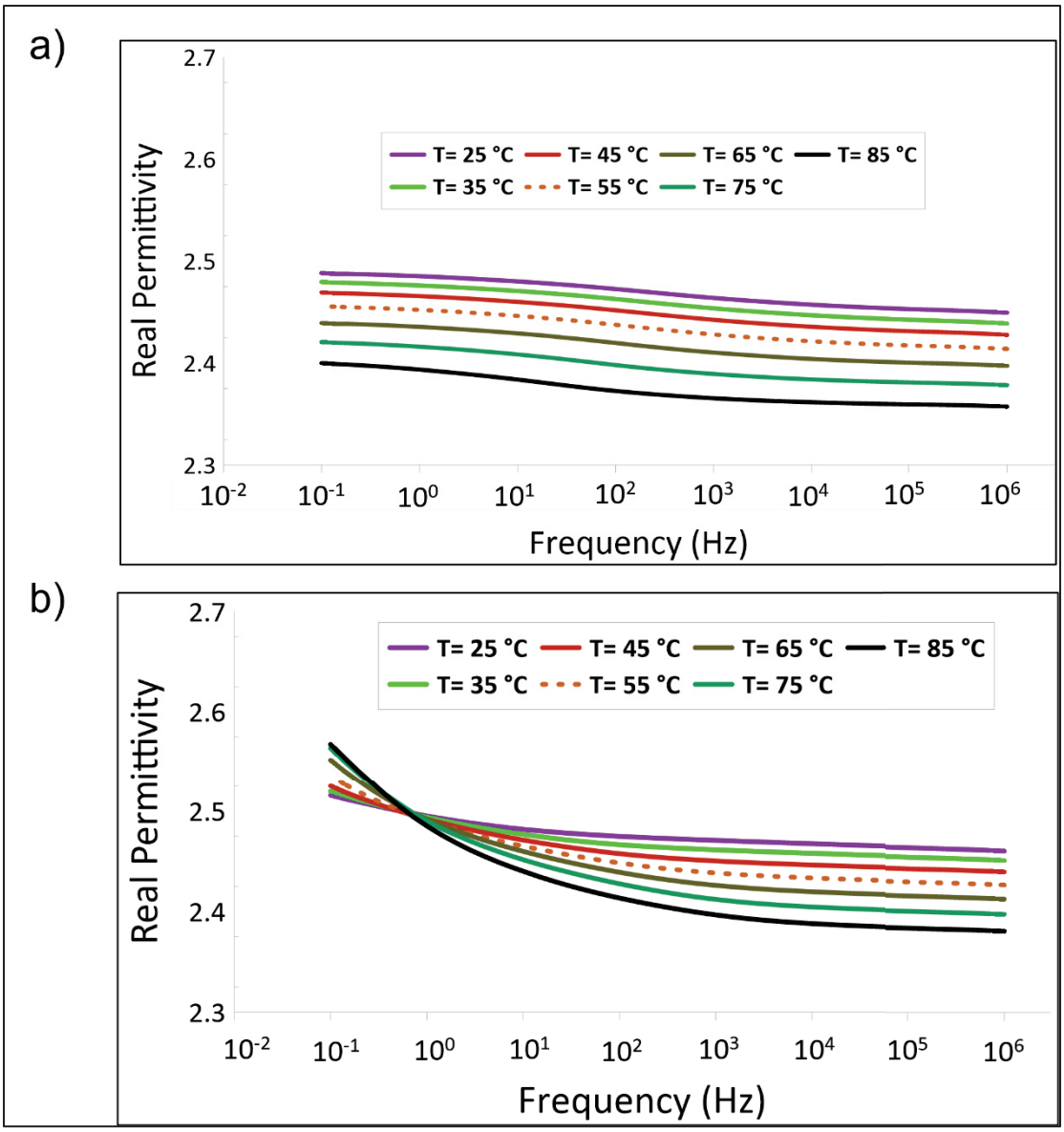

Figure 2.8 Dielectric constant of a) virgin polyethylene and b) recycled polyethylene (PCRF) at temperatures from 25 °C to 85 °C

Electrical breakdown is defined by a sudden dielectric failure of an insulation material which normally leads to carbonized puncturing of polymers. Different processes, mainly mechanical, thermal, and electronic can lead to electrical breakdown but it usually starts from defect, either

of void or an impurity within the insulation bulk. In any case, it is characterized by a failure that occurs rapidly at only one place and it is an irreversible and destructive event in solid materials (J. C. Fothergill, 2007).

Figure 2.9 displays the cumulative probability of failure for virgin HDPE compared with recycled materials as a function of the AC electrical field (RMS values). The two-parameter Weibull distribution was employed to calculate the cumulative probability of failure for the straight lines depicted in Figure 2.9, using the maximum likelihood technique. Meanwhile, the curve lines represent the 95% confidence bounds for each distribution. The scale parameter of the distribution was used as the characteristic breakdown strength for each material. The breakdown strength was found to be slightly lower for the two recycled materials than virgin HDPE with values of 128 kV/mm, 115 kV/mm, and 121 kV/mm, for HDPE, PCRF and PCRP respectively. The influence of inorganic particles within polyethylene on its breakdown strength is still not clear in the literature where it's possible to find a lot of contradictory results. However, there is some consensus (David et al., 2013; Eesaee et al., 2018) that the addition of nano-sized, well dispersed fillers leads to increase in breakdown strength over the base resin while in the case of micro-sized the effect is the opposite. In addition, there are many factors affecting the breakdown strength of filled polymers such as filler content, chemistry and size, matrix properties and type of applied voltage type (S. Li et al., 2010). In the case of filler content, below a certain value which is around 10 wt%, nano-fillers can affect breakdown strength positively (S. Li et al., 2010). On the other hand, the inclusion of micro-fillers usually leads to lower breakdown strength, when the short-term procedure is used to monitor the breakdown strength, at any concentration despite providing an higher resistance to partial discharge (Z. Li et al., 2011). In the case of our recycled material, particularly the PCRF material, the impurities were sometimes so large that they were clearly visible by naked-eye. There are several reports on the effect of filler size and concentration on breakdown strength (Mansour et al., 2021; S. Li et al., 2010; Tan, 2020) which in general leads to the conclusion that the breakdown strength of micro-size composites is similar or lower than the neat matrix (S. Li et al., 2010), while nano-composites can enhance the breakdown strength of matrix. Therefore, it can be concluded that the large size of impurities has detrimental effect on dielectric properties of the tested recycled materials. Moreover, changes in the structure of

polymer matrix during the processing is another factor that can affect the breakdown strength of recycled material due to some possible breaking of chemical bonds. Oxidation, cracking or cross-linking could also play a role since they all lead to the creation of carrier traps that can potentially capture electrical charges which disturb the electrical field.

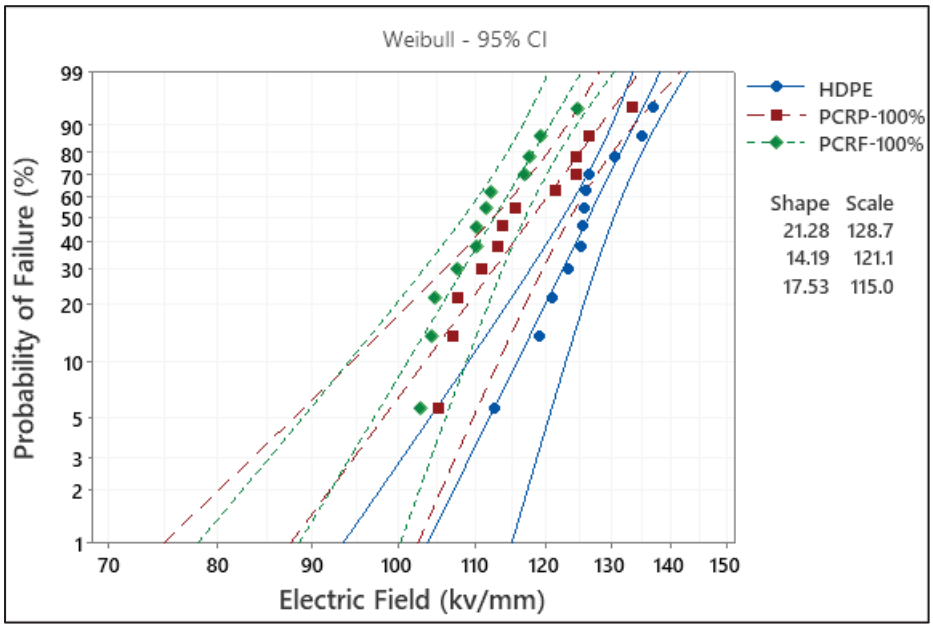

Figure 2.9 Breakdown strength of virgin PE, post-consumer recycled material in flake form (PCRF), and pellet form (PCRP)

2.4.4 Blending

The dielectric properties of the recycled PE were analyzed in the preceding section. As previously noted, these properties were found to be inferior to those of virgin PE. Therefore, to overcome the drawback of recycled PE properties, blending was used as a strategy. To prepare blend samples, flake and pellet forms of recycled material were blended with virgin HDPE. The composition of all prepared samples is listed in Table 2.

Table 2.2 Composition of blended recycled material, in flake (PCRF) or pellet (PCRP) form, with virgin HDPE

Sample	Weight percentage of virgin HDPE (%)	Weight percentage of flake form of recycled material- PCRF (%)	Weight percentage of pellet form of recycled material- PCRP (%)
HDPE	100	0	0
PCRP-100%	0	0	100
PCRP-85%	15	0	85
PCRP-70%	30	0	70
PCRP-50%	50	0	50
PCRP-30%	70	0	30
PCRP-15%	85	0	15
PCRF-100%	0	100	0
PCRF-85%	15	85	0
PCRF-70%	30	70	0
PCRF-50%	50	50	0
PCRF-30%	70	30	0
PCRF-15%	85	15	0

2.4.4.1 Thermal Analysis

Table 3 presents the degree of crystallinity, crystallization temperature, and melting temperature for different blends of virgin HDPE and post-consumer recycled materials. It was observed that the degree of crystallinity decreased as the proportion of recycled material increased in both PCRP and PCRF blends. For instance, the degree of crystallinity decreased from 70% to 58% for 100% virgin HDPE and to 100% recycled material. Similarly, the crystallinity of PCRF-50% and PCRP-50% which contains 50% of recycled material yielded intermediate values, 64% and 68% respectively. The same trend was observed for the melting temperature.

In addition to the nature of the polymer, the amount of impurities might affect the crystallinity of recycled polymers. Some reports suggested that at low filler loadings, the crystallinity increases, but decreases at higher filler loadings (Chen et al., 2018) which implies that there is a range of filler content leading to a maximum value of crystallinity. The simplest explanation would be that at low concentration impurities can act as nucleating agents and thus facilitate the crystallization process, while at higher concentrations, particularly above the rheological percolation threshold, the dominating effect is the increase of viscosity and the reduction of chain mobility leading to a decrease of crystallinity. Therefore, in the presence of impurity, according to concentration, the crystallinity may increase or decrease. However, here, the difference of crystallinity between neat and recycled materials is mainly due to the different grade of PE, and impurities not likely to play a significant role.

Table 2.3 Thermal properties of blended recycled materials calculated by DSC result

Polymer blend	**Degree of crystallinity (%)**	**Melting temperature (°C)**	**Crystallization temperature (°C)**	**Polymer blend**	**Degree of crystallinity (%)**	**Melting temperature (°C)**	**Crystallization temperature (°C)**
HDPE	70	137	118	-	-	-	-
PCRF-30%	68	136	120	PCRP-30%	70	134	118
PCRF-50%	64	136	120	PCRP-50%	68	135	118
PCRF-70%	63	135	120	PCRP-70%	64	135	117
PCRF-100%	58	133	118	PCRP-100%	58	133	117

2.4.4.2 Dielectric Response of Blend

Based on the results shown previously, the use of unmodified post-consumer materials in electrical insulation industry appears to be limited to unshielded or low voltage cables due to the high electrical loss that would be detrimental for AC shielded cables such as distribution or transmission cables (medium to high voltage). To decrease dielectric loss, a strategy could be blending recycled polymers with pure HDPE at different ratios. This strategy will decrease the impurity density and consequently lead to a decrease of dielectric loss.

Indeed, a significant decrease of dielectric losses for both PCRP and PCRF was observed when virgin HDPE was added, particularly at low frequencies (Figure 2.10) but also at power frequency (60 Hz) for which a decrease of about 50 % and 60 % of the losses was found for PCRP/HDPE and PCRF/HDPE blends respectively when an equal percentage of virgin and recycled material were blended. The dielectric loss of virgin HDPE that was extruded twice (HDPE-ext2) demonstrated that extrusion process to prepare sample doesn't significantly affect the dielectric properties.

Figure 2.11 illustrates the Weibull distributions of the breakdown data for virgin HDPE when blended with the recycled material, and Table 4 provides the scale and shape parameters for each sample. A slight increase in breakdown strength of recycled material by adding virgin HDPE was observed but the confidence bounds of the estimator for the scale parameter of the Weibull distribution were found to overlap for most of the data. Therefore, it can only be concluded that the general trend observed when the concentration of impurities is reduced by blending is the increase of AC breakdown strength. Similar behavior was observed by Cruz et al. (Cruz and Zanin, 2004; S. A. Cruz and M. Zanin, 2004), when higher concentrations of recycled material led to decreased performance and increased presence of conductive impurities. A decrease of 17% in breakdown strength was reported when using 100% recycled HDPE in comparison with virgin HDPE (Table 4). This value is around 10% when recycled PCRF was compared to virgin HDPE, can be related to the different experimental conditions and also different sources of recycled materials.

Since recycled materials could be viewed as composites with a low concentration of fillers, it could be helpful to understand the breakdown mechanism of polymer composites in order to understand their behavior. Generally, there are two main mechanisms to explain the breakdown strength of polymer composites. The first mechanism places emphasis on the role of particles and particle/polymer interfaces, which act as barriers to prevent the growth of discharge channels (S. Alapati and M. J. Thomas, 2012). The second mechanism highlights the significance of deep traps in capturing charge carriers, thereby decreasing their mobility and energy. Both are relevant to the total surface area and weight percentage of nanoparticles. Above a critical weight percentage of nanoparticles, the breakdown strength is decreased. It is generally attributed to the effect of particle distribution and agglomeration. At low concentration of nanoparticles, multiple trapping sites are introduced to charge carriers which increases breakdown strength consequently. The particles usually start to agglomerate at higher concentrations, so the overlapping interfacial regions can change the transport path of charge carriers, and subsequently increase the material conductivity and reduce the breakdown strength. In the tested recycled blends, the impurities can provide a short path of charge carriers which leads to low breakdown strength. Therefore, because of the dilution effect of blending, the blended samples tend to have a high breakdown strength.

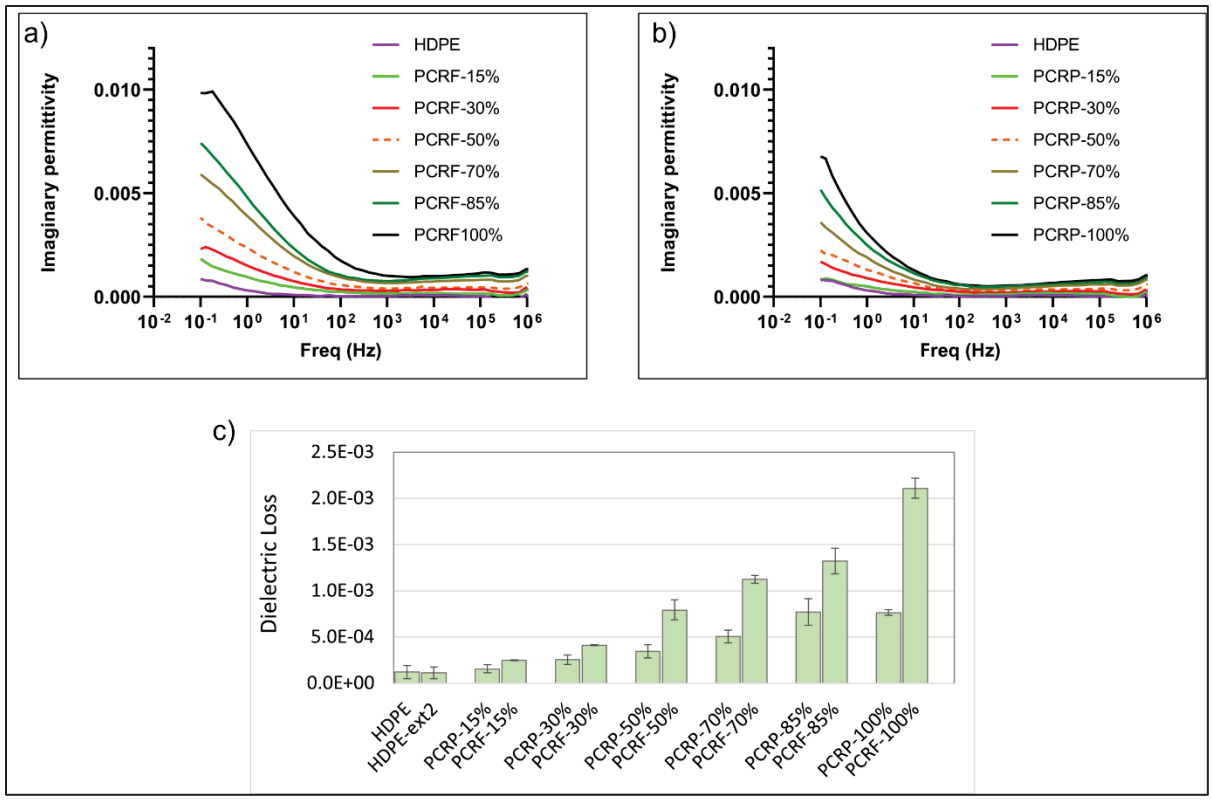

Figure 2.10 Dielectric loss post-consumer recycled material blended with virgin polyethylene at various concentration of recycled material at 25 °C, a) PCRF/HDPE, b) PCRP/HDPE at a range of frequencies from 10^{-1} to 10^{6} Hz, c) PCRF/HDPE and PCRP/HDPE at fixed power frequency (60 Hz)

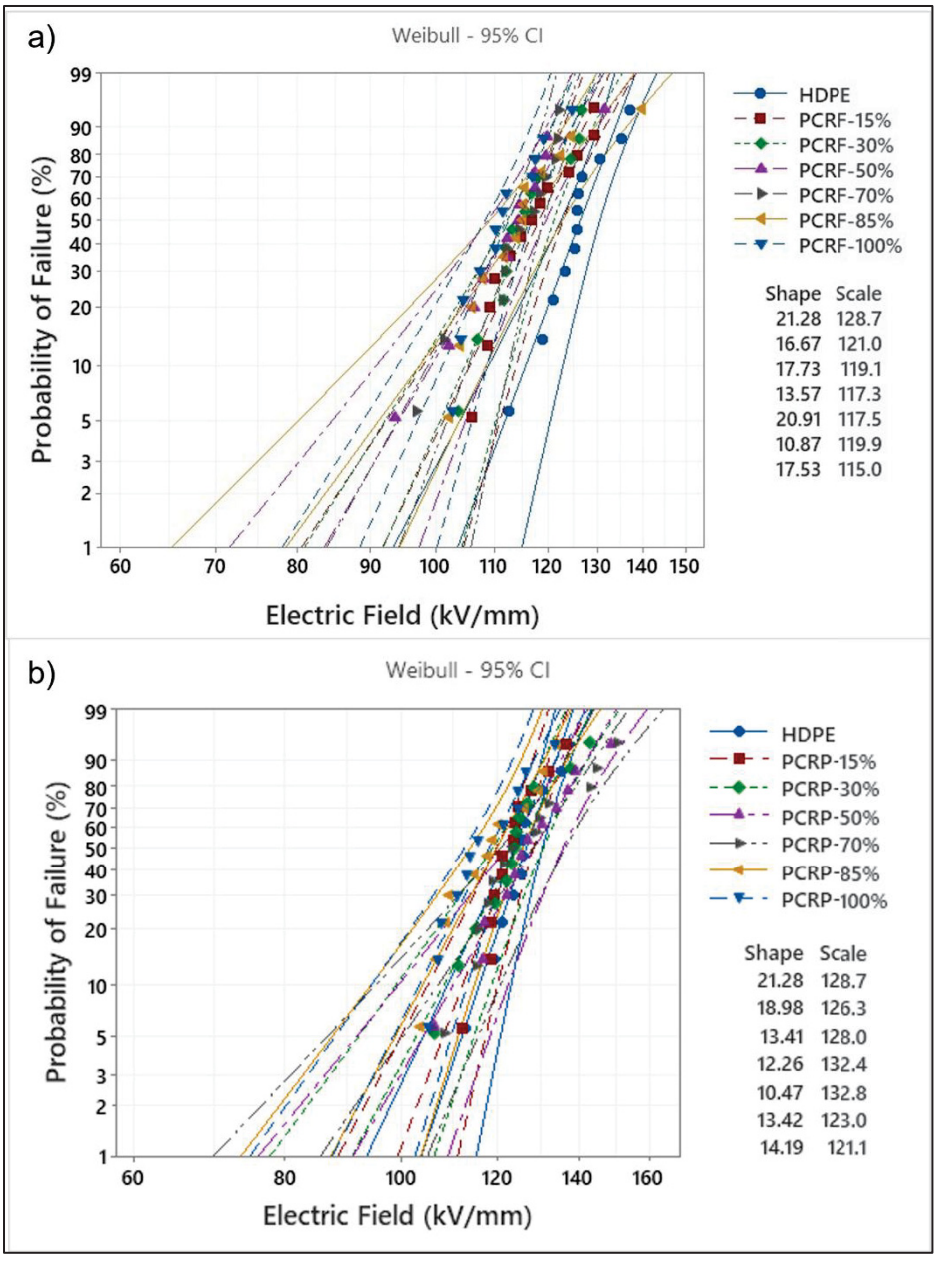

Figure 2.11 Breakdown strength of post-consumer recycled material blended with virgin PE; a) flake form (PCRF) and b) pellet form (PCRP), at different concentrations. The samples have been named with the percentage of recycled materials

Table 2.4 Weibull parameters for AC breakdown strength of HDPE/ Recycled polymers (PCRF, PCRP)

	Scale parameter (E_{Br})-kV/mm	**Shape parameter**		**Scale parameter (E_{Br})-kV/mm**	**Shape parameter**
HDPE	128	21	-	-	-
PCRF-15%	121	16	PCRP-15%	126	19
PCRF-30%	119	17	PCRP-30%	128	13
PCRF-50%	117	13	PCRP-50%	132	12
PCRF-70%	117	20	PCRP-70%	132	10
PCRF-85%	119	10	PCRP-85%	123	13
PCRF-100%	115	17	PCRP-100%	121	14

2.5 Conclusion

The dielectric properties of recycled HDPE were investigated. Thermal and chemical characterization was used to assess any possible organic (such as mixed stream) or inorganic impurities within the provided waste stream of HDPE. The results showed no significant amount of mixed plastic but some content of inorganic impurities, about 1.5 wt% and 1.0 wt% for two different grades of recycle PE. In both cases, it was observed that the high level of

impurities had a significant adverse impact on the dielectric properties of the recycled material. The level of impurity was found to be sufficiently high that it caused a considerable increase in dielectric losses for recycled polyethylene when compared to virgin HDPE. Although the real part of permittivity remained almost constant for both recycled materials and virgin PE across the measured frequency range, the imaginary part of the permittivity of recycled material was higher at low frequencies by about an order of magnitude, exhibiting an interfacial relaxation peak.

Additionally, breakdown strength was also influenced by contamination, but the effect was less pronounced compared to that observed in the dielectric response. The general trend was that higher values of contamination led to lower breakdown strength.

To overcome the decrease of the dielectric properties, blending was used as a strategy to partially restore the material properties. It was indeed shown that blending can significantly improve the dielectric property of recycled material whereas a 50% decrease in dielectric loss was observed when 50% of virgin material was added. Consequently, the result showed that recycled material blended with virgin HDPE can be a good candidate with satisfactory properties for most cables & wires applications, including low voltage or medium voltage cables.

CHAPTER 3

ENHANCING THE DIELECTRIC PROPERTIES OF RECYCLED POLYOLEFIN STREAMS THROUGH BLENDING

Iman Shirzaei Sani [a], Nicole R. Demarquette [b], Eric David [c]

[a,b,c] Department of Mechanical Engineering, École de Technologie Supérieure, 1100 Notre-Dame West, Montreal, Quebec, Canada H3C 1K3

Paper published in *Sustainability journal*, May 2025
DOI: 10.3390/su17094123

Chapter Outline: Chapter 3 explores the dielectric, thermal, and chemical properties of recycled HDPE and HDPE/PP blends. The chapter begins with an abstract and introduction that highlight the challenges of polyolefin waste, the limitations of recycled materials, and the motivation for blending with virgin polyethylene. Then the methods used for chemical, thermal, and dielectric analysis were discussed. The results and discussion show that blending recycled materials with virgin HDPE improves their dielectric behavior. The chapter concludes by emphasizing blending as both a sustainable solution and a practical approach to enhance the electrical performance of recycled polyolefins for insulation applications.

Abstract: The extensive use of polyolefins, such as polyethylene (PE) and polypropylene (PP), has led to a substantial accumulation of plastic waste, raising growing concerns about environmental impact and sustainability. In this study, the dielectric, thermal, and chemical properties of recycled materials were investigated, and blending with virgin polyethylene was examined as a sustainable strategy to enhance their electrical performance and promote material reuse. Dielectric analysis demonstrated that blending recycled materials with virgin polyethylene effectively reduced dielectric losses. With the addition of only 15% virgin HDPE, the dielectric loss was significantly lowered by 40% for recycled HDPE (rHDPE) and 30% for the recycled PE-PP blend (r(PE-PP))—compared to their unblended forms. Although the original recycled materials exhibited much higher dielectric losses than virgin HDPE—24 and

28 times greater for rHDPE and r(PE-PP), respectively, at 60 Hz—the blending approach clearly improved their electrical behavior. Overall, the results highlight blending as a practical and sustainable strategy to improve the dielectric performance of recycled polyolefins, enabling their reuse in applications such as electrical cable insulation while contributing to plastic waste reduction.

Keywords: recycled polyolefins; sustainable materials; plastic waste; dielectric properties; polymer blends; polyethylene; circular economy

3.1 Introduction

Polyolefins, such as polyethylene (PE) and polypropylene (PP), are widely used as dielectric insulating materials due to their excellent electrical insulating properties, chemical stability, low cost, and processability suitable with the cable industry. Dielectric insulation is a crucial component in various electrical and electronic devices, including transformers, capacitors, and cables. The low dielectric constant and low dielectric loss of polyolefins also make them suitable for use in high-frequency applications (Geyer et al., n.d.; Jambeck et al., 2015).

Despite the significant advantages of polyolefins, the increasing global demand for plastics has led to a significant rise in the generation of plastic waste, resulting in considerable environmental challenges. Addressing this issue requires innovative approaches, particularly through the reuse and recycling of plastic waste. Utilizing recycled polyolefins in dielectric applications is a promising solution that not only improves the environmental burden of plastic waste but also conserves natural resources and mitigates the greenhouse gas emissions associated with producing virgin materials (Geyer et al., n.d.).

One strategy for improving the properties of recycled polyolefins is to blend them with virgin polyolefins, such as virgin high-density polyethylene (HDPE) (Cecon et al., 2021; X. Huang et al., 2019). The blending of recycled polyolefins with virgin materials enhances the mechanical and thermal properties of recycled polyolefins (Jones et al., 2023; Yin et al., 2015; Zhang et al., 2023). In addition, blending can also improve their dielectric properties, making them more attractive for use in electric and electronic applications (X. Huang et al., 2019). Previous studies have investigated different properties of recycled materials, including their

mechanical and photodegradation behavior (Sultana et al., 2024a, 2023). However, their electrical performance, specifically dielectric and thermal properties, needs further exploration.

In this study, we investigated the possibility of using recycled materials in the electrical cable industry for low- to high-voltage applications as a continuation of our previous study referenced in (Shirzaei Sani et al., 2023). The dielectric, thermal, and chemical properties of recycled materials were characterized, along with the effect of impurities on these properties. Furthermore, we studied how blending recycled materials with virgin materials could improve their dielectric properties, with the goal of addressing the challenges associated with using waste material.

In summary, the significance of this study is the investigation of the dielectric properties of recycled materials and, secondly, enhancing the properties of recycled materials through blending.

3.2 Materials and Methods

3.2.1 Materials

There were two different waste materials. The first waste material was high-density polyethylene supplied in flake form with a melt flow index (MFI) of 0.60 g/10 min measured at 190 °C. The second waste material was a mix of polyethylene and polypropylene provided by the supplier (MFI ≥ 4), with the reported PP content ranging from 45 wt% to 55 wt%. Both recycled materials sourced from local recyclers in Quebec come from post-consumer recycled streams.

For the virgin material, high-density polyethylene (HDPE) with a density of 0.952 g/cm^3 and MFI of 6.8 g/10 min (at 190 °C under 2.16 kg load) was supplied from Dow in pellet form.

3.2.2 Sample Preparation

A twin-screw extruder with a length-to-diameter ratio of 40 was utilized to blend waste material with virgin HDPE. The temperature was set at 200 °C from the hopper to the die, while the screw rate was set at 100 rpm. The recycled and blended materials were hot-pressed into disk-shaped samples using a hydraulic press for the purpose of analyzing their dielectric properties. The proportion of recycled material in the blend was 15%, 30%, 50%, 70%, and 85% wt. The blending process was repeated twice to ensure adequate mixing. The thickness of the samples for broadband dielectric spectroscopy measurements was around 300 μm, while a mold with 500 μm thickness was used for dielectric breakdown strength testing. In preparation, a preheating step of 5 min was carried out, followed by hot-pressing at 175 °C for another 5 min under a pressure of 10 MPa. The samples were then cooled under constant pressure with circulating water at a rate of 10 °C per minute until they reached an ambient temperature.

3.2.3 Characterization

3.2.3.1 Chemical Characterization

The chemical composition of the recycled materials was determined using Fourier Transform Infrared Spectroscopy (FT-IR) in transmission mode, with a wavenumber range from 400 to 4000 cm^{-1}, using a Nicolet 6700 FT-IR Spectrometer (manufactured by Thermo Fisher Scientific Inc, Waltham, USA). The content of inorganic impurities was analyzed on the surface of waste materials using SEM-EDX (Scanning Electron Microscopy Energy-Dispersive X-ray Spectroscopy), which was performed using a Hi tachi SU3500 SEM, manufactured by Hitachi Science Systems, Ltd., Tokyo, Japan.

3.2.3.2 Thermal Characterization

Thermogravimetric analysis (TGA) was performed using a Pyris Diamond model from PerkinElmer technology (TG/DTA, Shelton, CT, USA) to examine the thermal degradation of

the material and measure the weight quantity of inorganic impurities. The samples were heated under a nitrogen atmosphere with a flow rate of 100 mL/min from 50 °C to 600 °C with a heating rate of 10 °C/min. To verify the TGA results, pyrolysis was performed on larger samples in an oven at 450 °C.

Differential scanning calorimetry (DSC) using a Perk in Elmer, Pyris1 (Shelton, USA), was used to determine the degree of crystallinity, melting temperature, and crystallization temperature of the samples. The samples were first heated from 70 °C to 180 °C with a heating rate of 10 °C/min under a nitrogen flow rate of 20 mL/min to eliminate any thermal history of the material. Then, they were cooled from 180 °C to 70 °C at a cooling rate of 10 °C/min, followed by a second heating cycle from 70 °C to 180 °C at a rate of 10 °C/min. The results from the second heating cycle were used for calculation purposes. The degree of crystallinity (X_c) was calculated using Equation (3.1), according to ASTM D-3418 (*ASTM D-3418, Standard Test Method for Transition Annual book of ASTM,* 2015),

$$X_c = 100 \times \frac{\Delta H_m}{\Delta H_m^\circ} \tag{3.1}$$

where X_c is the weight fraction of the crystalline phase, ΔH_m° is the fusion enthalpy of 100% crystalline PE (293.6 J/g), and ΔH_m is the fusion enthalpy of the sample extracted from DSC thermograms.

3.2.3.3 Dielectric Response

Dielectric response measurements were performed in the frequency domain using a broadband dielectric spectrometer (Novocontrol Technologies GmbH & Co. KG, Montabaur, Germany). The samples used were disk-shaped with a thickness of 300 μm and a diameter of 30 mm and were placed between two parallel plate electrodes with a thickness of 2 mm. The spectrometer was set to apply a 3 Vrms excitation voltage.

The measurements were conducted using three different strategies in order to investigate the dielectric response of the materials in detail. The three different strategies are as follows:

(1) The dielectric response was assessed at various temperatures ranging from 25 °C to 95 °C across a frequency spectrum from 10^{-1} to 10^{6} Hz with steps of 10 °C between each isothermal scan, with the measuring chamber continuously purged with dry nitrogen. After reaching the highest temperature, the sample cooled down to 25 °C, and the dielectric spectrum was measured again in order to examine the effect of the heating process on the dielectric response.

(2) The samples were kept at a constant temperature of 70 °C, and the dielectric response was measured every 10 min to analyze the effect of high temperature on dielectric response.

(3) The samples were subjected to heating and cooling cycles between 25 °C and 70 °C to mitigate the limits of evaluating the dielectric response at higher temperatures observed in the previous step. In each cycle, the sample was held at 70 °C for 10 min, then cooled back to 25 °C before measurements were performed at this temperature.to mitigate the limits of evaluating the dielectric response at higher temperatures observed in the previous step. In each cycle, the sample was held at 70 °C for 10 min, then cooled back to 25 °C before measurements were performed at this temperature.

3.2.3.4 Dielectric Breakdown Strength

AC short-term breakdown tests were performed using a Baur DTA100 device, manufactured by BAUR GmbH, Sulz, Austria. The samples were positioned between two 4 mm diameter ball-shaped electrodes, surrounded by mineral oil as the insulating medium. The tests followed the ASTM D-149 method A (*ASTM D-149, Standard Test Method for Dielectric Breakdown Voltage and Dielectric Strength of Solid Electrical Insulating Materials at Commercial Power Frequencies*, 2020), with a voltage increase rate of 2 kV/s and frequency of 60 Hz. The mineral oil was degassed for a minimum of two hours in a vacuum oven to increase its dielectric strength and decrease the risk of flashovers. The surrounding oil was replaced periodically with new, clean, and degassed mineral oil to avoid any failure caused by oil impurities.

The electrodes were cleaned when the oil was refreshed to maintain accuracy. To account for variations in sample thickness, the measurements were adjusted to a standard thickness of 400 μm. The estimated breakdown strength (E_2) at a thickness of 400 μm was calculated using the

power–law relationship in Equation (3.1), where E_1 is the measured breakdown strength at the actual thickness (d_1), and d_2 has a standardized thickness of 400 μm (*IEEE-930, IEEE Guide for the Statistical Analysis of Electrical Insulation Breakdown Data*, 2005). To account for the statistical variability of dielectric breakdown, 15 samples of the same material were tested, and the results were analyzed using a two-parameter Weibull distribution, as shown by Equation (3.2).

$$E_2 = E_1\left(\frac{d_2}{d_1}\right)^{-0.4} \tag{3.1}$$

$$P = 1 - \exp\left[-\frac{E}{E_0}\right]^{\beta} \tag{3.2}$$

P represents the cumulative probability of failure at electrical fields lower than or equal to E. The scale parameter E_0 represents the electrical field for which 63.2% of the samples broke down. The shape parameter β shows the scattering of data, and a high value of β indicates a low standard deviation of breakdown strength measurements. The maximum likelihood method was used to determine the scale and shape parameters of the distribution, and the 95% confidence bounds were calculated numerically. The scale parameter was used to represent the breakdown strength of each material (1992). Further information on the statistical analysis of breakdown measurements can be found in (*IEEE-930, IEEE Guide for the Statistical Analysis of Electrical Insulation Breakdown Data*, 2005).

3.3 Results and Discussion

3.3.1 Chemical Characterization of Recycled Samples

Figure 3.1 displays the FT-IR spectra of virgin HDPE and recycled materials. In both virgin and recycled HDPE (rHDPE), the peaks at 2915 cm^{-1} and 2850 cm^{-1} correspond to the asymmetric and symmetric stretching vibrations of C-H bonds in methylene groups, respectively (Gala et al., 2020; Smith, 2021a). Additionally, the bending and rocking vibration

modes of C-H bonds can be observed at 1460 cm^{-1} and 720 cm^{-1}, respectively (Andreassen, 1999; Camacho and Karlsson, 2001; Fang et al., 2012).

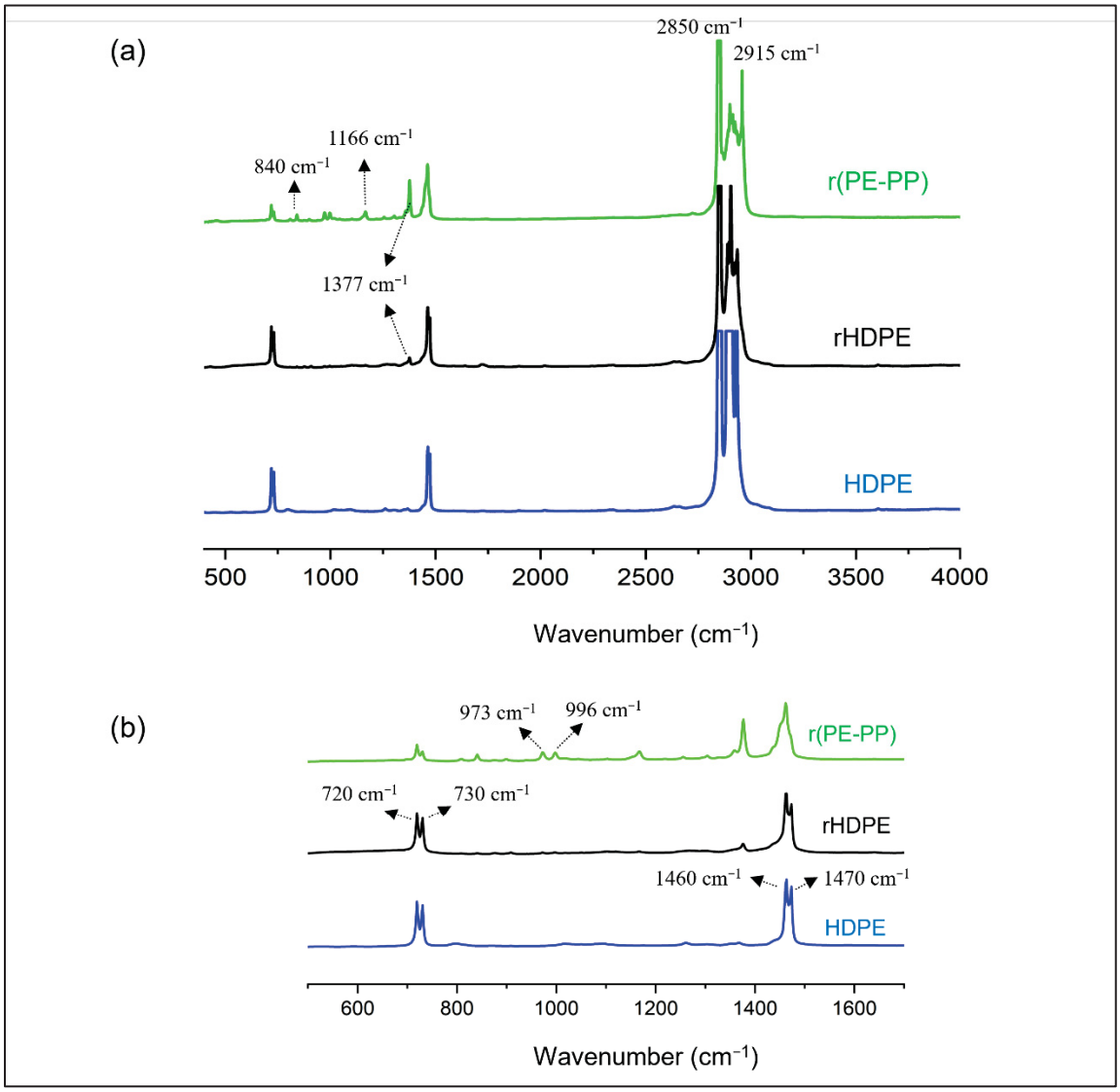

Figure 3.1 FT-IR spectra of recycled waste materials and virgin HDPE at spectral ranges from (a) 400 cm^{-1} to 4000 cm^{-1} and (b) 500 cm^{-1} to 1700 cm^{-1}. rHDPE and r(PE–PP) refer to recycled high-density polyethylene and a recycled polyethylene/ polypropylene blend, respectively

The FT-IR spectra of rHDPE and virgin HDPE present a high degree of similarity, confirming that the recycled material is mainly composed of polyethylene. The main difference is the presence of a weak absorbance band at 1377 cm^{-1} in the IR spectrum of the rHDPE sample. This peak is associated with the symmetrical bending vibrations of C-H bonds in methyl groups and may indicate contamination with PP (Gala et al., 2020; Heydariaraghi et al., 2016). Furthermore, the presence of the band at 1377 cm^{-1} can be used as an indicator to differentiate between different types of branched polyethylene (PE), such as LDPE, LLDPE, and HDPE. HDPE typically exhibits a higher peak between 1400 cm^{-1} and 1300 cm^{-1} without an additional band at 1377 cm^{-1} (Gall et al., 2021).

In Figure 3.1b, weak peaks at lower wavenumbers are observed in the r(PE-PP) sample, which are not present in the rHDPE or virgin PE samples. These peaks can be attributed to polypropylene. The peak at 840 cm^{-1} corresponds to the C-H rocking vibration, while the medium peaks at 973 cm^{-1} and 996 cm^{-1} are associated with the C-C stretching or rocking vibration of the methylene group in polypropylene. Additionally, the rocking vibration of the methyl group or bending vibration of the C-H bond can be observed at 1166 cm^{-1} [13].

Further analysis shows that the peak at 720 cm^{-1} is split into two separate peaks at slightly different wavenumbers for all three materials. Figure 3.1b illustrates two distinct in-phase and out-of-phase rocking vibrations, resulting in separate peaks at 720 cm^{-1} and 730 cm^{-1}. This splitting phenomenon is characteristic of solid, long-chain alkanes like HDPE. In contrast, a polymer like LDPE lacks this splitting due to the presence of side chains that hinder the crystallization of methylene chains by keeping them apart (Smith, 2021a). As this split peak pattern is typically found in PE materials or a very weak one in PP copolymers, the detection of medium intensity in r(PE-PP) is, therefore, attributed to the presence of PE in a polyolefin blend or PP copolymer, or both (Andreassen, 1999; Gall et al., 2021). Similarly, further analysis shows that the peak at 1460 cm^{-1} is split into two separate peaks at 1460 cm^{-1} and 1470 cm^{-1} for virgin HDPE and recycled HDPE, but this splitting is not observed for the

recycled r(PE-PP) sample. These peaks correspond to the crystalline structure of HDPE in both virgin HDPE and recycled HDPE (Smith, 2021a). Several weak peaks in the region from 800 cm^{-1} to 1300 cm^{-1} are characteristic of PP, as observed in previous studies (Smith, 2021b). Similar peaks are also commonly detected in plastic waste from various sources (Turku et al., 2017). Therefore, the spectral features in this region may be attributed to impurities present within the polymer matrix, PP, or both.

Inorganic impurities present in the recycled material were identified using SEM-EDX analysis, which is a technique that combines high-resolution imaging of a material's surface with chemical identification of its elemental composition. The detected elements are listed in Table 1, indicating the presence of Ti, Ca, Si, and Al as the most prominent elements in waste materials. Previous studies have also reported on the potential sources of these inorganic impurities in recycled polyethylene (Turku et al., 2017). Soil impurities are believed to be the primary source of silicon (Si). Titanium may originate from pigment components. It has been suggested that the fire retardants or catalysts used during polymerization could contribute to the presence of impurities. In the case of neat HDPE, the Si content can provide further support to the previous discussion regarding the existence of soil impurities. Figure 3.2 presents the SEM-EDX map of the r(PE-PP) sample, revealing the simultaneous detection of elements such as Ca and Si or Al and Si in the same locations. This suggests the presence of inorganic contamination, possibly in the form of calcium silicate or aluminosilicate components.

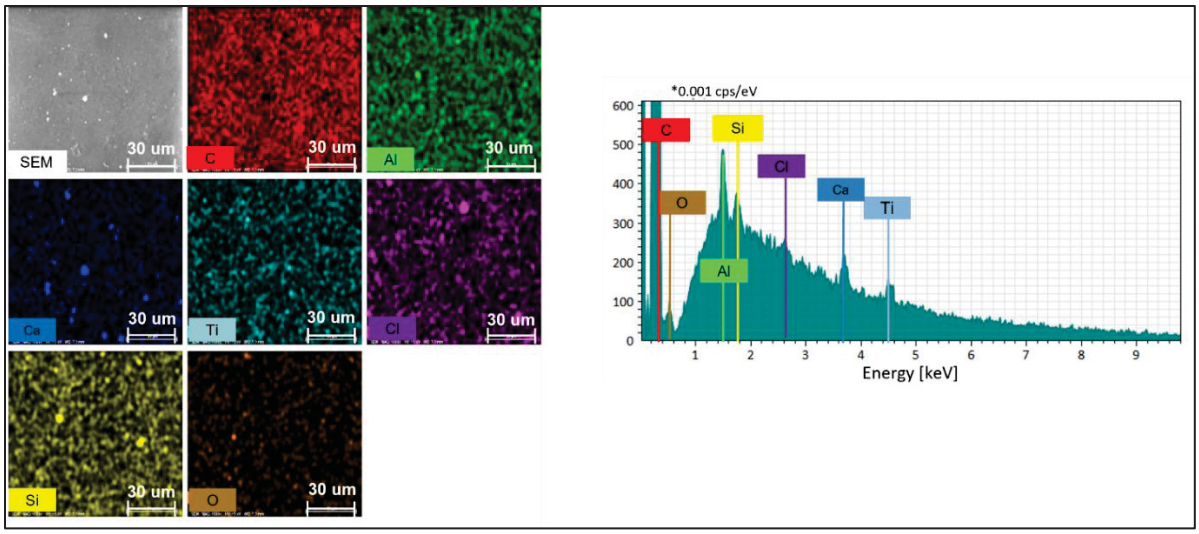

Figure 3.2 SEM-EDX map of post-consumer-recycled polyethylene/polypropylene, r(PE-PP). * Intensity scale: 0.001 cps/eV (counts per second per electron volt)

Table 3.1 Proportions of elements (%) on the surface of virgin and recycled materials

Sample/Element	C	O	Ti	Ca	Si	Al	S	Cl	k	Mg	Na
rHDPE	96.49	1.91	0.88	0.23	0.1	0.22	0.05	0.04	0.08	-	-
r(PE-PP)	97.47	1.51	0.39	0.25	0.08	0.27	-	0.04	-	-	-
HDPE	98.09	1.06	-	-	0.71	0.14	-	-	-	-	-

3.3.2 Thermal Analysis (DSC, TGA, Pyrolysis) of Recycled HDPE

Figure 3.3a presents the results of the differential scanning calorimetry (DSC) analysis for virgin HDPE, recycled HDPE, and recycled r(PE-PP) materials. Virgin high-density polyethylene (HDPE) exhibits a single melting transition (T_m) at 132 °C. For the recycled r(PE-PP) material, two separate peaks were observed at 129° C and 160 °C, corresponding to HDPE and PP, respectively. However, no evidence of additional melting peaks, indicating contamination with LDPE or PP, was observed for the rHDPE sample. The only melting peak detected for rHDPE was at around 133 °C, which is consistent with the recycler's identification of mainly HDPE content. However, this finding may differ from the FTIR results, which indicated the presence of inorganic impurities. This discrepancy could be attributed to the varying sensitivities of different analytical techniques. In this regard, Thoden et al. (Thoden

van Velzen et al., 2021) reported detecting as low as 2 wt% of polypropylene using DSC, confirming that rHDPE is mainly composed of HDPE.

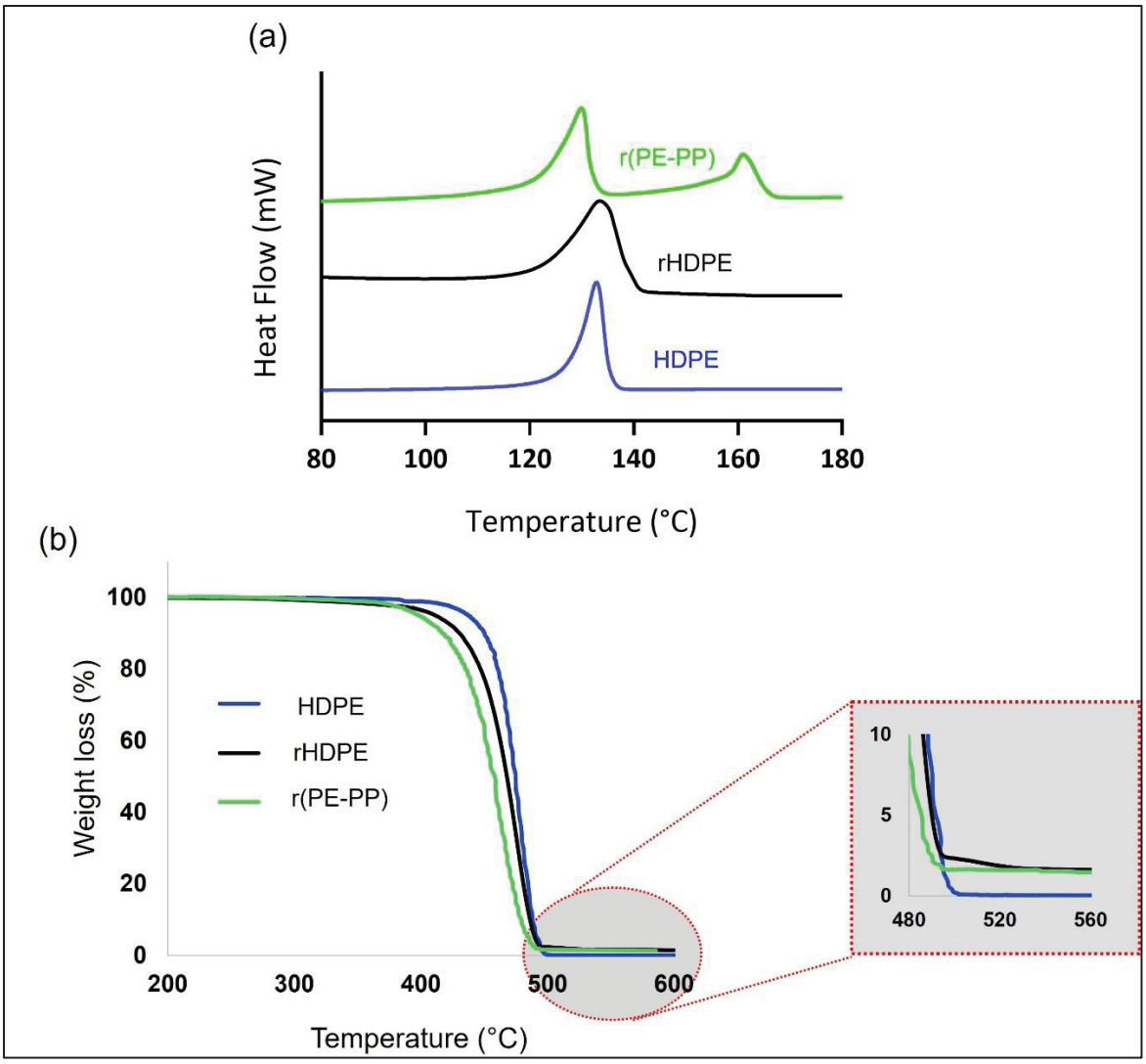

Figure 3.3 Thermal behavior of HDPE, rHDPE, and r(PE-PP). (a) DSC curve at temperatures from 80 to 180 °C; (b) TGA curve at temperatures from 200 to 600 °C. HDPE, rHDPE and r(PE–PP) refer to virgin high-density polyethylene, recycled high-density polyethylene and a recycled polyethylene/polypropylene blend, respectively

The DSC method used here is a common approach to determine polymer blend compositions based on their melt enthalpy, enabling the distinction of each component's specific melting temperature (T_m) in immiscible polyolefin blends. The results of DSC and FTIR discussed earlier suggest that the rHDPE sample predominantly consists of HDPE with the minimal presence of other organic impurities, while the r(PE-PP) sample is a blend of HDPE and PP.

Figure 3.3b displays the thermal gravimetric analysis (TGA) curves of recycled materials. The decomposition of these recycled materials was observed to start at approximately 350 °C. The majority of the weight loss occurred within the temperature range of 400 °C to 500 °C. The residual mass at 600 °C was determined to be approximately 1.4 wt% for both rHDPE and r(PE-PP) samples. However, these values exhibited minor variations across different samples, primarily due to the limitations of TGA in accurately quantifying impurities, including the inhomogeneous dispersion of impurities, overlapping decomposition events, the atmospheric effects on decomposition, and sensitivity limitations in detecting low-level impurities.

To address the accuracy of these values, conventional pyrolysis was carried out on larger samples using a pyrolysis oven. Unlike TGA, pyrolysis enables the complete thermal degradation of the polymer matrix in a controlled environment, leaving behind only non-volatile inorganic residues. The results indicated impurity contents of (1.45 ± 0.01) wt% for rHDPE and (0.44 ± 0.01) wt% for r(PE-PP). The values of inorganic impurities obtained from both TGA and pyrolysis were similar for the rHDPE sample. However, there was a noticeable difference in the results for r(PE-PP) waste material. This difference was mainly due to the presence of carbon black, as reported by the material supplier. Carbon black is a conductive filler that does not fully combust under the standard nitrogen atmosphere used in TGA, leading to the overestimation of residual mass. However, in pyrolysis, where controlled oxygen-rich or oxidative conditions are used for complete combustion, a more precise determination of actual impurity levels is achieved.

3.3.3 Dielectric Properties of Recycled Materials

In Figure 3.4, the imaginary part of complex permittivity is plotted against the temperature for two recycled materials over a range of 25 °C to 95 °C. The low dielectric loss of polyolefins ($\sim 10^{-4}$), which is an intrinsic property of these materials, makes the measurements highly sensitive to molecular and inorganic contaminants. A relaxation peak appears at low frequencies (1–10^2 Hz) in Figure 3.4a, attributed to interfacial polarization, commonly known as Maxwell–Wagner polarization (T. W. Dakin, 2006). This effect arises from ionic carrier

accumulation at polymer–electrode interfaces (electrode polarization) or at contaminant–polymer interfaces due to the differences in electrical conductivity among constituents.

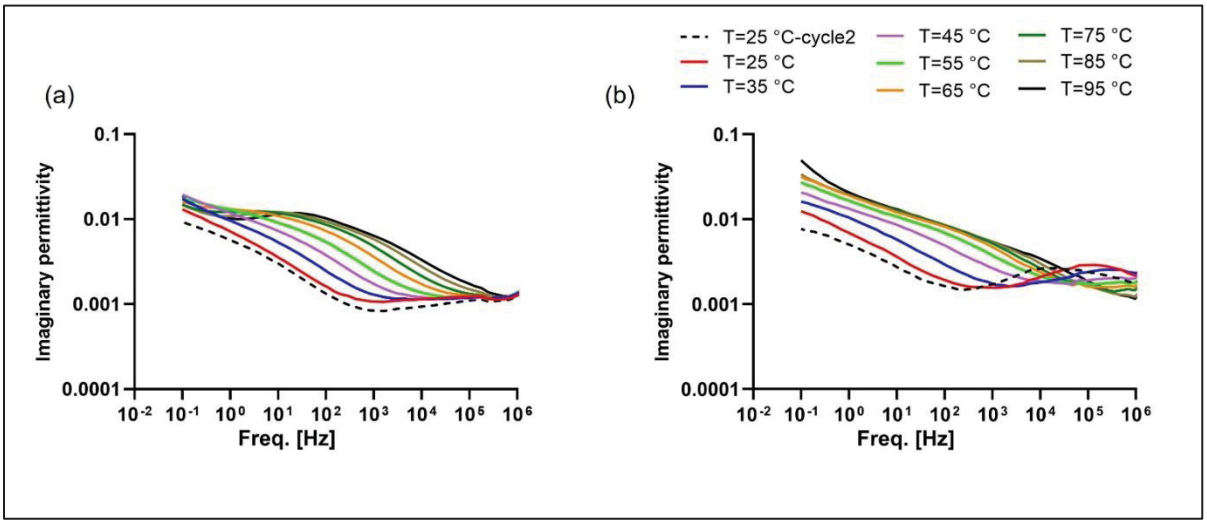

Figure 3.4 The imaginary permittivity of (a) recycled polyethylene (rHDPE) and (b) recycled polymer, with a mix of polyethylene and polypropylene r(PE-PP), at temperatures ranging from 25 °C to 95 °C

As depicted in Figure 3.4, the relaxation peak shifts toward higher frequencies as the temperature rises. This change could likely be attributed to an increase in the conductivity of ionic or micro-scale impurities. The latter explanation carries more significance and correlates with earlier investigations into the dielectric response in the frequency domain of polyethylene containing minor concentrations of metallic or non-metallic oxides (F. Ciuprina et al., 2010). Figure 3.4b represents the imaginary part of the complex permittivity of r(PE-PP) as a function of frequency. In this figure, two distinct relaxation modes are observable at high and low frequencies. The interfacial relaxation peak overlaps with the DC conductivity at low frequencies from 1 to 100 Hz. The dielectric loss of r(PE-PP) is slightly higher than rHDPE at low frequencies due to higher DC conductivity. Zois et al. (Zois et al., 1999) reported a dielectric loss of around 10^{-1} for the polypropylene/carbon black system with a 6 wt% percolation threshold. Additionally, another relaxation peak can be observed at higher frequencies, ranging from 10^4 to 10^5, which gradually shifts to higher frequencies with increasing temperature. The second peak can be attributed to the absorbed water that is usually

observable at higher frequencies, or it can be connected to the dipolar polarization of carbon-black-containing systems.

Figure 3.5 represents the relaxation behavior of r(PE-PP) under different temperature conditions. In Figure 3.5a, when the sample is gradually heated and then cooled to an initial temperature of 25 °C, the relaxation peak shifts to lower frequencies. This behavior has also been observed for samples that contain absorbed water. Indeed, due to the presence of hydrophilic inorganic impurities, water may have been absorbed. In order to investigate the possible presence of absorbed water, samples were heated at 70 °C for 70 min, as shown in Figure 3.5b. According to Figure 3.5b,c, no change in either the magnitude or the frequency of the position of the relaxation peak was observed after ten minutes of drying. Furthermore, it shows that although the dried sample has a lower relaxation peak intensity than the original sample, the peak does not disappear completely. In other words, although the relaxation peak is affected by the absorbed water between the impurity and polymer interlayer, it is not solely attributed to water. Moreover, the relaxation peak shifted to lower frequencies. This relaxation peak, which is almost 10^3 faster than the other relaxation peak, can be attributed to the presence of carbon black. Such a bimodal peak pattern has been documented in earlier studies involving polymer/clay nanocomposites (Böhning et al., 2005; Tomer et al., 2011; Tripathi et al., 2018) and can also be observed in carbon black, which contains polyolefins below the percolation concentration.

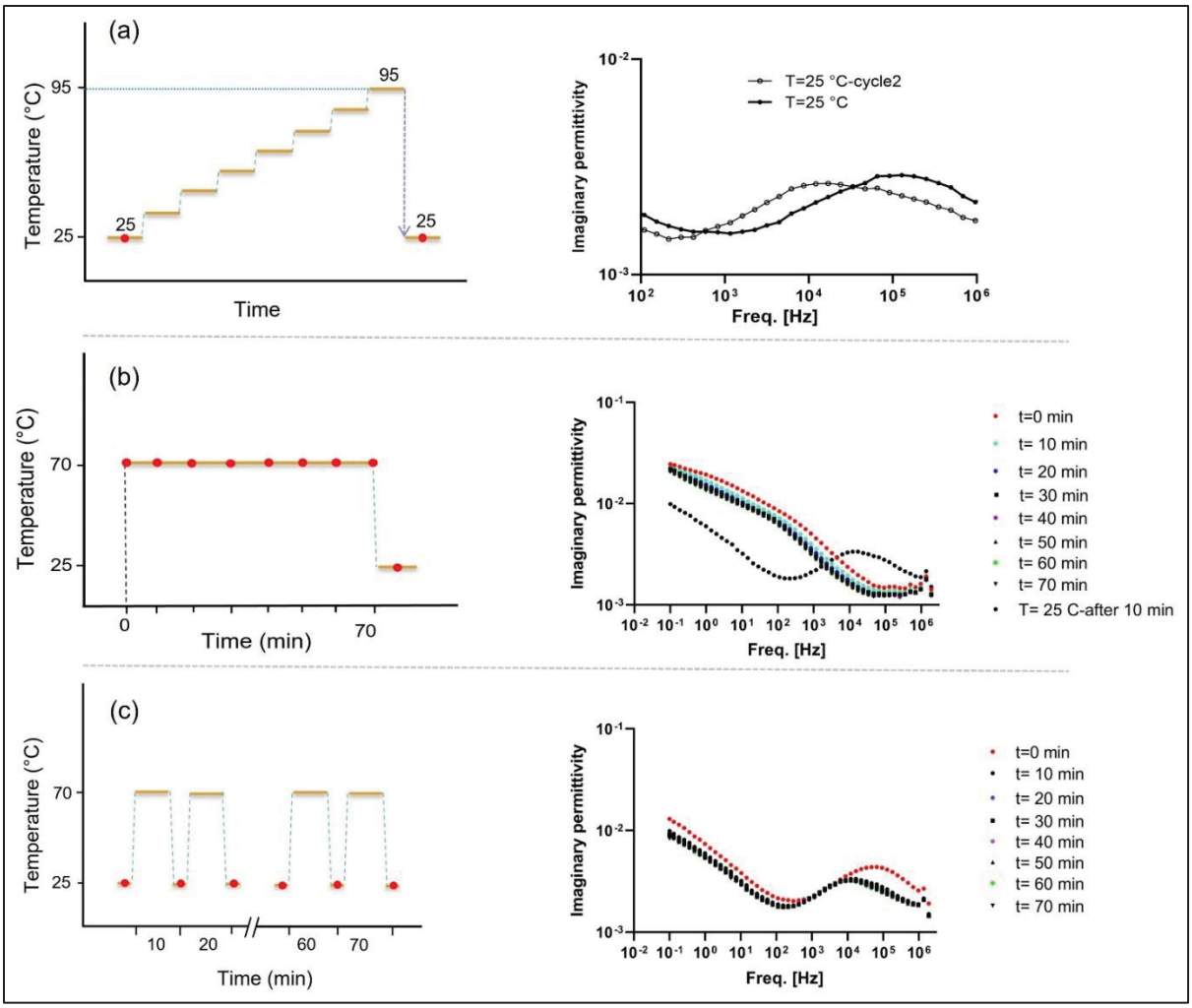

Figure 3.5 The imaginary permittivity of r(PE-PP) under different temperature profiles: (a) gradual tempera-ture increase; (b) steady high temperature; and (c) cyclic temperature changes between 25 °C and 70 °C

After normalization, collected data from the AC breakdown tests were analyzed using a two-parameter Weibull distribution to determine the breakdown strength of virgin HDPE and recycled materials. Statistical evaluation was conducted using commercial software, revealing differences in the electrical breakdown behavior of these materials. Further information on the statistical analysis of breakdown measurements can be found in (*IEEE-930, IEEE Guide for the Statistical Analysis of Electrical Insulation Breakdown Data*, 2005).

Figure 3.6 illustrates the cumulative Weibull distribution function for the breakdown strength. The scale parameter of the distributions, which is commonly used as the characteristic

breakdown strength for a material, indicates that virgin PE, recycled HDPE, and recycled r(PP-PE) have breakdown strengths of 84, 83, and 93 kV/mm, respectively. These values are lower than those we obtained for virgin and recycled HDPE in our previous research (Shirzaei Sani et al., 2023). The difference may stem from differences in environmental conditions and the difference in the increasing voltage rate, which was 2 kV/s compared to the previous 5 kV/s. However, the influence of inorganic impurities on breakdown strength in recycled polyethylene is not clear, but there is agreement that the inclusion of micro-fillers typically results in breakdown strengths similar to or lower than those of the neat matrix, particularly when employing short-term test procedures to monitor breakdown strength (Cheng et al., 2018; Nelson and Fothergill, 2004; Z. Li et al., 2011).

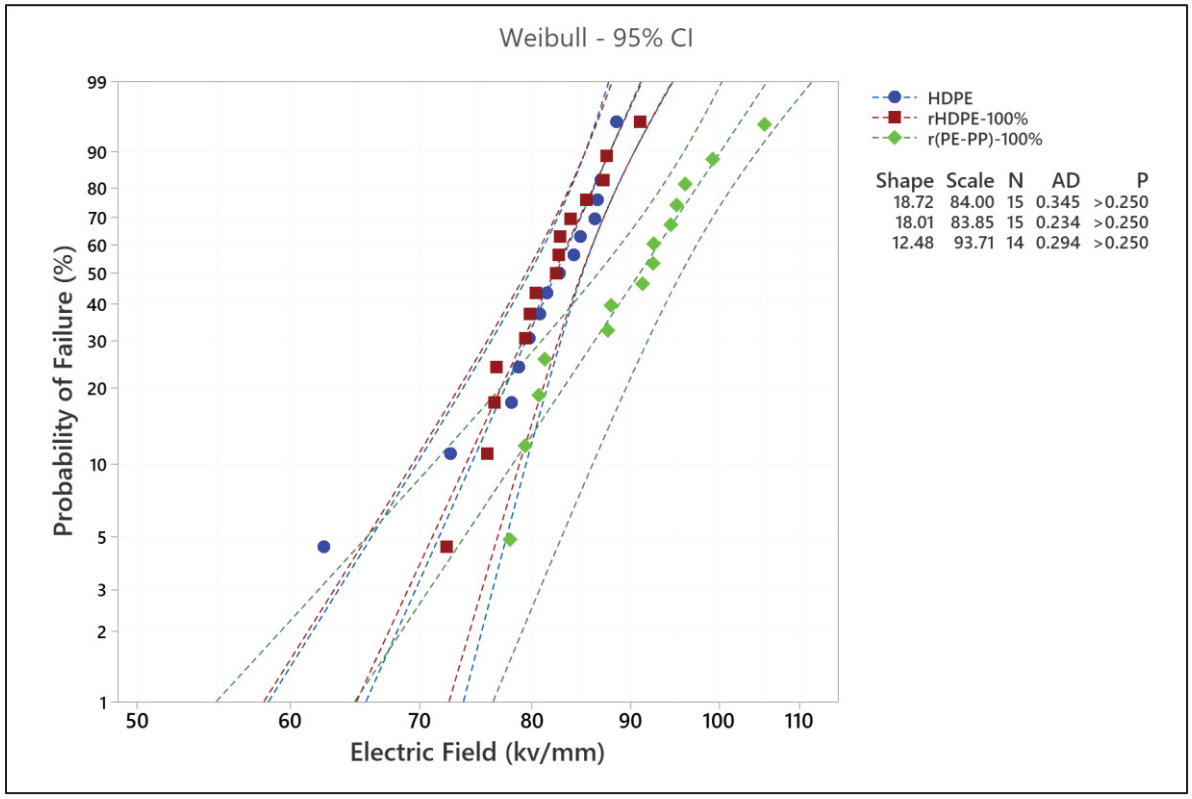

Figure 3.6 Breakdown strength of virgin HDPE, recycled HDPE, and r(PE-PP)

The dielectric breakdown strength of recycled r(PE-PP) exceeds that of recycled HDPE and virgin PE. This is likely due to the higher polypropylene dielectric breakdown strength in

comparison to polyethylene, as polypropylene is a component of recycled r(PE-PP) (Angalane and Kasinathan, 2022).

3.3.4 Blending

In the previous section, an in-depth analysis of the dielectric properties of recycled materials was carried out. These materials showed lower performance compared to virgin polyethylene (PE), mainly due to higher losses at least ten times larger at power frequency (60 Hz). This highlights the need for practical solutions to improve their properties. To address these issues, a blending method was used, combining recycled r(PE-PP) and recycled HDPE with virgin high-density polyethylene (HDPE). This method aimed to incorporate the advantageous properties of virgin HDPE to enhance the overall quality of recycled materials. The details of the blend sample compositions, which were prepared to improve dielectric properties, are provided in Table 2. This blending approach shows promise in addressing the limitations of recycled materials.

Table 3.2 Composition of blended recycled material, both recycled HDPE and recycled PE-PP, with virgin HDPE

Sample	wt% of Virgin HDPE	wt% of Recycled rHDPE	wt% of Recycled r(PE-PP)
HDPE	100	0	0
r(PE-PP)-100%	0	0	100
r(PE-PP)-85%	15	0	85
r(PE-PP)-70%	30	0	70
r(PE-PP)-50%	50	0	50
r(PE-PP)-30%	70	0	30
r(PE-PP)-15%	85	0	15
rHDPE-100%	0	100	0
rHDPE-85%	15	85	0
rHDPE-70%	30	70	0
rHDPE-50%	50	50	0
rHDPE-30%	70	30	0
rHDPE-15%	85	15	0

3.3.4.1 Thermal Analysis

In our previous study (Shirzaei Sani et al., 2023), it was shown that the degree of crystallinity decreased as the proportion of recycled material increased. The same trend was observed for the melting temperature. The nature of the polymer structure, as well as the number of impurities, might affect the crystallinity of recycled polymers. At low filler loadings, the crystallinity increases but decreases at higher filler loadings, which implies that a range of filler content leads to the maximum value of crystallinity.

Table 3 presents the melting temperature, degree of crystallinity, crystallization temperature, and melting enthalpy of each portion of blended recycled materials. In the r(PE-PP) material, each sample displays distinct melting temperatures. The lower melting temperature signifies

the T_m of the high-density polyethylene (HDPE) component, while the higher melting temperature corresponds to the T_m of the polypropylene (PP) component. This double-peak characteristic was consistently identified in all examined blends. Due to the overlap in crystallization temperature, only the peaks with a percentage composition exceeding 50% of recycled material exhibited a clear distinction.

Table 3.3 Thermal properties of blended recycled materials calculated using the DSC result

Polymer Blend	$\mathbf{T_m^{PE}}$	$\mathbf{T_m^{PP}}$	$\mathbf{T_C^{PE}}$	$\mathbf{T_C^{PP}}$	$\mathbf{\Delta H_{PE}}$	$\mathbf{\Delta H_{total}}$	**PP%**
HDPE	133	-	120	-	233.2	233.2	0
r(PE-PP)-30%	132	161	121	-	178.2	190.2	7
r(PE-PP)-50%	132	161	121	-	145.1	167.3	13
r(PE-PP)-70%	131	160	121	123	121.1	156.5	22
r(PE-PP)-100%	130	161	119	124	69.6	119	43

Note: T_m: melting temperature, T_C: crystallization temperature of polyethylene and polypropylene in the polymer blend.

The distinct melting temperatures of PE and PP in the primary recycled material demonstrate that blends of PP and PE are basically incompatible. The findings from Table 3 indicate a gradual decrease in the melting temperature of PE and an increase in the melting temperature of PP as the PP content increases. This outcome aligns with the results reported by Wong et al. (Wong and Lam, 2002).

The percentage of polypropylene (PP) in the polymer blend was determined using differential scanning calorimetry (DSC), following the methodology outlined by Kazemi et al. (Kazemi et al., 2015). The calculated PP content ranged from 7% for the sample r(PE-PP)-30% to 43% for the sample r(PE-PP)-100%. The values obtained through this method are lower than those calculated using the blending rules for the blends.

Figure 3.7 displays the TGA curves for the recycled material r(PE-PP) combined with virgin HDPE. The decomposition of the recycled materials was initiated at around 350 °C, with

primary weight loss occurring within the temperature range of 400 °C to 500 °C. The decomposition of the recycled material blend with virgin HDPE occurred earlier in comparison to the decomposition of virgin HDPE alone. Moreover, with the increase in the recycled material content (r(PE-PP)), the composites started decomposing at a lower temperature. This finding aligns with our earlier investigation into a recycled HDPE blend (Shirzaei Sani et al., 2023). This could be due to the lower decomposition temperature of polypropylene compared to polyethylene (PE), attributed to the lower thermal stability of polypropylene.

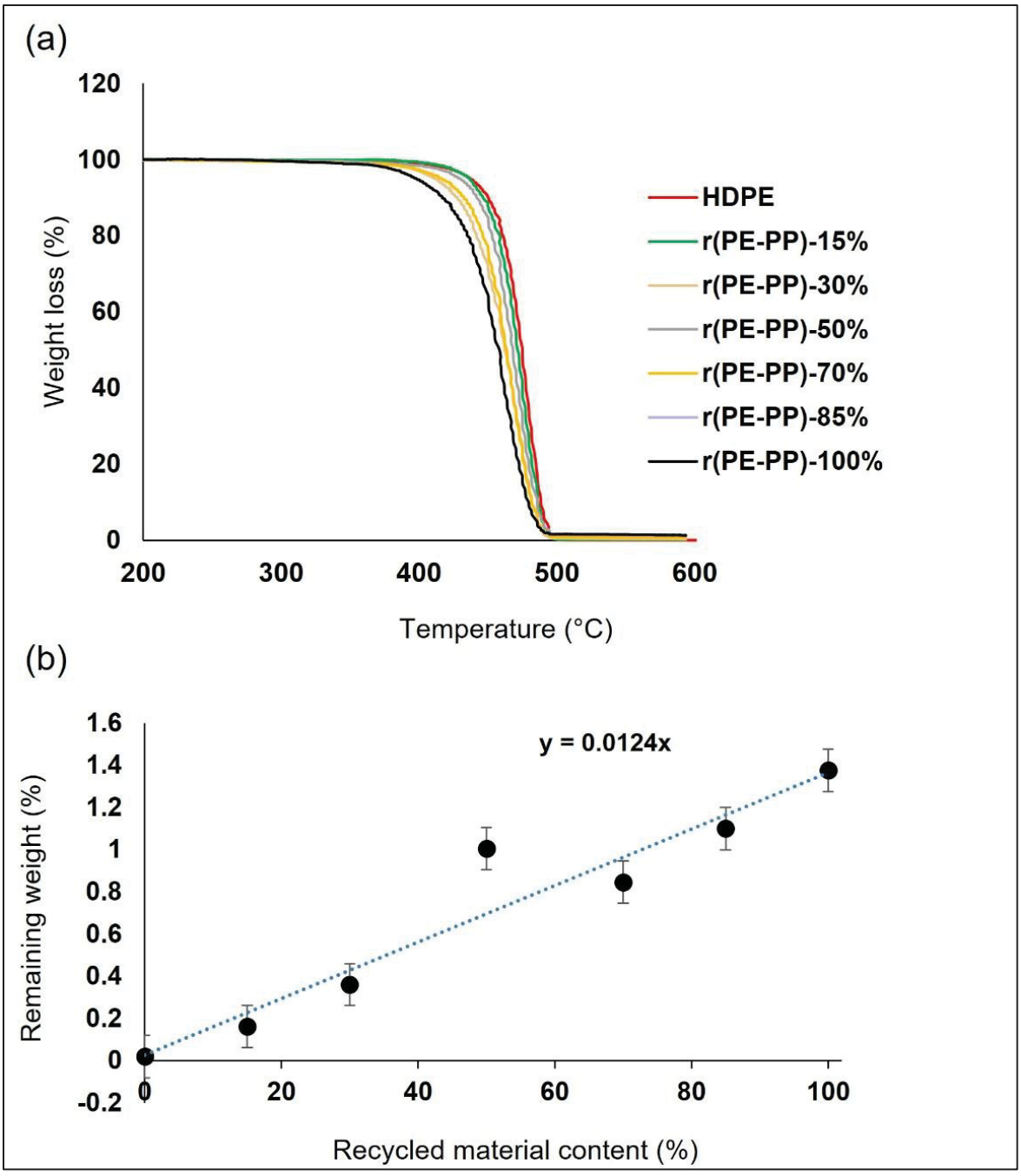

Figure 3.7 (a) TGA curve, and (b) the remaining weight (%) at 600 °C derived from the TGA curve for the recycled material r(PE-PP) blended with virgin HDPE at various ratios. In figure 3.7b, the black dots represent experimental data, while the blue dotted line is the linear fit, showing a positive correlation between the residual weight and the recycled content (y = 0.0124x)

In Figure 3.7b, the residual weight (%) versus the percentage of recycled material is illustrated. The residual content was 1.4 wt% for r(PE-PP)-100%. Based on the experimental results obtained, the quantity of the residual content could be determined using the linear equation provided in Figure 3.7b.

3.3.4.2 Dielectric behavior of blended material

The utilization of unaltered post-consumer materials in the electrical insulation industry seems confined to unshielded or low-voltage cables, as their high electrical loss poses risks for shielded AC cables like distribution or transmission cables (with a medium-to-high voltage). To mitigate dielectric loss, one potential strategy involves blending recycled polymers with pure HDPE at varying ratios. This approach aims to reduce the concentration of impurities, thereby lowering dielectric loss. Notably, a significant reduction in dielectric losses was observed for both rHDPE and r(PE-PP) upon the addition of virgin HDPE, particularly at lower frequencies (Figure 3.8). With the power frequency (60 Hz), the dielectric loss of rHDPE and r(PE-PP) was approximately 24 and 28 times higher, respectively, than that of virgin HDPE (Figure 3.9). Introducing just 15% of virgin HDPE decreases the dielectric loss of rHDPE and r(PE-PP) by almost 40% and 30%, respectively. Furthermore, when an equal composition of virgin and recycled material is used, the dielectric loss decreases by 62% and 57% for rHDPE and r(PE-PP), respectively, compared to the original recycled materials at 60 Hz.

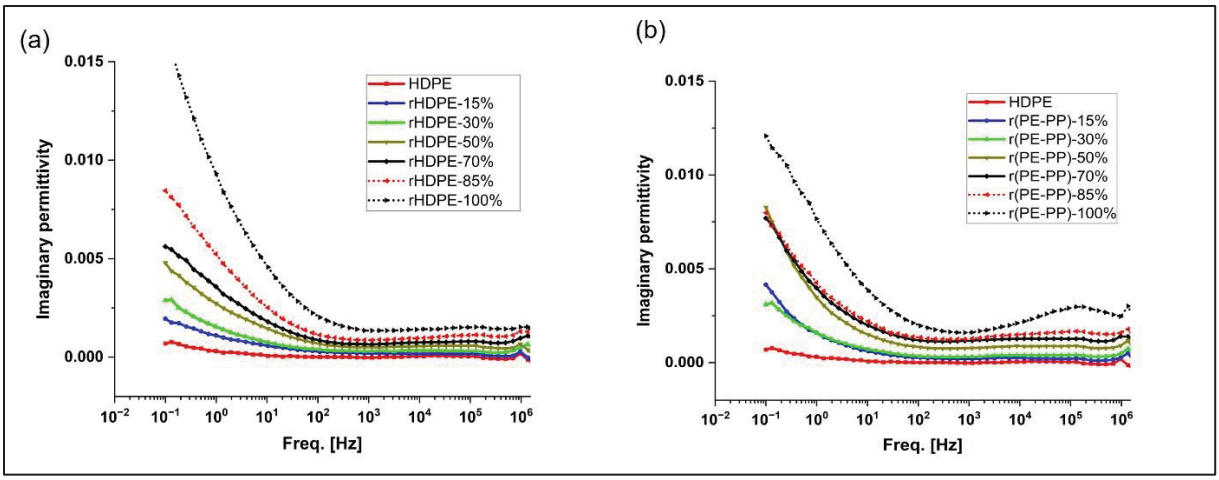

Figure 3.8 The imaginary permittivity of recycled materials blended with virgin polyethylene at various concentrations: (a) recycled HDPE (rHDPE); (b) recycled polyethylene/polypropylene, r(PE-PP), at a range of frequencies from 10^{-1} to 10^{6} Hz and at the temperature 25 °C

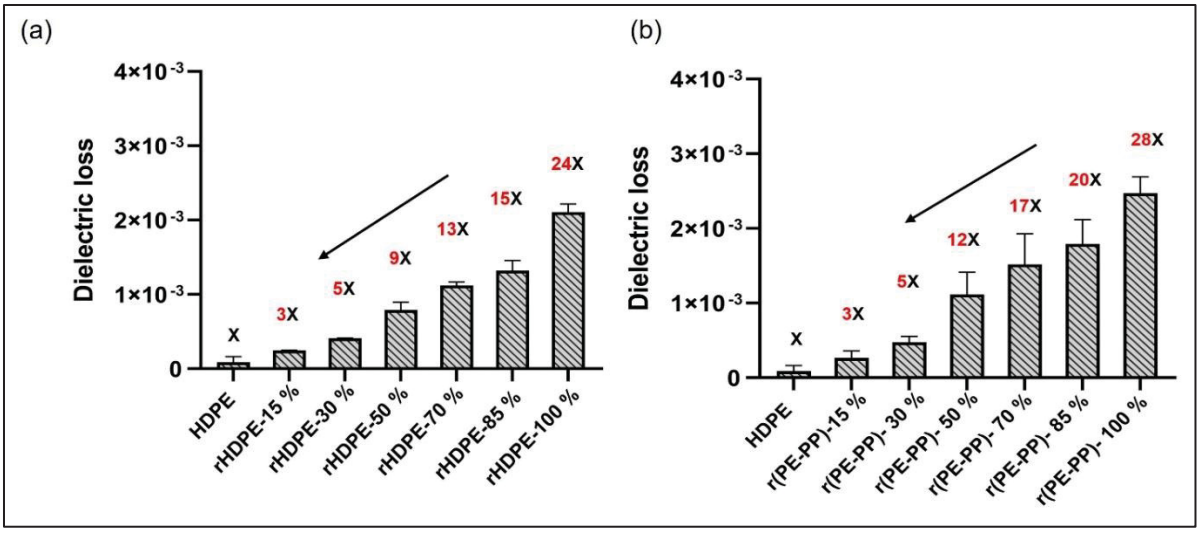

Figure 3.9 The dielectric loss of the blend of recycled materials and virgin polyethylene at various concentra-tions: (a) recycled PE, rHDPE; (b) recycled polyethylene/polypropylene blend, r(PE-PP), at a fixed frequency (60 Hz) and a temperature of 25 °C

Figure 3.10 illustrates the Weibull distributions of breakdown data for virgin HDPE when blended with recycled material. Contrary to the findings in our previous study (Shirzaei Sani et al., 2023), where blending with virgin HDPE was shown to enhance the breakdown strength

of recycled material by reducing the concentration of impurities, our current study yielded different results. For instance, in Figure 3.10a, no significant difference was observed when virgin HDPE was added to recycled polyethylene (rHDPE). In the case of recycled PE-PP samples, the dielectric breakdown strength decreased from 93 to 89 kV/mm as the percentage of virgin HDPE increased from 0 to 70%. This was attributed to the composition of the polymer matrix blend. Typically, the breakdown strength of PP is higher than that of PE; thus, the addition of virgin material to the recycled blend resulted in reduced breakdown strength. However, Dabbak et al. (Ahmed Dabbak et al., 2018) showed opposite results. In their case, the addition of HDPE increased the breakdown strength of the HDPE/PP blend.

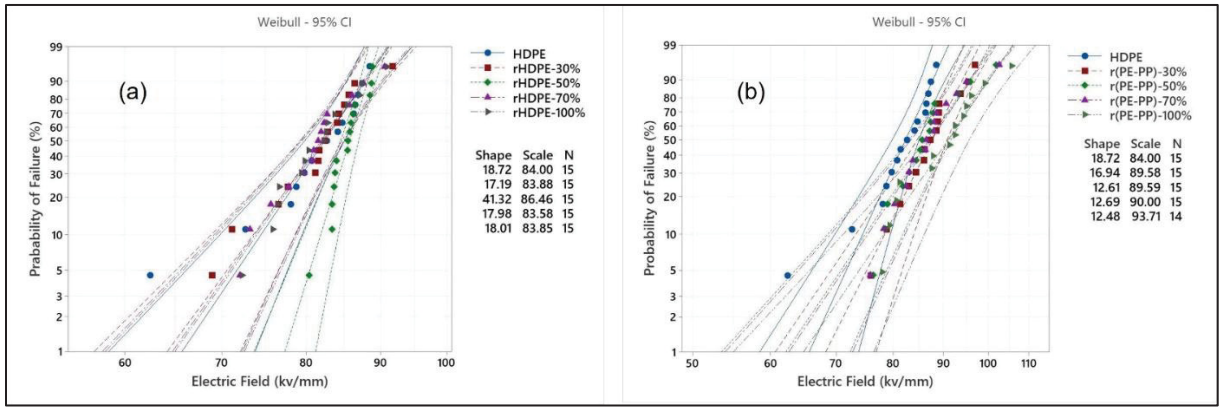

Figure 3.10 Dielectric breakdown strength of the blend of (a) recycled polyethylene (rHDPE) and (b) recycled polyethylene/polypropylene mixture, r(PE-PP), at different ratios with virgin high-density polyethylene. The samples are labeled according to the sample name and the percentage of recycled material included

3.4 Conclusions

This research focused on the characterization of recycled materials mainly containing polyethylene or a mixture of polyethylene/polypropylene. Furthermore, the potential use of recycled polyolefins as possible materials for dielectric insulation, with blending strategies, was investigated. Several findings and conclusions can be drawn based on the investigation conducted in this study:

Chemical analysis using SEM-EDX showed the presence of inorganic impurities in the recycled materials, mainly identified as soil impurities and pigment components. Thermal analysis, DSC, exhibited the first recycled material, which was mainly composed of HDPE. The results confirm the supplier's information regarding the second recycled material, which is composed of two different polymers: HDPE and PP. These results were also confirmed by specific FT-IR absorbance peaks at 720 cm^{-1}, 1460 cm^{-1} attributed to HDPE, and several weak peaks in the range of the 800 cm^{-1}–1300 cm^{-1} region attributed to PP. The thermal degradation behavior of the polymer, using TGA, represents the presence of impurities at around 1.4 wt% for both recycled materials. However, pyrolysis results showed a lower content of inorganic impurities (around 0.4 wt%) for the recycled material containing polypropylene, which was probably caused by the decomposition of carbon black in the presence of air at high temperatures.

Dielectric analysis showed considerably higher losses for recycled materials compared to virgin HDPE, especially at low frequencies where the dielectric losses of recycled rHDPE and recycled r(PE-PP) were 24 and 28 times lower than virgin polyethylene, respectively. The addition of virgin material was found to extensively reduce the dielectric loss of recycled materials. Indeed, adding only 15 wt% of virgin HDPE reduced the dielectric loss by about 40% and 30% for recycled rHDPE and recycled r(PE-PP), respectively. This result suggests the potential of blending in order to enhance dielectric properties. On the other hand, the addition of virgin material reduces the breakdown strength of the recycled material containing polypropylene due to the lower breakdown strength of PE compared to PP.

CHAPTER 4

DIELECTRIC RELAXATION OF RECYCLED PE AND RECYCLED (PE-PP)

Iman Shirzaei Sani [a], Nicole R. Demarquette [b], Eric David [c]

[a,b,c] Department of Mechanical Engineering, École de Technologie Supérieure,
1100 Notre-Dame West, Montreal, Quebec, Canada H3C 1K3

To be submitted to *Polymer Engineering and Science journal*, August 2025

Chapter outline: Chapter 4 explores the dielectric behavior of recycled polyolefins, specifically recycled HDPE and recycled HDPE-PP blends, in comparison with virgin HDPE. It begins with an abstract summarizing the main findings, followed by an introduction that emphasizes environmental impact of using recycled materials in insulation. The materials and methods section outlines the preparation of samples under wet, dry, and untreated conditions, as well as the modeling approach using the Havriliak-Negami function. The results and discussion section analyzes the effects of impurities, moisture absorption, and temperature on dielectric relaxation. The chapter concludes with a summary of the result.

Abstract: High cost, time consuming and environmental hazards are some of the challenges in producing new materials. Hence, the use of recycled materials has always been of interest. In this study, the dielectric properties of two different recycled materials, mainly recycled HDPE and recycled HDPE-PP, were investigated under three distinct conditions: wet, dry, and untreated. For comparison, virgin HDPE was also used to assess the differences in dielectric behavior between recycled and non-recycled materials. The Havriliak-Negami function was used to model and fit the results, providing a detailed understanding of the relaxation processes and related parameters. The presence of impurities in recycled polyolefins considerably affects their dielectric behavior and also water absorption content. Results showed that the dielectric loss of recycled materials is much higher than that of virgin materials. Moisture absorption significantly influenced dielectric relaxation, dipolar and interfacial polarization, with broader

peaks and higher dielectric losses after 10 days of immersion in water. Drying over the same period revealed that heating could cause degradation in virgin HDPE, leading to further changes in its dielectric properties through increased DC conductivity. The Havriliak-Negami (HN) function was used to characterize the relaxation processes, showing that the maximum frequency at which the relaxation peak appears increases with rising temperature. This behavior was successfully fitted to experimental data. These findings contribute to understanding the potential of recycled materials in insulation applications while addressing the challenges posed by impurities and environmental factors such as moisture absorption, and thermal aging.
Keywords: recycled polyolefins; water absorption; thermal aging; broadband dielectric spectroscopy; Havriliak–Negami function; dielectric relaxation

4.1 Introduction

Emphasis on environmental sustainability and the circular economy has encouraged industries to use recycle materials. Polyolefins, such as PE and PP, are broadly used in the insulation industry due to their excellent dielectric properties combining low losses and high breakdown strength, low cost, chemical resistance, and suitable processability. On the other side, high cost, time consuming and environmental hazards are some of the challenges in producing new industrial materials. Hence, the use of recycled materials has always been of interest for new applications such as dielectric insulation industry. However, recycled polyolefins often contain inorganic and organic impurities that can significantly influence their dielectric properties(I. Shirzaei Sani et al., 2021; Shirzaei Sani et al., 2023).

Moisture, temperature, and degradation in insulation materials are crucial factors that can profoundly affect dielectric properties like dielectric loss, conductivity, breakdown strength, and consequently the performance of the materials as an electrical insulation materials(Cimbala et al., 2015). Dielectric relaxation, which is the material's response to an alternating electric field, is a critical parameter in assessing the electrical insulation properties of a polymer. Understanding these changes is crucial to optimize the performance of recycled materials and determining their potential applications within the insulation industry. While

many studies have focused on various properties of waste materials, such as mechanical, thermal, and chemical characteristics(Borovanska et al., 2014; Calero et al., 2018; Gala et al., 2020; Gall et al., 2021; Mylläri et al., 2016), only a limited investigations have been done on the dielectric properties of these materials. Although many studies have focused on water absorption (Couderc Hugues et al., 2014; Hosier et al., 2017; Hui et al., 2013; Kochetov et al., 2016) and aging (Densley, 2001; Li et al., 2024; Liang et al., 2023; Tantipattarakul et al., 2020; Zheng et al., 2023) of polyolefins and their composites, there is a lack of studies on the effect of those factors on dielectric properties of waste materials.

In our previous study, we have characterized the impurity of recycled materials and their influence on dielectric properties of recycled materials(Shirzaei Sani et al., 2023). In this study, we have focused more profoundly on the dielectric properties of two different materials: recycled polyethylene (rPE) and recycled polyethylene-polypropylene blends (r(PE-PP)). We have investigated the dielectric properties in three different states: dry, wet, and untreated samples. For the dry and wet samples, the process was conducted over a duration of 10 days. Additionally, we discussed the effect of impurities in all these situations. Finally, we employed advanced analytical methods, using the Havriliak-Negami (HN) function, to provide a detailed understanding of relaxation processes and the factors driving dielectric losses.

4.2 Materials and Methods

4.2.1 Materials

Virgin material used was high-density polyethylene (HDPE) with a density of 0.952 g/cm³ and an MFI of 6.8 g/10 min at 190°C under a 2.16 kg load. This HDPE was supplied by Dow in pellet form.

Also, two type of waste material were used. The initial waste material, rPE, was mainly high-density polyethylene (HDPE) provided in flake form, with a melt flow index (MFI) of 0.60 g/10 min at 190°C. The second waste material, r(PE-PP), was a blend of polyethylene and polypropylene, containing 45% to 55% polypropylene by weight, and exhibiting an MFI index of 4 or higher.

4.2.2 Sample preparation

The recycled material, rPE, was initially provided in colorful flake form by a supplier. It was pelletized using a twin-screw extruder (Model Haake Rheomix OSPTW16, Thermo Fisher Scientific Inc., USA), with a length-to-diameter ratio of 40 (L/d=40). To ensure uniform sample preparation through mixing, the material was extruded twice before any further characterization. The processing temperature was consistently maintained at 180 °C from the hopper to the die, with the screw speed set at 100 rpm.

For further characterization, the pelletized materials were hot-pressed into disc-shaped samples using a hydraulic press. For broadband dielectric spectroscopy analysis, the samples' thicknesses were approximately 500 μm.

The preparation process included a 5-minute preheating step, followed by hot-pressing at 175 °C for another 5 minutes under a pressure of 10 MPa. After pressing, the samples were cooled under sustained pressure with circulating water at a cooling rate of 10°C per minute until they reached ambient temperature.

4.2.3 Characterization

4.2.3.1 Scanning Electron Microscopy (SEM)

Scanning Electron Microscope (SEM) imaging was performed using a Hitachi SEM S3600-N (Model: MEB-3600-N, Hitachi Science Systems, Ltd., Tokyo, Japan) to investigate the microstructure of the cryo-fractured surface of the samples. Before imaging, the sample surfaces were gold coated to improve the imaging quality.

4.2.3.2 Water Absorption and Loss

After preparing the samples, they were conditioned to different levels of water content. Ambient samples were kept in an air-conditioned environment at room temperature. Dry

samples were subjected to vacuum drying at 70°C for 3,6 and 10 days. Wet samples were submerged in water for 3,6 and 10 days. To quantify water absorption, samples of each material, with a thickness of 500 µm, were characterized at 3, 6, and 10 days of drying or wetting. Their mass was recorded at regular intervals with an accuracy of ±0.0001 g. Water absorption or desorption was determined using equation (4.1) where M_t is the sample mass at the specific drying or wetting times (3, 6, 10 days), and M_0 is the initial mass of the sample at ambient temperature before the start of the drying or wetting process(Shirzaei Sani et al., 2021). The samples were characterized in three states of wet, dry and untreated.

$$W = \frac{M_t - M_0}{M_0} \times 100 \tag{4.1}$$

4.2.3.3 Dielectric Spectroscopy

Dielectric response measurements were conducted in the frequency domain using a broadband dielectric spectrometer (Novocontrol Technologies GmbH & Co. KG, Montabaur, Germany). The samples, which were disk-shaped with a thickness of 500 µm and a diameter of 30 mm, were positioned between two parallel plate electrodes with a thickness of 2 mm. A 3 Vrms excitation voltage was applied during the measurements.

To thoroughly investigate the dielectric response of the materials, three different experimental strategies were employed:

1. The dielectric response was evaluated at various temperatures ranging from 25°C to 95°C, covering a frequency range from 10^{-1} to 10^{6} Hz, with isothermal scans taken at 10°C intervals. The measuring chamber was continuously purged with dry nitrogen. After reaching the maximum temperature, the samples were cooled back to 25°C, and the dielectric spectrum was measured again to assess the impact of the heating process on the dielectric response. For r(PE-PP) sample, to better analyse the relaxation behaviour at high frequencies, the sample were cooled to low temperatures and were analyzed in the range of -25°C to 95°C.

2. In order to analyze the relaxation behavior of wet samples and to ensure the removal of water, the samples underwent repeated heating and cooling cycles between 25°C and 70°C. During each cycle, the sample was held at 70°C for 10 minutes, then cooled to 25°C before measurements were taken at this temperature.

4.2.3.4 Fitting Procedure

Among the commonly used relaxation functions for predicting dielectric properties, empirical Havriliak-Negami (HN) function stands out as the most effective function. This is due to its capability to model a wide and asymmetric distribution of relaxation times. The complex dielectric permittivity can then be accurately described by combining the HN function with a conductivity term related to free charge fluctuations. The complex dielectric permittivity can then be expressed as:

$$\hat{\varepsilon}(\omega) = \varepsilon'(\omega) - i\varepsilon''(\omega) \tag{4.2}$$

$$\hat{\varepsilon}(\omega) = b(i\omega)^{n-1} + \sum_{k=1}^{N}\left[\frac{\Delta\varepsilon_k}{(1+(i\omega\tau_k)^{\alpha_k})^{\beta_k}} + \varepsilon_{\infty k}\right] \tag{4.3}$$

Where ω is the angular frequency, $\hat{\varepsilon}$ the complex dielectric permittivity, ε' the real part of the complex dielectric permittivity also known as the dielectric constant and ε'' the imaginary part of dielectric permittivity known as the dielectric loss.

In equation (4.3), the first and second parts of the left side are a general expression characterizing the charge fluctuation and a summation of Havriliak-Negami (HN) terms related to relaxation processes, respectively. The parameter n is an exponential factor, varying between 0 and 1 and characterizing the nature of the charge hopping process. The case n=0 corresponds to pure electronic conduction with $b=\sigma_0/\varepsilon_0$ while none-zero values lead to low frequency dispersion, a still poorly understood but commonly observed phenomena (Jonscher, 1983). $\Delta\varepsilon_k$, τ_k, $\varepsilon_{\infty k}$, α_k and β_k are the dielectric relaxation strength, the relaxation time, the real permittivity at much higher frequencies than the relaxation frequency, the width and asymmetry parameters of the k^{th} relaxation process, respectively. α_k and the product $\alpha_k*\beta_k$ are also related to the asymptotic slope of the low and high frequency tails of the k^{th} relaxation

process (in a log-log plot). Finally, N is the number of relaxation processes appearing in the experimental frequency window.

The fitting process was carried out using a commercially software using the Levenberg-Marquardt numerical technique to calculate the unknown parameters in equation (3) with both the real and imaginary parts of the experimentally measured dielectric spectra included in the fitting process. This was performed iteratively until a reasonable fitting was achieved, which was determined by the mean square deviation (MSD). The software calculated the MSD throughout the fitting procedure, and a threshold of less than 10^{-4} was established as the criterion for a stable fit. However, at least three iterations were performed at each step to ensure accuracy.

4.3 Results and Discussion

4.3.1 Characterization of Recycled Material

The impurities inside the material causes some properties to drop, which can influence the use of recycled material in insulation industry. Hence, firstly the effect of impurities on dielectric properties has been studied to know to what extend contamination affect these properties. The effects of moisture and drying on relaxation responses were studied. Additionally, the Havriliak-Negami function was used to examine the fitting of the experimental data.

4.3.1.1 Morphology of Recycled Materials

Figure 4.1 illustrates the microstructure of two types of recycled materials examined. In contrast to Figure 4.1b, which exhibits a single-phase morphology corresponding to polyethylene (PE), Figure 4.1a shows two distinguishable phases, indicating a droplet-dispersed morphology. The smooth and spherical droplets are attributed to the polypropylene (PP) phase (the minor component), while the continuous rough matrix corresponds to the PE phase. This confirms that PP and PE form an immiscible blend. In immiscible polymer blends where the two phases have different electrical conductivities, the phase morphology can

significantly influence the dielectric response of the material (Kremer and Schönhals, 2003). The composition of recycled PE (rPE) and recycled PE/PP (r(PE-PP)) blends was discussed in our previous study (Shirzaei Sani et al., 2025, 2023). Furthermore, similar morphology of phase-separated structure of waste PE/PP materials has been investigated by Nourin et al. (Sultana et al., 2024a, 2024b).

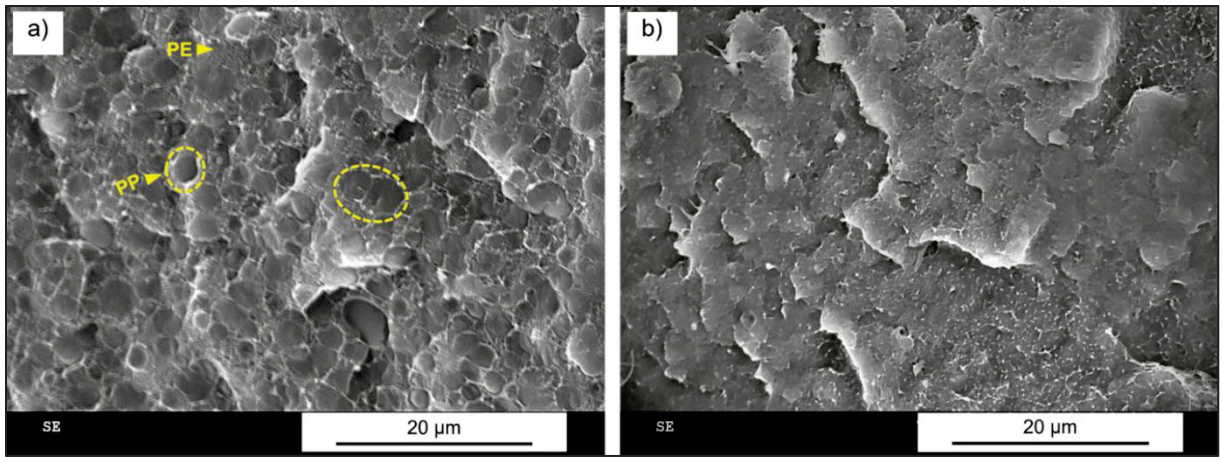

Figure 4.1 SEM images of recycled materials: a) recycled PE/PP (r(PE-PP)), droplets representing PP phase; b) recycled PE (rPE)

4.3.1.2 Dielectric response

In Figure 4.2, the graph exhibits the variation of the imaginary component of complex permittivity as a function of frequency and temperature for two types of recycled materials, covering a temperature range from 25 to 95 °C. Polyethylene, with low inherent dielectric losses (around 10^{-4}), showed sensitivity to molecular and inorganic contaminants due to these low losses. Figure 4.1a and 1b show a relaxation process at frequencies around 100 Hz, which is associated with interfacial or Maxwell-Wagner polarization. This type of polarization occurs due to charge accumulation at the interfaces between the polymer and electrodes - known as electrode polarization - or at the interfaces between contaminant particles and the polymer within the sample. The latter case is mainly due to differences in electrical conductivity between the components.

As shown in Figure 4.1, the relaxation peak shifts to higher frequencies with increasing temperature. This shift is due to an increase in the conductivity of either ionic impurities or

secondary phases containing micro-scale impurities. The latter explanation is particularly relevant and aligns with previous studies on the dielectric response of polyethylene with small amounts of metallic oxides. Furthermore, for the particular case of spheroidal inclusions of conductivity σ_f, the solution of the Laplace equation for a dilute solution (the so-called Maxwell approximation), leads to a relaxation time inversely proportional to the filler conductivity which gives a theoretical explanation for the temperature dependency of the dielectric response (Banhegyi, 1986)]. However, in the case of hydrophilic impurities included in a hydrophobic matrix, the composite's dielectric behavior becomes much more complex as the relaxation time is also very sensitive to the thickness of the water layer at the particle-matrix interface to the point that it can lead to a completely opposite temperature dependency (David and Frechette, 2013).

Figure 4.2b illustrates the imaginary part of the complex permittivity for the r(PE-PP) sample as a function of frequency and temperature. In Figure 4.1b, two distinct relaxation modes are observed at both high and low frequencies. The interfacial relaxation peak overlaps with the DC conductivity at low frequencies, from 1 to 100 Hz. Additionally, a second relaxation peak is evident at higher frequencies, ranging from 10^3 to 10^5 Hz, which shifts progressively to higher frequencies with increasing temperature. This second relaxation peak is likely attributable to multiple mechanisms. One possibility is the presence of absorbed water, which is known to produce dielectric relaxation at higher frequencies due to the reorientation of water molecules under an AC current (Lau et al., 2013). Alternatively, this peak may come from a dipolar polarization, especially in carbon black-containing systems, where conductive fillers enhance interfacial polarization effects. A similar peak pattern has been reported in polymer/clay nanocomposites (Tomer et al., 2011; Tripathi et al., 2018). Another contributing factor could be Maxwell–Wagner–Sillars (MWS) interfacial polarization, which becomes significant in heterogeneous polymer blends with phase-separated (immiscible) microstructures. In such systems, where the components are immiscible or only partially miscible, the dielectric response may exhibit two distinct relaxation peaks, each corresponding to the glass transition temperature (T_g) of the individual phases. Additionally, when the two phases differ in electrical conductivity—such as in blends of polar and non-polar polymers—charge accumulation at the interfaces can occur under an external electric field, giving rise to

interfacial polarization effects (Kremer and Schönhals, 2003). The latter effect is examined and discussed in more detail in Figure 4.4.

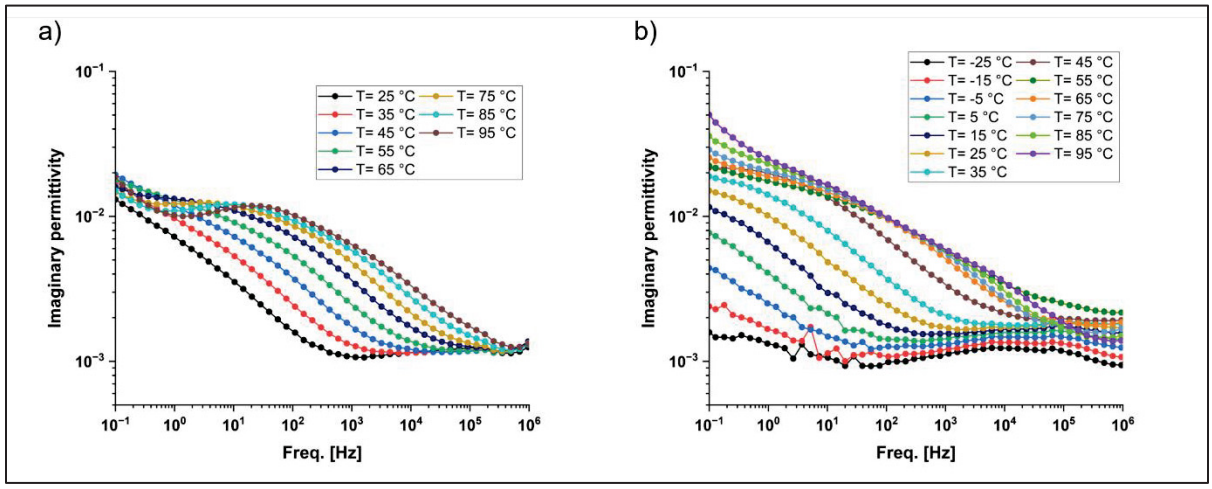

Figure 4.2 Imaginary permittivity of recycled materials. a) Recycled polyethylene at temperatures ranging from 25 °C to 95 °C (rPE) and b) recycled blend of polyethylene and polypropylene (r(PE-PP)), at temperatures ranging from -25°C to 95 °C

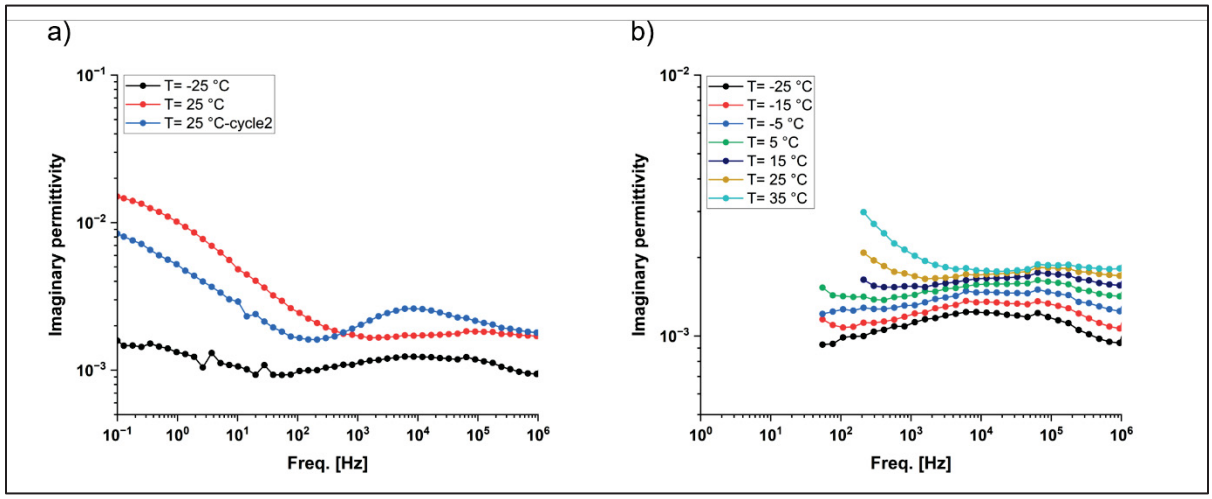

Figure 4.3 Imaginary permittivity of recycled blend of polyethylene and polypropylene (r(PE-PP)), a) effect of cycling; b) polarization at high frequencies

Figure 4.3a shows the imaginary permittivity of r(PE-PP) at 25°C, where the untreated sample was tested from 25°C to 95°C and then cooled back to 25°C. It shows that the relaxation peak

at high frequency slightly shifted to a lower frequency due to water loss during the first cycle. Additionally, at -25°C, the intensity of the relaxation peak at low temperatures is much lower than at medium temperatures (25°C). Figure 4.3b shows the magnified scale of imaginary permittivity of r(PE-PP) at high frequencies, ranging from -25°C to 35°C. In this temperature range, dipolar polarization at high frequencies is clearly observable. The peaks shift to higher frequencies as the temperature increases. At higher temperatures, the peak shifts out of the measurement range (T > 45°C).

To better understand the origin of the high-frequency relaxation peak observed in the r(PE-PP) sample, virgin PP and PE were blended in the same ratios as those found in the recycled material, and their dielectric responses were compared (Figure 4.4). Additionally, LDPE was blended with PP to investigate the influence of polymer type on the relaxation behavior. As discussed earlier, the recycled PE-PP (r(PE-PP)) blend exhibits a droplet-type morphology due to the immiscibility between HDPE and PP (Figure 4.1). Although both PE and PP are nonpolar polymers, the difference in their electrical conductivities, combined with droplet morphology, may lead to interfacial polarization. A similar phenomenon was reported by Ginzburg et al. (Ginzburg et al., 2020), where the interfacial polarization in a PP/polycarbonate (PC) blend with droplet morphology was observed. Moreover, impurities present in the recycled material (such as residual carbon black (Shirzaei Sani et al., 2025)) may preferentially localize in one of the phases, which would further enhance charge carrier accumulation. For example, Nourin et al. (Sultana et al., 2024a) have shown that graphene particles exhibit a greater affinity for the PE phase than the PP phase in a PE/PP blend.

According to Figure 4.4, no high-frequency peak was observed in the virgin HDPE-PP blend. However, a comparable but weaker peak was detected in the virgin LDPE-PP blend. It should be noted that the recycled materials include PP and PE from unknown grades and sources, which may influence the morphology and interfacial characteristics of the blend.

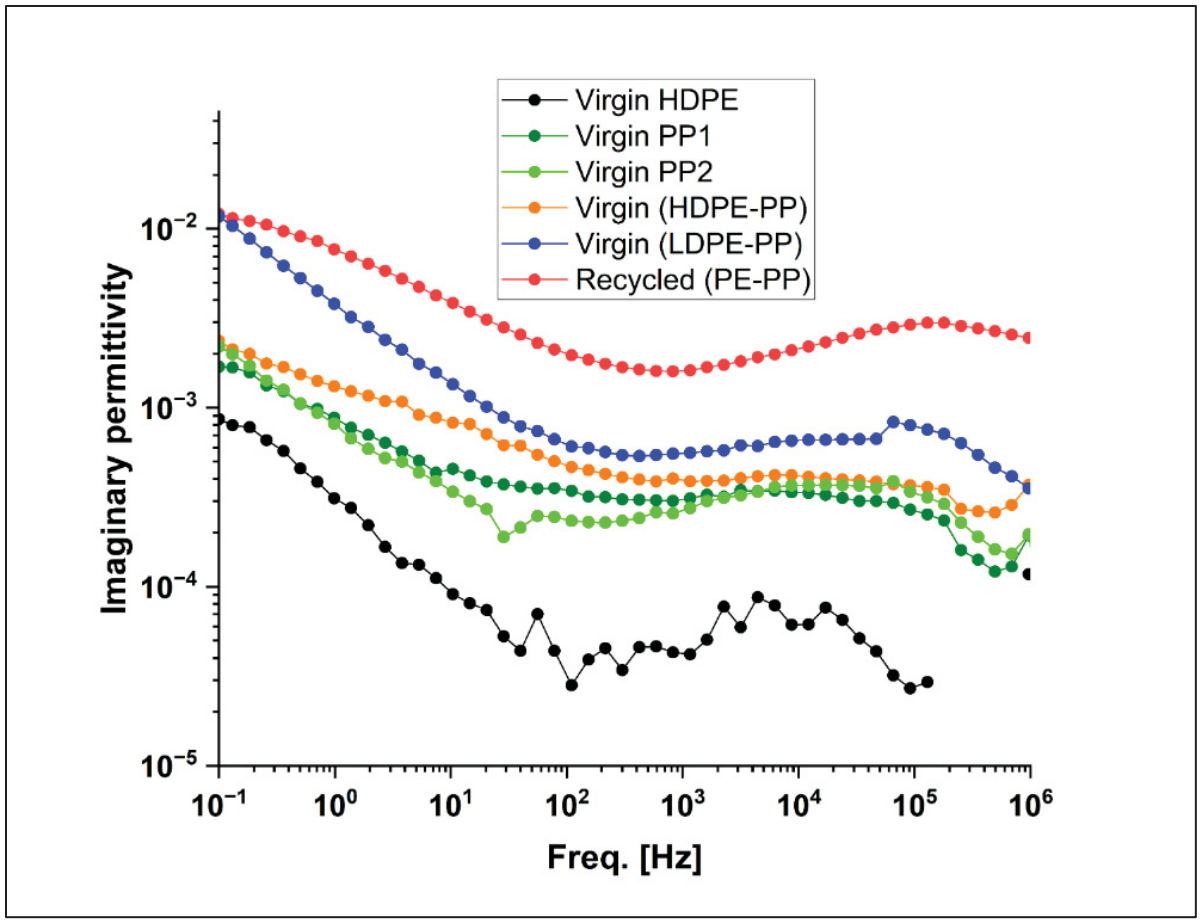

Figure 4.4 Comparison of the imaginary permittivity of three polymer blends; recycled PE/PP, virgin HDPE/PP, and virgin LDPE/PP, the virgin blends containing 40 wt% polypropylene

4.3.1.3 Water Uptake and Water Loss

Figure 4.5 illustrates how the sample mass changes over time during conditioning. All data have been normalized relative to the specimen's mass measured at equilibrium under ambient conditions. For both dry and wet conditioning, the mass variation of the unfilled system falls within the measurement uncertainty (±0.02%), suggesting that there is minimal change in water content whether the sample is in a vacuum or immersed in water. The accumulation mass change increase until approach a steady value after approximately 6 days, particularly for the drying process. Mass variation can be attributed to the inherent properties of the polymer, impurity level and type of impurities. Polyethylene is well-known for nonpolar structure, so it

is expected to absorb very low amount of water. Whereas the presence of impurities in recycled materials can increased the water absorption. In Figure 4.5, the result of water uptake after 10 days shows that just a minimal change was observed for virgin HDPE, however for recycled materials it was around 0.3 %.

At the molecular scale, the free volume of polyolefin has a radius of about 0.6 nm, while the size of a water molecule is about 0.2 nm (Xi et al., 2024). Although the polymer structure is hydrophobic, water molecules can still penetrate the polymer structure due to the concentration difference. In recycled materials, water absorption is primarily due to impurities rather than concentration difference diffusion. In polyolefin/nanoparticle composites , the absorbed water is usually located on the surface of the filler particles rather than within the hydrophobic polymer matrix(Zou et al., 2007). Both rPE and r(PE-PP) have absorbed nearly the same amount of water because of the similar impurity levels they contain. The volume of water uptake observed in this study is comparable to that reported in other studies, which used up to 5 wt% particle concentration in PE/Silica systems(Lau et al., 2012), and up to 10 wt% of nanoparticles in PP/nano-aluminium nitride systems (Wang et al., 2020).

The drying process shows the water content in both recycled rPE and r(PE-PP) was higher than in virgin HDPE, ranging between 0.1 to 0.2%, in comparison with initial weight at ambient temperature. These findings clearly indicate that both recycled materials, when stored under ambient conditions, retain a some amount of water. Moreover, surprisingly virgin HDPE shows approximately 0.1% mass loss during the drying process after 10 days. This observation does not align with the water uptake of HDPE over the same period. This disagreement suggests that mass loss may mostly be attributed to the volatilization of residual solvents introduced during polymerization, rather than water loss.

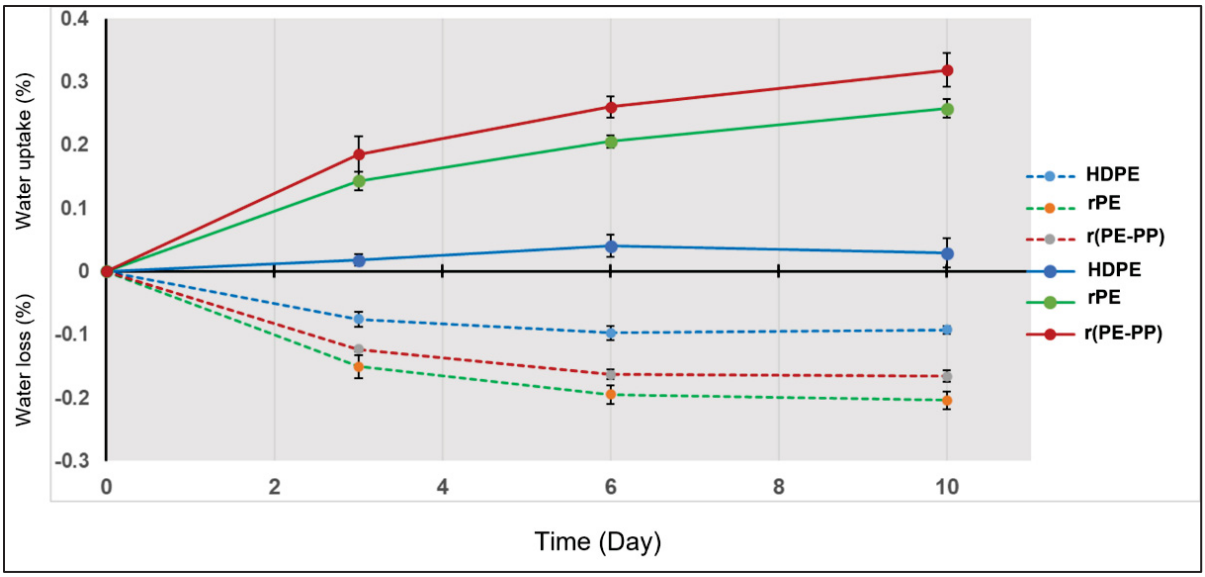

Figure 4.5 Water uptake and water loss of virgin HDPE, recycled PE and recycled blend of PE-PP

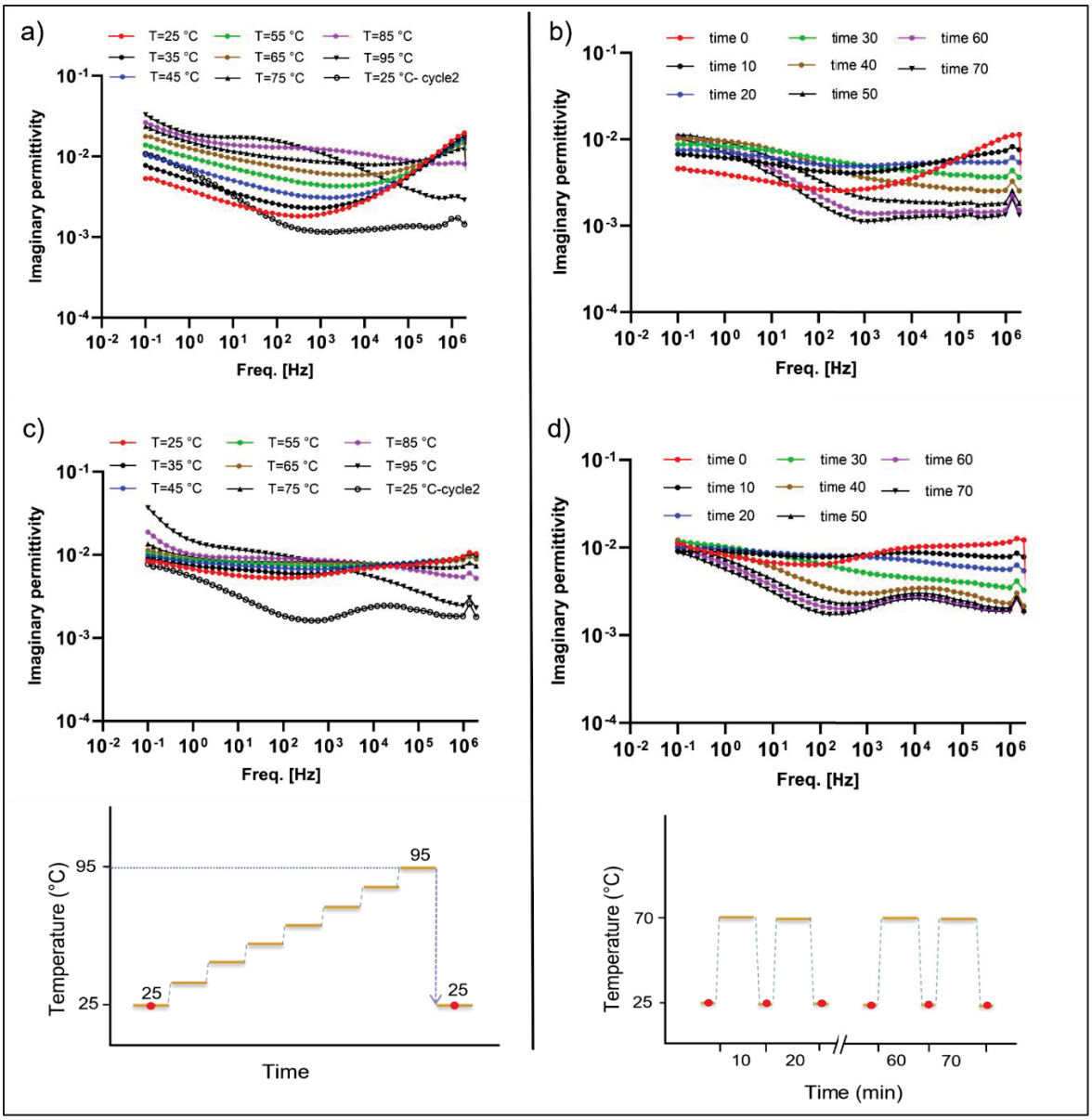

Figure 4.6 Imaginary permittivity of recycled a,b) polyethylene (rPE), and c,d) polyethylene/polypropylene (r(PE-PP)), at two different temperature conditions: temperature increasing at a rate of 10 °C, ranging from 25 to 95 °C (a,c); temperature cycling between 25°C and 70°C, with a 10 minutes hold at 70°C (b,d)

Figure 4.6, shows the dielectric loss as a function of frequency ranging from 10^{-1} to 10^{6} Hz, for two types of recycled consumer waste materials: (a, b) mainly HDPE (rPE) and (c, d) a supplier blend of HDPE and PP (r(PE-PP)). The samples were characterized following 10 days of water immersion, and their dielectric responses were evaluated under two temperature

conditions. Figure 4.6a,c depicts the dielectric response during a regular stepwise temperature increase of 10 °C and Figure 4.6b,d, represent the dielectric response measured at 25 °C during a heating cycle from 25°C to 70°C, with the sample held for 10 minutes at 70 °C.

As the heating time increases (Figures 4.6b and 4.6d), the interfacial relaxation peak related to inorganic impurities was observed to shift from high to low frequencies causing a decrease of the losses at high frequency as well as an increase at lower frequencies. Indeed, in Figure 4.6b, at time 0, where the water content is highest, a broad relaxation peak appears at a high frequency (~10^6 Hz). Over time, by water removal, this peak shifted to the lower frequencies with a slightly decreasing intensity. A similar behavior was observed by Hoiser et al. (Lau et al., 2013) and Couderc at al [9], both for the case of polyethylene containing a few % of nano-silica. At low frequencies, the dielectric response is further complexified due to the overlapping phenomena of interfacial polarization (both electrode-type and at the phases boundaries) and bulk charge fluctuation leading low-frequency dispersion. This is particularly obvious in Figure 4.6a and 6c for which the water removal becomes significant for the isothermal scans at 85 and 95ºC, causing a shift of the interfacial peak towards lower frequencies while the thermally-activated charge fluctuation increases. The comparison between the first and the second run at 25ºC is particularly revealing as a broad peak related to adsorbed water forming an interlayer between particles and the matrix is clearly observable at 25°C during the first heating cycle at high frequencies while it was observed to be shifted by 5-6 orders of magnitude towards lower frequencies (Figure 4.6a).

The wide peaks observed in wet samples can be explained considering a three-component system in which the water interlayer is more conductive than both the particles and the matrix. This particular case of an heterogenous material with interfacial layer being considerably more conductive than the two other phases was theoretically investigated (once again using the Maxwell approximation) and the complex dielectric response of such system was shown to behave as a Debye relaxation process for which the relaxation time is inversely proportional the thickness of the water layer (Steeman and Maurer, 1990). Higher water absorption is believed to increase the presence of loosely bound water(Lau et al., 2013), resulting in the observed loss peak shifting to higher frequencies. In reality, the experimental observed relaxation process is considerably broader than a simple Debye process since the impurities in

the waste material can vary in size (as demonstrated in our previous research(Shirzaei Sani et al., 2023)), can create structurally diverse interfacial regions, leading to a wider peak compared to materials with a narrower particle size distribution. Thus, a broad peak in interfacial polarization may reflect a wide range of particle size distribution. Also, different types and sizes of impurities introduce varied states of water bonding at interfaces, further contributing to the observed broad loss peaks.

For the r(PE-PP) samples (Figures 4.6c and 4.6d), the high-frequency fixed peak around 10^4 Hz was masked at drying times of 40 minutes or less due to the presence of an interfacial relaxation peak caused by adsorbed water. However, as the drying time increases (time > 40 min), this high-frequency peak gradually became unmasked. In these samples, the dielectric loss at lower frequencies is dominated by DC conductivity or interfacial polarization related to electrode-sample or impurity-polymer.

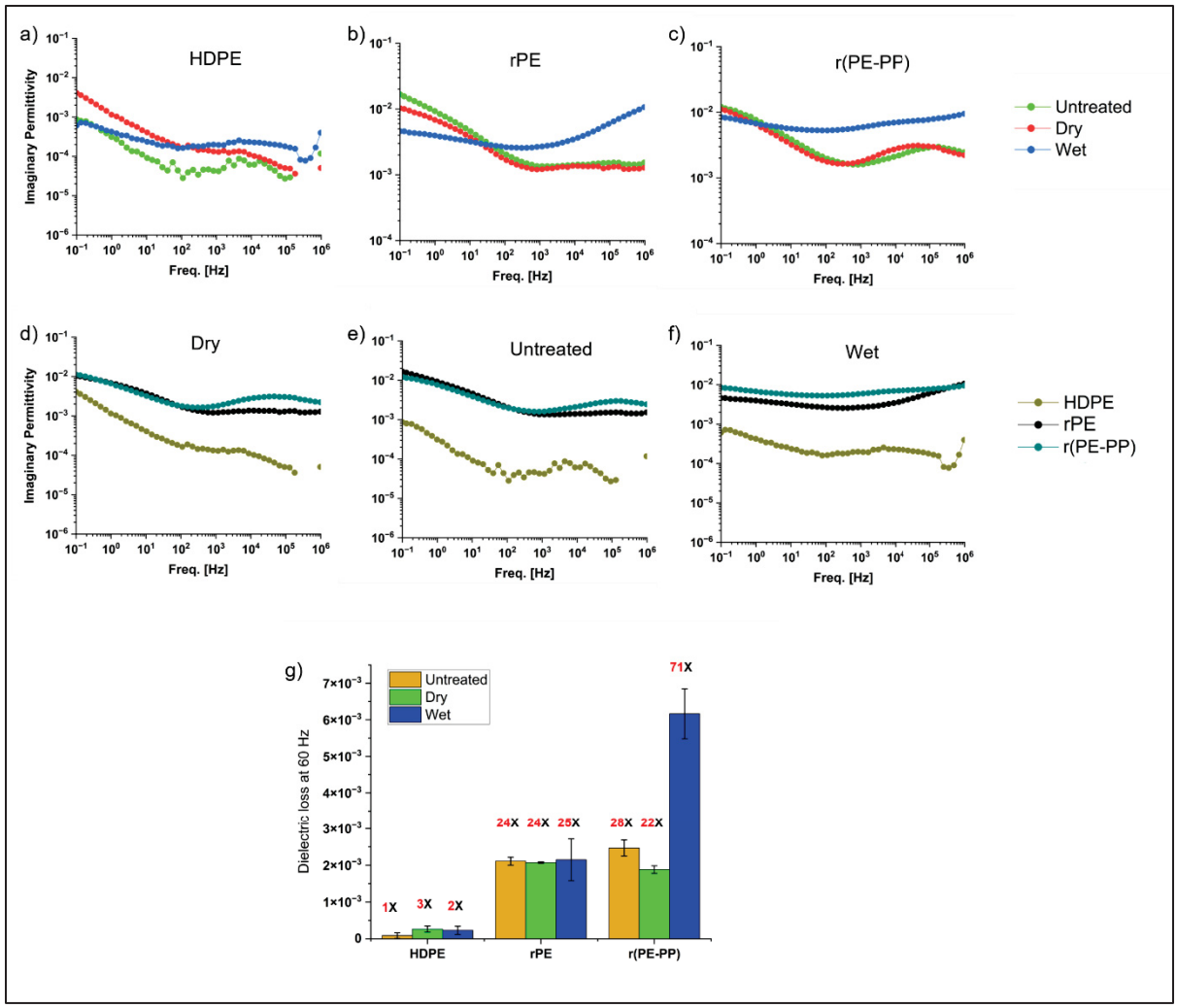

Figure 4.7 Imaginary permittivity of a) virgin HDPE, b) rPE, and c) r(PE-PP) (influence of wettability). Comparison imaginary permittivity of virgin HDPE, rPE, and r(PE-PP), at different condition d) dry, e) untreated, f) wet, after 10 days immersion in water; (influence of polymer type), g) dielectric loss at 60 Hz

Figure 7a-f illustrates the dielectric loss of virgin HDPE, rPE, and r(PE-PP), highlighting the effects of wettability and polymer type at different moisture content. Due to the higher dielectric loss of recycled materials, the scales for Figures 4.7b and 4.7c differ from the others. Figures 4.7a, 4.7b, and 4.7c show that samples immersed in water for 10 days exhibit an increase in dielectric loss at high frequencies. In the case of wet samples, the dielectric loss peak shifts toward higher frequencies, whereas for dry and untreated samples, it shifts toward lower frequencies. In general, the relaxation peak in wet samples is attributed to the volume

fraction of absorbed water and the conductivity of the interfacial layer (Kremer and Schönhals, 2003). The relaxation time is inversely proportional to the volume fraction of the interfacial layer. As a result, the dielectric loss of wet samples is lower than that of dry and untreated samples at low frequencies (e.g., 0.1 Hz), as clearly seen in Figures 4.7a-c. A similar result was observed by Lau et al. (Lau et al., 2013, 2012) in a 2% nanosilica-polyethylene system, where the dielectric loss of the nanocomposite at low frequency in the untreated state was higher compared to the that of absorbed water sample. For HDPE sample, which is a nonpolar polymer, it can still absorb a small amount of water primarily through penetration (Figure 4.5). Hence, HDPE absorbs approximately 15 times less water than the recycled materials, its corresponding relaxation peak is expected to appear at a lower frequency (Figure 4.7f). Therefore, in the wet state, the relaxation peak of HDPE becomes comparable to that of the recycled material, with the dielectric loss at power frequency (60 Hz) being 71 times and 2 times higher for r(PE-PP) and HDPE, respectively, relative to the untreated sample (Figure 4.7g).

Unlike the recycled materials, which don't show a significant difference between their dried and untreated states (Figure 4.7b,c), HDPE, shows a distinct variation in its dielectric loss curve (Figure 4.7a). Specifically, the dried HDPE exhibits approximately 5 times and 1.6 times higher dielectric loss compared to the untreated sample at 0.1 Hz and 10 kHz, respectively. Also, at power frequency (60 Hz), the dielectric loss is 3 times higher (Figure 4.7g). This increase can be attributed to the aging effects caused by prolonged thermal exposure. During aging, new polar groups may form, particularly in the amorphous regions, leading to the creation of additional interfaces between polar groups and the polymer matrix, thereby enhancing interfacial polarization.

Additionally, in the early stages of heating, the recrystallization of polymer chains may generate new "crystal–amorphous" interfaces, which also contribute to an increase in interfacial polarization. Similar increases in dielectric loss due to thermal degradation and aging have been reported by other researchers (Cimbala et al., 2015).

Furthermore, dielectric loss is composed of conduction loss and relaxation loss. This considerable rise in dielectric loss at low frequencies may result from a simultaneous strengthening of interfacial polarization and conductivity. The new interfaces introduced by

created polar groups may also offer additional pathways for charge carriers, which enhances DC conductivity. However during the recrystallization process, it has been reported that DC conductivity initially may decrease due to the suppression of charge carrier movement by the crystalline regions(Li et al., 2024), but with extended heating, free volume increases reduce the crystalline regions, which ultimately enhances charge carrier mobility and DC conductivity(Danikas et al., 2020; Liang et al., 2023).

4.3.1.4 Fitting relaxation response

Figure 4.8 illustrates the relaxation rates of recycled materials, both rPE and r(PE-PP), as a function of increasing temperature, providing insights into their dielectric behavior under varying thermal conditions. The relaxation times corresponding to the peak maximum frequency at each temperature were determined using the Havriliak-Negami (HN) fitting method and Equation (4.1), ensuring an accurate representation of the material's relaxation dynamics. Figure 4.8 further complements this analysis by plotting the characteristic relaxation rates (f_{max}) for the two relaxation processes against the inverse temperature. Although the Maxwell-Wagner-Sillars (MWS) and dipolar relaxation peaks are not distinctly separated at all temperatures, the fitting software successfully predicted the data even under challenging conditions.

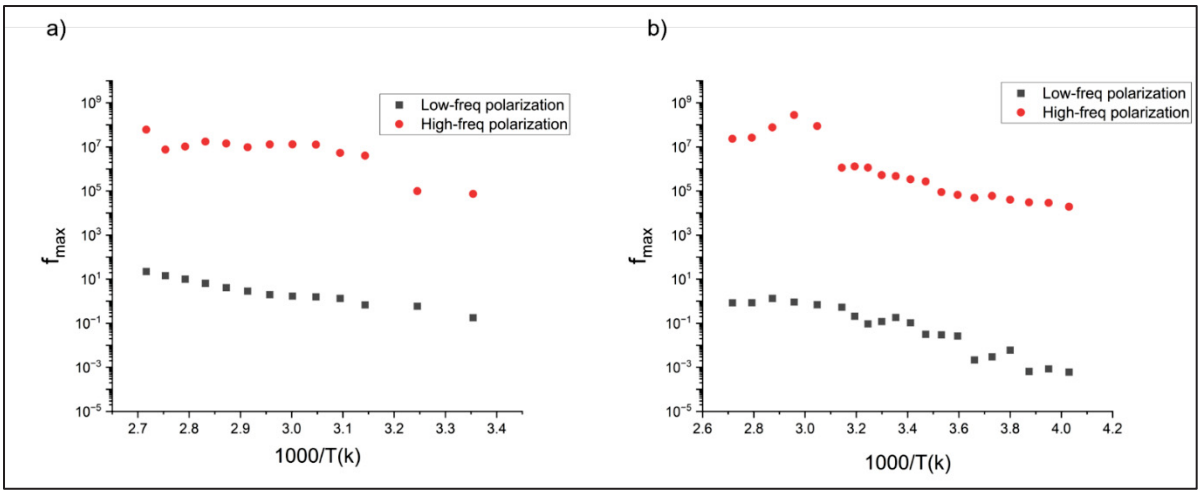

Figure 4.8 Relaxation rate (fmax) of the interfacial and dipolar polarization processes of a) Recycled polyethylene (rPE) and b) recycled blend of polyethylene and polypropylene (r(PE-PP)), at different temperatures

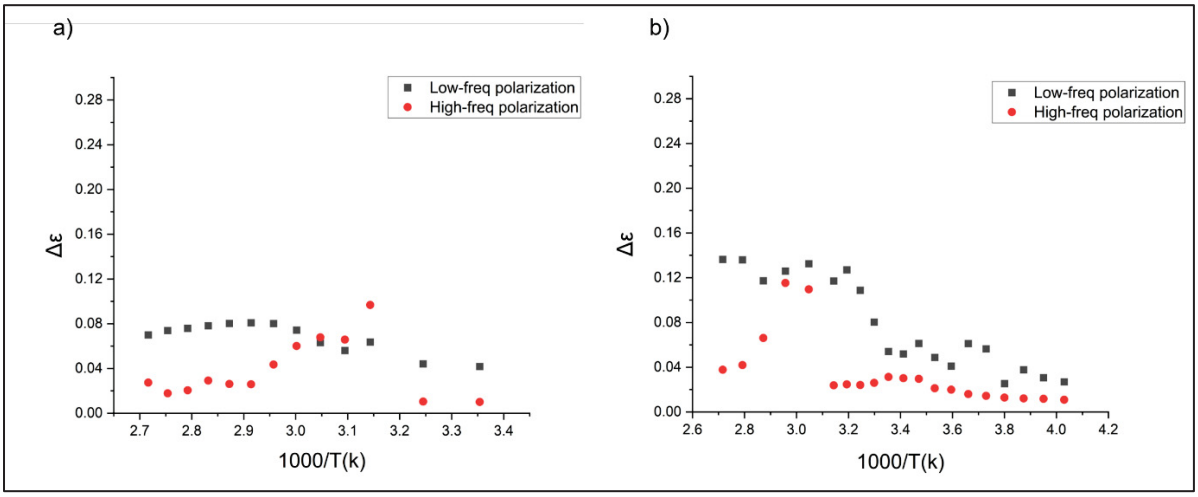

Figure 4.9 Δε of low-frequency and high-frequency polarization of the recycled materials, a) rPE and (b) r(PE-PP); as a function of reciprocal temperature

According to Figure 4.8, for both recycled materials, the dipolar and interfacial polarization rates increase as the temperature rises. This trend is particularly evident in Figure 4.2 and Figure 4.3b, where the interfacial polarization shifts toward higher frequencies with increasing temperature, indicating enhanced molecular mobility or charge transport at high temperatures.

The same behavior was observed for high-frequency polarization. For r(PE-PP), the high-frequency polarization also shifts to higher frequencies as the temperature increases, regardless of the influence of thermal energy on dipolar alignment or charge accumulation at the interfaces.

Figure 4.9, illustrating the dielectric relaxation strength of recycled materials as a function of reciprocal temperature. For both recycled materials, the electrical relaxation strength of low-frequency polarization is slightly higher than that of high-frequency polarization. Dielectric relaxation strength is defined as the difference in a material's ability to store energy at high and low frequencies when external electric field is applied. The impurity content can affect the strength of the dielectric relaxation, as impurities can introduce new dipoles, potentially increasing the dielectric relaxation strength. Also, new interfaces can also affect the dielectric strength. Eesaee et al (Eesaee et al., 2020), showed that while the temperature doesn't remarkably affect the dielectric strength, particle concentration has a significant impact.

Table 4.1 Optimum fitting parameters of recycled (PE-PP), obtained from the HN function

Temperature (°C)	f_{max}	Δε-low	α-low	β -low	f_{max}	Δε-high	α -high	β -high
-25	-	--	--	--	1.94×10^{4}	1.10×10^{-2}	0.27	0.95
-15	--	--	--	--	3.06×10^{4}	1.21×10^{-2}	0.27	0.92
-5	--	--	--	--	5.98×10^{4}	1.44×10^{-2}	0.33	0.45
5	--	--	--	--	6.65×10^{4}	2.00×10^{-2}	0.43	0.19
15	3.14×10^{-2}	0.0612	0.62	0.58	2.70×10^{5}	2.96×10^{-2}	0.47	0.10
25	1.83×10^{-1}	0.0540	0.63	0.59	4.73×10^{5}	3.14×10^{-2}	0.47	0.10
35	9.36×10^{-2}	0.1088	0.39	1	1.14×10^{6}	2.41×10^{-2}	0.40	0.18
45	5.38×10^{-1}	0.1171	0.42	1	1.13×10^{6}	2.39×10^{-2}	0.40	0.18
55	6.92×10^{-1}	0.1325	0.31	1	--	--	--	--
65	9.15×10^{-1}	0.1258	0.34	1	--	--	--	--
75	1.34	0.1173	0.34	1	--	--	--	--
85	8.48×10^{-1}	0.1360	0.32	1	-	--	--	--
95	8.43×10^{-1}	0.1364	0.32	1	--	--	--	--

The shape parameters (α, β), maximum frequency at relaxation peak (f_{max}), and dielectric strength (Δε) of the relaxation peaks of r(PE-PP) are presented in Table 4.1. Data for the low-frequency polarization curve was excluded at low temperatures (T < 15°C) due to the lack of clarity. Similarly, at high-frequency range, the data was cut off at high temperatures (T > 45°C) where the relaxation curve was not distinct. The parameter α, known as the width parameter, indicates the broadness of the relaxation curve and ranges from -1 to 1 ($-1 \leq \alpha \leq 1$). When the value of the width parameter α is low, the relaxation curve becomes broader. In other words, a decrease in α results in a wider relaxation curve. As temperature increased, the width parameter α for low-frequency polarization of r(PE-PP) decreased, indicating a broader relaxation curve. Conversely, for high-frequency polarization, α increased with rising temperature, resulting in

a narrower peak. For instance, in Figure 4.3a, the width parameter of high-frequency relaxation peak increased from 0.47 to 0.54 after heating cycling. This change might be attributed to the removal of water molecules, which are known to cause a wide peak (Lau et al., 2013). In wet samples, different states of water bonding could exist at various interfaces which contribute to the broad loss peaks observed. These various bounds could polarize across a range of frequencies, leading to broader dielectric loss peaks. Other research has also shown that the concentration of inorganic compound could influence the broadness of the peak (C. Zhang and G. C. Stevens, 2008; Steeman et al., 1991). The second parameter β is attributed to the asymmetry of relaxation peak and ranges from -1 to 1 ($-1 \leq \beta \leq 1$). At low frequencies, the asymmetry parameter increased toward unity as the temperature increased. At higher frequencies, in the high-frequncy polarization area, it decreased with an increase in temperature.

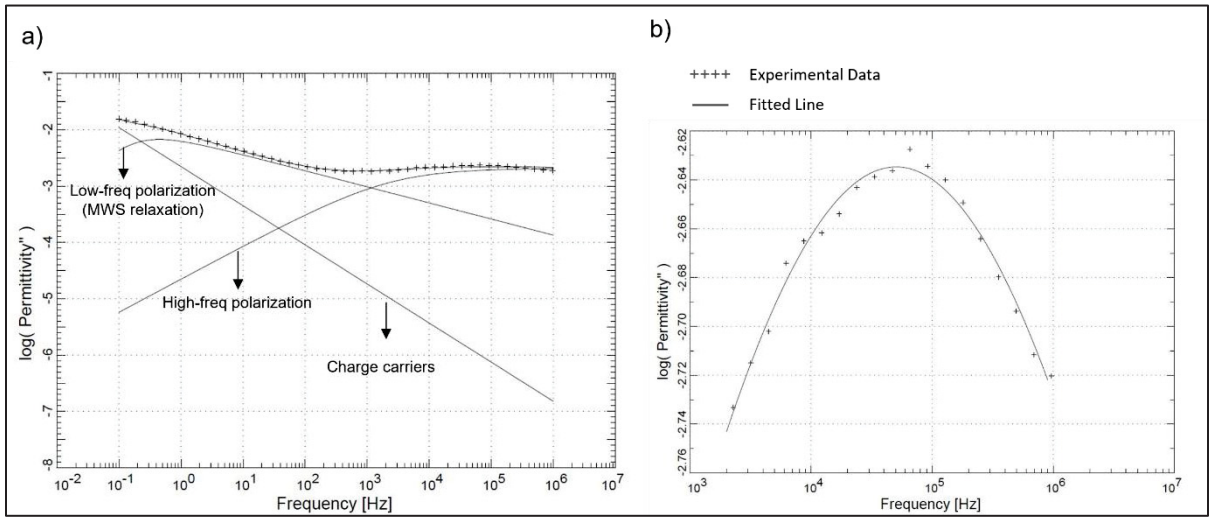

Figure 4.10 Fitting corresponding to recycled blend of polyethylene and polypropylene (r(PE-PP)): (a) over the full frequency range (10^{-1} to 10^{6} Hz); (b) magnified view of the high-frequency region at 25 °C

Figure 4.10 shows the fitting plot of data using equation (4.3) for recycled sample r(PE-PP) at 25 °C. The fitting parameters of the HN function are shown in Table 4.1. As illustrated in Figure 4.10a and 4.10b, the real data fit well with the HN function. The slope of the logarithmic plot of imaginary permittivity versus frequency at low frequencies, which represents DC

conductivity exponent, is approximately 0.56. If the slope were close to unity, it would suggest ideal electronic conductivity that was primarily due to charge leakage through the sample. However, in this case, the slope indicates the contribution of charge blockage by electrode polarization which is charge blockage in the interface of polymeric material and metallic electrode (Eesaee et al., 2020).

4.4 Conclusion

This study provides the analysis of relaxation process of recycled polyethylene (rPE) and polyethylene-polypropylene blends, r(PE-PP), under various thermal and environmental conditions. The results demonstrated that recycled materials have shown higher dielectric loss compared to virgin materials, primarily due to impurities, moisture absorption and microstructural boundaries. Moisture was identified as a critical factor influencing relaxation behavior, with wet samples showing higher dielectric loss. On the other hand, heating resulted in lower dielectric loss for recycled materials but higher dielectric loss for virgin HDPE, representing potential thermal aging in the virgin material, particularly through higher polarization effects and increased conductivity. The successful application of the Havriliak-Negami function in fitting the experimental data highlights its functionality in characterizing relaxation processes in recycled polyolefins. These findings show the importance of controlling environmental conditions and impurities, to optimize the performance of recycled materials in insulation applications.

CONCLUSION

This section outlines the primary findings based on the objectives of the study.

Objective 1: To understand how impurities influence the dielectric behavior and performance of recycled polyolefins used in insulation applications

The investigation confirmed that inorganic impurities, primarily soil and pigment components, are present in recycled polyolefins at levels of approximately 1.0-1.5 wt%. These impurities have a significant adverse effect on dielectric performance. Specifically, they cause a substantial increase in dielectric losses up to 28 times higher than virgin material by introducing a strong interfacial relaxation mechanism, which is most prominent at low frequencies. Furthermore, the presence of these contaminants leads to a reduction in the material's dielectric breakdown strength, though this effect was less pronounced than the impact on dielectric losses.

Objective 2: To investigate the dielectric properties of recycled polyolefins under varying thermal and environmental conditions (dry, wet, and ambient) in order to determine their impact on dielectric performance

The dielectric properties of recycled polyolefins are highly sensitive to environmental and thermal conditions. Exposure to moisture (wet conditions) significantly degrades performance, leading to higher dielectric losses and more pronounced interfacial and dipolar polarization compared to ambient conditions. Conversely, thermal treatment (drying) reduced the dielectric loss in recycled materials by removing moisture. However, the same heating process was found to cause thermal degradation in virgin HDPE, paradoxically increasing its dielectric loss. This highlights a key difference in how recycled and virgin materials respond to thermal stress, with the properties of recycled materials being dominated by impurity and moisture content.

Objective 3: To explore performance-enhancing techniques, such as blending with virgin polymer, to restore the dielectric performance of recycled polyolefins in insulation applications

Blending recycled polyolefins with virgin HDPE was confirmed as an effective and practical technique for restoring dielectric performance. This approach significantly improves key properties, with the addition of just 15 wt% virgin HDPE reducing dielectric loss by up to 40%. A more substantial 50/50 blend was shown to decrease dielectric loss by 50% while also improving the dielectric breakdown strength. These results demonstrate that blending is a viable strategy to enhance the electrical properties of recycled materials, making them suitable candidates for insulation applications in low and medium voltage cables.

RECOMMENDATIONS

The findings of this research highlight the significant influence of impurities and moisture, on the dielectric performance of recycled polyolefins. Also blending has found to be an useful strategy to improve the dielectric performance. However, several studies have done on recycled materials, further studies could help to better understand it. These recommendations aim to address identified knowledge gaps, improve material performance, and expand the applicability of recycled polymers in the electrical industry.

- Study the impact of exposure time and temperature on thermal degradation of both virgin HDPE and recycled materials. This help to understand how aging can influence the dielectric property of PE/PP blend.

- Blend virgin HDPE and PE/PP with controlled amounts of mineral elements and evaluate their dielectric properties. This will allow the effect of impurities on the dielectric response to be studied under controlled conditions, eliminating the uncertainty present in recycled materials.

- In an immiscible PE/PP blend, introduce a coupling agent to modify the morphology and then study its effect on both dielectric response and morphology. This approach will help distinguish the influence of miscibility from the intrinsic effects of the coupling agent itself.

- Evaluate the dielectric properties of post-consumer versus post-industrial recycled polymers.

- Study how processing cycles influence the dielectric response of both virgin PE/PP blends and recycled PE/PP blends. Processing can alter droplet-phase morphology in

immiscible blends, which may affect interfacial polarization and dielectric behavior. Furthermore, this process can cause mechanical and thermal aging, which in turn affects the dielectric responses.

LIST OF BIBLIOGRAPHICAL REFERENCES

Ahmed Dabbak, S.Z., Illias, H.A., Ang, B.C., Abdul Latiff, N.A., Makmud, M.Z., 2018. Electrical Properties of Polyethylene/Polypropylene Compounds for High-Voltage Insulation. Energies 11. https://doi.org/10.3390/en11061448

Andreassen, E., 1999. Infrared and Raman spectroscopy of polypropylene, in: Karger-Kocsis, J. (Ed.), Polypropylene: An A-Z Reference. Springer Netherlands, Dordrecht, pp. 320–328. https://doi.org/10.1007/978-94-011-4421-6_46

Angalane, S.K., Kasinathan, E., 2022. A review on polymeric insulation for high-voltage application under various stress conditions. Polymer Composites 43, 4803–4834. https://doi.org/10.1002/pc.26793

ASTM D-149, Standard Test Method for Dielectric Breakdown Voltage and Dielectric Strength of Solid Electrical Insulating Materials at Commercial Power Frequencies, 2020.

ASTM D-3418, Standard Test Method for Transition Annual book of ASTM, 2015. . Philadelphia.

Banhegyi, G., 1986. Comparison of electrical mixture rules for composites. Colloid and polymer science 264, 1030–1050.

Blythe, A.R., Bloor, D., 2005. Electrical Properties of Polymers, Cambridge solid state science series. Cambridge University Press.

Böhning, M., Goering, H., Fritz, A., Brzezinka, K.-W., Turky, G., Schönhals, A., Schartel, B., 2005. Dielectric Study of Molecular Mobility in Poly(propylene-graft-maleic anhydride)/Clay Nanocomposites. Macromolecules 38, 2764–2774. https://doi.org/10.1021/ma048315c

Borovanska, I., Krastev, R., Benavente, R., Pradas, M.M., Lluch, A.V., Samichkov, V., Iliev, M., 2014. Ageing effect on morphology, thermal and mechanical properties of impact modified LDPE/PP blends from virgin and recycled materials. Journal of Elastomers & Plastics 46, 427–447.

Boz Noyan, E.C., Venkatesh, A., Boldizar, A., 2022. Mechanical and Thermal Properties of Mixed PE Fractions from Post-Consumer Plastic Packaging Waste. ACS Omega 7, 45181–45188. https://doi.org/10.1021/acsomega.2c05621

C. Zhang, G. C. Stevens, 2008. The Dielectric Response of Polar and Non-Polar Nanodielectrics. IEEE Transactions on Dielectrics and Electrical Insulation 15, 606–617. https://doi.org/10.1109/TDEI.2008.4483483

Calero, M., Martín-Lara, M.A., Godoy, V., Quesada, L., Martínez, D., Peula, F., Soto, J.M., 2018. Characterization of plastic materials present in municipal solid waste: Preliminary study for their mechanical recycling. Detritus 4, 104–112.

Camacho, W., Karlsson, S., 2001. NIR, DSC, and FTIR as quantitative methods for compositional analysis of blends of polymers obtained from recycled mixed plastic waste. Polymer Engineering & Science 41, 1626–1635.

Cecon, V.S., Da Silva, P.F., Vorst, K.L., Curtzwiler, G.W., 2021. The effect of post-consumer recycled polyethylene (PCRPE) on the properties of polyethylene blends of different densities. Polymer Degradation and Stability 190, 109627.

Chen, B., Berretta, S., Evans, K., Smith, K., Ghita, O., 2018. A primary study into graphene/polyether ether ketone (PEEK) nanocomposite for laser sintering. Applied Surface Science 428, 1018–1028. https://doi.org/10.1016/j.apsusc.2017.09.226

Cheng, Y., Bai, L., Yu, G., Zhang, X., 2018. Effect of particles size on dielectric properties of nano-ZnO/LDPE composites. Materials 12, 5.

Cimbala, R., German-Sobek, M., Bucko, S., 2015. The assessment of influence of thermal aging to dielectric properties of XLPE insulation using dielectric relaxation spectroscopy. ACTA electrotechnica et informatica 15, 14–17.

Couderc Hugues, David Eric, Frechette Michel, 2014. Study of Water Diffusion in PE-SiO2 Nanocomposites by Dielectric Spectroscopy. Transactions on Electrical and Electronic Materials 15, 291–296. https://doi.org/10.4313/TEEM.2014.15.6.291

Cruz, S., Zanin, M., 2004. Dielectric strength of the blends of virgin and recycled HDPE. Journal of applied polymer science 91, 1730–1735.

Danikas, M., Vardakis, G.E., Sarathi, R., 2020. Some Factors Affecting the Breakdown Strength of Solid Dielectrics: A Short Review. Eng. Technol. Appl. Sci. Res 10, 5505–5511.

David, E., Frechette, M., 2013. Polymer nanocomposites-major conclusions and achievements reached so far. IEEE Electrical Insulation Magazine 29, 29–36.

David, E., Fréchette, M., Zazoum, B., Daran-Daneau, C., Ngô, A.D., Couderc, H., 2013. Dielectric Properties of PE/Clay Nanocomposites. Journal of Nanomaterials 2013, 703940. https://doi.org/10.1155/2013/703940

Densley, J., 2001. Ageing mechanisms and diagnostics for power cables-an overview. IEEE electrical insulation magazine 17, 14–22.

Dissado, L. A., and Fothergill, J. C., 1992. Electrical Degradation and Breakdown in Polymers, Statistical features of breakdown. 319-355.

Eesaee, M., David, E., Demarquette, N.R., 2020. Dielectric Relaxation Dynamics of Clay-Containing Low-Density polyethylene Blends and Nanocomposites. Polymer Engineering & Science 60, 968–978. https://doi.org/10.1002/pen.25352

Eesaee, M., David, E., Demarquette, N.R., Fabiani, D., 2018. Electrical Breakdown Properties of Clay-Based LDPE Blends and Nanocomposites. Journal of Nanomaterials 2018, 7921725. https://doi.org/10.1155/2018/7921725

F. Ciuprina, I. Plesa, P. V. Notingher, T. Zaharescu, P. Rain, D. Panaitescu, 2010. Dielectric properties of LDPE-SiO2 nanocomposites, in: 2010 10th IEEE International Conference on Solid Dielectrics. Presented at the 2010 10th IEEE International Conference on Solid Dielectrics, pp. 1–4. https://doi.org/10.1109/ICSD.2010.5568097

Fang, J., Zhang, L., Sutton, D., Wang, X., Lin, T., 2012. Needleless Melt-Electrospinning of Polypropylene Nanofibres. Journal of Nanomaterials 2012, 382639. https://doi.org/10.1155/2012/382639

Fothergill, J.C., Montanari, G.C., Stevens, G.C., Laurent, C., Teyssedre, G., Dissado, L.A., Nilsson, U.H., Platbrood, G., 2003. Electrical, microstructural, physical and chemical characterization of HV XLPE cable peelings for an electrical aging diagnostic data base. IEEE Transactions on Dielectrics and Electrical Insulation 10, 514–527. https://doi.org/10.1109/TDEI.2003.1207480

G, E., Hauver, 2014. the dielectric constant of polyei ’ hy under shock c pression.

Gala, A., Guerrero, M., Serra, J.M., 2020. Characterization of post-consumer plastic film waste from mixed MSW in Spain: A key point for the successful implementation of sustainable plastic waste management strategies. Waste Management 111, 22–33. https://doi.org/10.1016/j.wasman.2020.05.019

Gall, M., Freudenthaler, P.J., Fischer, J., Lang, R.W., 2021. Characterization of Composition and Structure–Property Relationships of Commercial Post-Consumer Polyethylene and Polypropylene Recyclates. Polymers 13, 1574.

Gao, J., Ju, H., Yao, Z., Zhang, G., Jiang, Q., Guo, H., 2023a. Effect of zinc oxide nanoparticle size on the dielectric properties of polypropylene-based nanocomposites. Polymer Engineering & Science n/a. https://doi.org/10.1002/pen.26370

Gao, J., Ju, H., Yao, Z., Zhang, G., Liu, Y., Niu, J., 2023b. Effect of silicon dioxide and organized montmorillonite on the crystalline morphology and dielectric properties of polypropylene-based composites. Polymer Composites 44, 2804–2815. https://doi.org/10.1002/pc.27281

Garofalo, E., Di Maio, L., Scarfato, P., Pietrosanto, A., Protopapa, A., Incarnato, L., 2021. Study on Improving the Processability and Properties of Mixed Polyolefin Post-Consumer Plastics for Piping Applications. Polymers 13. https://doi.org/10.3390/polym13010071

Geyer, R., Jambeck, J.R., Law, K.L., 2017. Production, use, and fate of all plastics ever made. Science advances 3, e1700782.

Geyer, R., Jambeck, J.R., Law, K.L., n.d. Production, use, and fate of all plastics ever made. Science Advances 3, e1700782. https://doi.org/10.1126/sciadv.1700782

Ginzburg, A., Ramakrishnan, V., Rongo, L., Rozanski, A., Bouyahyi, M., Jasinska-Walc, L., Duchateau, R., 2020. The influence of polypropylene-block/graft-polycaprolactone copolymers on melt rheology, morphology, and dielectric properties of polypropylene/polycarbonate blends. Rheologica Acta 59, 601–619. https://doi.org/10.1007/s00397-020-01223-7

Helal, E., David, E., Fréchette, M., Demarquette, N.R., 2017. Thermoplastic elastomer nanocomposites with controlled nanoparticles dispersion for HV insulation systems: Correlation between rheological, thermal, electrical and dielectric properties. European Polymer Journal 94, 68–86. https://doi.org/10.1016/j.eurpolymj.2017.06.038

Heydariaraghi, M., Ghorbanian, S., Hallajisani, A., Salehpour, A., 2016. Fuel properties of the oils produced from the pyrolysis of commonly-used polymers: Effect of fractionating column. Journal of Analytical and Applied Pyrolysis 121, 307–317. https://doi.org/10.1016/j.jaap.2016.08.010

Hosier, I.L., Praeger, M., Vaughan, A.S., Swingler, S.G., 2017. The effects of water on the dielectric properties of aluminum-based nanocomposites. IEEE Transactions on Nanotechnology 16, 667–676.

Hui, L., Schadler, L.S., Nelson, J.K., 2013. The influence of moisture on the electrical properties of crosslinked polyethylene/silica nanocomposites. IEEE Transactions on Dielectrics and Electrical Insulation 20, 641–653.

I. Shirzaei Sani, E. David, N. R. Demarquette, 2021. Dielectric properties of recycled city and industrial waste polyethylene, in: 2021 IEEE Conference on Electrical Insulation and Dielectric Phenomena (CEIDP). Presented at the 2021 IEEE Conference on Electrical Insulation and Dielectric Phenomena (CEIDP), pp. 49–52. https://doi.org/10.1109/CEIDP50766.2021.9705467

IEEE-930, IEEE Guide for the Statistical Analysis of Electrical Insulation Breakdown Data, 2005. . Electrical Insulation Society.

J. C. Fothergill, 2007. Ageing, Space Charge and Nanodielectrics: Ten Things We Don’t Know About Dielectrics, in: 2007 IEEE International Conference on Solid Dielectrics. Presented at the 2007 IEEE International Conference on Solid Dielectrics, pp. 1–10. https://doi.org/10.1109/ICSD.2007.4290739

Jambeck, J.R., Geyer, R., Wilcox, C., Siegler, T.R., Perryman, M., Andrady, A., Narayan, R., Law, K.L., 2015. Plastic waste inputs from land into the ocean. Science 347, 768–771. https://doi.org/10.1126/science.1260352

Jones, H., McClements, J., Ray, D., Hindle, C.S., Kalloudis, M., Koutsos, V., 2023. Thermomechanical Properties of Virgin and Recycled Polypropylene—High-Density Polyethylene Blends. Polymers 15. https://doi.org/10.3390/polym15214200

Jonscher, A.K., 1991. Low-frequency dispersion in volume and interfacial situations. Journal of Materials Science 26, 1618–1626. https://doi.org/10.1007/BF00544672

Jonscher, A.K., 1983. Dielectric relaxation in solids. Chelsea Dielectrics Press Ltd.

Juan, R., Paredes, B., García-Muñoz, R.A., Domínguez, C., 2021. Quantification of PP contamination in recycled PE by TREF analysis for improved the quality and circularity of plastics. Polymer Testing 100, 107273. https://doi.org/10.1016/j.polymertesting.2021.107273

Karaagac, E., Koch, T., Archodoulaki, V.-M., 2021. The effect of PP contamination in recycled high-density polyethylene (rPE-HD) from post-consumer bottle waste and their compatibilization with olefin block copolymer (OBC). Waste Management 119, 285–294.

Kazemi, Y., Ramezani Kakroodi, A., Rodrigue, D., 2015. Compatibilization Efficiency in Post-Consumer Recycled Polyethylene/Polypropylene Blends: Effect of Contamination. Polymer Engineering and Science. https://doi.org/10.1002/pen.24125

Kochetov, R., Tsekmes, I.-A., Morshuis, P.H.F., Smit, J.J., Wanner, A.J., Wiesbrock, F., Kern, W., 2016. Effect of water absorption on dielectric spectrum of nanocomposites, in: 2016 IEEE Electrical Insulation Conference (EIC). IEEE, pp. 579–582.

Kremer, F., Schönhals, A., 2003. Broadband dielectric spectroscopy.

Kuffel, E., 2000. Chapter 6 – Breakdown in solid and liquid dielectrics. High Voltage Engineering 367–394.

Larsen, Å.G., Olafsen, K., Alcock, B., 2021. Determining the PE fraction in recycled PP. Polymer Testing 96, 107058. https://doi.org/10.1016/j.polymertesting.2021.107058

Lau, K.Y., Vaughan, A.S., Chen, G., Hosier, I.L., 2012. Dielectric response of polyethylene nanocomposites: The effect of surface treatment and water absorption, in: 2012 Annual Report Conference on Electrical Insulation and Dielectric Phenomena. IEEE, pp. 275–278.

Lau, K.Y., Vaughan, A.S., Chen, G., Hosier, I.L., Holt, A.F., 2013. On the dielectric response of silica-based polyethylene nanocomposites. Journal of Physics D: Applied Physics 46, 095303.

Li, Yamei, Peng, Z., Xu, D., Huang, S., Gao, Y., Li, Yuan, 2024. Research on the Thermal Aging Characteristics of Crosslinked Polyethylene Cables Based on Polarization and Depolarization Current Measurement. Energies 17, 2274.

Liang, B., Lan, R., Zang, Q., Liu, Z., Tian, L., Wang, Z., Li, G., 2023. Influence of thermal aging on dielectric properties of high voltage cable insulation layer. Coatings 13, 527.

M. Roy, J. K. Nelson, R. K. MacCrone, L. S. Schadler, C. W. Reed, R. Keefe, 2005. Polymer nanocomposite dielectrics-the role of the interface. IEEE Transactions on Dielectrics and Electrical Insulation 12, 629–643. https://doi.org/10.1109/TDEI.2005.1511089

Mansour, D.-E.A., Abdel-Gawad, N.M.K., El Dein, A.Z., Ahmed, H.M., Darwish, M.M.F., Lehtonen, M., 2021. Recent Advances in Polymer Nanocomposites Based on Polyethylene and Polyvinylchloride for Power Cables. Materials 14. https://doi.org/10.3390/ma14010066

Mylläri, V., Hartikainen, S., Poliakova, V., Anderson, R., Jönkkäri, I., Pasanen, P., Andersson, M., Vuorinen, J., 2016. Detergent impurity effect on recycled HDPE: Properties after repetitive processing. Journal of Applied Polymer Science 133.

Nelson, J.K., Fothergill, J.C., 2004. Internal charge behaviour of nanocomposites. Nanotechnology 15, 586.

Pandey, J.C., Singh, M., 2021. Dielectric polymer nanocomposites: Past advances and future prospects in electrical insulation perspective. SPE Polymers 2, 236–256. https://doi.org/10.1002/pls2.10059

Polyethylene Insulation Materials Market Size and Forecast 2030 [WWW Document], 2022. . Alliedmarketresearch, report code A01757 ,. URL https://www.alliedmarketresearch.com/polyethylene-insulation-materials-market (accessed 4.12.23).

Polyethylene Market Size to Hit US$ 151.85 Billion by 2030 [WWW Document], 2021. . The Dow Chemical Company, precedenceresearch, report code 1440 ,. URL https://www.precedenceresearch.com/polyethylene-market (accessed 4.12.23).

Ragaert, K., Delva, L., Van Geem, K., 2017. Mechanical and chemical recycling of solid plastic waste. Waste management 69, 24–58.

Roosen, M., Mys, N., Kusenberg, M., Billen, P., Dumoulin, A., Dewulf, J., Van Geem, K.M., Ragaert, K., De Meester, S., 2020. Detailed Analysis of the Composition of Selected Plastic Packaging Waste Products and Its Implications for Mechanical and Thermochemical Recycling. Environ. Sci. Technol. 54, 13282–13293. https://doi.org/10.1021/acs.est.0c03371

S. A. Cruz, M. Zanin, 2004. Assessment of dielectric behavior of recycled/virgin high density polyethylene blends. IEEE Transactions on Dielectrics and Electrical Insulation 11, 855–860. https://doi.org/10.1109/TDEI.2004.1349791

S. Alapati, M. J. Thomas, 2012. Electrical treeing and the associated PD characteristics in LDPE nanocomposites. IEEE Transactions on Dielectrics and Electrical Insulation 19, 697–704. https://doi.org/10.1109/TDEI.2012.6180265

S. Li, G. Yin, G. Chen, J. Li, S. Bai, L. Zhong, Y. Zhang, Q. Lei, 2010. Short-term breakdown and long-term failure in nanodielectrics: a review. IEEE Transactions on Dielectrics and Electrical Insulation 17, 1523–1535. https://doi.org/10.1109/TDEI.2010.5595554

Shirzaei Sani, I., Demarquette, N.R., David, E., 2025. Enhancing the Dielectric Properties of Recycled Polyolefin Streams Through Blending. Sustainability 17. https://doi.org/10.3390/su17094123

Shirzaei Sani, I., Demarquette, N.R., David, E., 2023. Investigation and characterization of dielectric, thermal, and chemical properties of recycled high-density polyethylene blended with virgin polyethylene. Polymer Engineering & Science 63, 3254–3267. https://doi.org/10.1002/pen.26441

Shirzaei Sani, I., Rezaei, M., Baradar Khoshfetrat, A., Razzaghi, D., 2021. Preparation and characterization of polycaprolactone/chitosan-g-polycaprolactone/hydroxyapatite electrospun nanocomposite scaffolds for bone tissue engineering. International Journal of Biological Macromolecules 182, 1638–1649. https://doi.org/10.1016/j.ijbiomac.2021.05.163

Singh, M.K., Mohanty, A.K., Misra, M., 2023. Upcycling of waste polyolefins in natural fiber and sustainable filler-based biocomposites: A study on recent developments and future perspectives. Composites Part B: Engineering 263, 110852.

Smith, B., 2021a. The Infrared Spectra of Polymers II: Polyethylene. Spectroscopy, September 2021 36, 24–29.

Smith, B., 2021b. The infrared spectra of polymers III: Hydrocarbon polymers.

Steeman, P.A.M., Maurer, F.H.J., 1990. An interlayer model for the complex dielectric constant of composites. Colloid and Polymer Science 268, 315–325. https://doi.org/10.1007/BF01411674

Steeman, P.A.M., Maurer, F.H.J., Van Es, M.A., 1991. Dielectric monitoring of water absorption in glass-bead-filled high-density polyethylene. Polymer 32, 523–530.

Sultana, S.M.N., Helal, E., Gutiérrez, G., David, E., Moghimian, N., Demarquette, N.R., 2024a. The Influence of a Commercial Few-Layer Graphene on the Photodegradation Resistance of a Waste Polyolefins Stream and Prime Polyolefin Blends. Recycling 9. https://doi.org/10.3390/recycling9020029

Sultana, S.M.N., Helal, E., Gutiérrez, G., David, E., Moghimian, N., Demarquette, N.R., 2024b. The Influence of a Commercial Few-Layer Graphene on Electrical Conductivity, Mechanical Reinforcement and Photodegradation Resistance of Polyolefin Blends. Crystals 14. https://doi.org/10.3390/cryst14080687

Sultana, S.M.N., Helal, E., Gutiérrez, G., David, E., Moghimian, N., Demarquette, N.R., 2023. Effect of Few-Layer Graphene on the Properties of Mixed Polyolefin Waste Stream. Crystals 13. https://doi.org/10.3390/cryst13020358

T. W. Dakin, 2006. Conduction and polarization mechanisms and trends in dielectric. IEEE Electrical Insulation Magazine 22, 11–28. https://doi.org/10.1109/MEI.2006.1705854

Tan, D.Q., 2020. The search for enhanced dielectric strength of polymer-based dielectrics: A focused review on polymer nanocomposites. Journal of Applied Polymer Science 137, 49379.

Tantipattarakul, S., Vaughan, A.S., Andritsch, T., 2020. Ageing behaviour of a polyethylene blend: influence of chemical defects and morphology on charge transport. High Voltage 5, 270–279. https://doi.org/10.1049/hve.2019.0402

Thoden van Velzen, E.U., Chu, S., Alvarado Chacon, F., Brouwer, M.T., Molenveld, K., 2021. The impact of impurities on the mechanical properties of recycled polyethylene. Packaging Technology and Science 34, 219–228. https://doi.org/10.1002/pts.2551

Tiemblo, P., Hoyos, M., Gómez-Elvira, J.M., Guzmán, J., García, N., Dardano, A., Guastavino, F., 2008. The development of electrical treeing in LDPE and its nanocomposites with spherical silica and fibrous and laminar silicates. Journal of Physics D: Applied Physics 41, 125208.

Tomer, V., Polizos, G., Randall, C.A., Manias, E., 2011. Polyethylene nanocomposite dielectrics: Implications of nanofiller orientation on high field properties and energy storage. Journal of Applied Physics 109, 074113. https://doi.org/10.1063/1.3569696

Tripathi, N., Thakur, A.K., Shukla, A., Marx, D.T., 2018. Dielectric, transport and thermal properties of clay based polymer- nanocomposites. Polymer Engineering & Science 58, 220–227. https://doi.org/10.1002/pen.24549

Turku, I., Kärki, T., Rinne, K., Puurtinen, A., 2017. Characterization of plastic blends made from mixed plastics waste of different sources. Waste Manag Res 35, 200–206. https://doi.org/10.1177/0734242X16678066

Wang, X., Qiang, D., Hosier, I., Zhu, Y., Chen, G., Andritsch, T., 2020. Effect of water on the breakdown and dielectric response of polypropylene/nano-aluminium nitride composites. Journal of materials science 55, 8900–8916.

Wong, A.C.-Y., Lam, F., 2002. Study of selected thermal characteristics of polypropylene/polyethylene binary blends using DSC and TGA. Polymer Testing 21, 691–696. https://doi.org/10.1016/S0142-9418(01)00144-1

X. Huang, J. Zhang, P. Jiang, T. Tanaka, 2019. Material progress toward recyclable insulation of power cables. Part 1: Polyethylene-based thermoplastic materials: Dedicated to the 80th birthday of professor Toshikatsu Tanaka. IEEE Electrical Insulation Magazine 35, 7–19. https://doi.org/10.1109/MEI.2019.8804330

Xi, R., Jiang, Q., Cao, L., Li, C., He, J., Zhang, Y., He, G., Gui, Y., Tang, C., 2024. Effects of Water Absorption on the Insulating Properties of Polypropylene. Energies 17, 4576.

Yin, S., Tuladhar, R., Shi, F., Shanks, R.A., Combe, M., Collister, T., 2015. Mechanical reprocessing of polyolefin waste: A review. Polymer Engineering & Science 55, 2899–2909. https://doi.org/10.1002/pen.24182

Z. Li, K. Okamoto, Y. Ohki, T. Tanaka, 2011. The role of nano and micro particles on partial discharge and breakdown strength in epoxy composites. IEEE Transactions on Dielectrics and Electrical Insulation 18, 675–681. https://doi.org/10.1109/TDEI.2011.5931052

Zhang, J., Hirschberg, V., Rodrigue, D., 2023. Blending Recycled High-Density Polyethylene HDPE (rHDPE) with Virgin (vHDPE) as an Effective Approach to Improve the Mechanical Properties. Recycling 8. https://doi.org/10.3390/recycling8010002

Zheng, Y., Long, Y., Yi, D., Zhang, H., Gao, J., Wu, K., Li, J., 2023. Correlation between antioxidant depletion kinetic model and ageing behaviour of cross-linked polyethylene cable insulation. High Voltage 8, 231–238.

Zois, H., Apekis, L., Omastova, M., 1999. Electrical properties and percolation phenomena in carbon black filled polymer composites, in: 10th International Symposium on Electrets (ISE 10). Proceedings (Cat. No.99 CH36256). pp. 529–532. https://doi.org/10.1109/ISE.1999.832101

Zou, C., Fothergill, J.C., Rowe, S.W., 2007. A" water shell" model for the dielectric properties of hydrated silica-filled epoxy nano-composites, in: 2007 IEEE International Conference on Solid Dielectrics. IEEE, pp. 389–392.